

Fortschr. Phys. **34** (1986) 11, 687–751

On the 1-Loop Renormalization of the Electroweak Standard Model and its Application to Leptonic Processes

M. BÖHM, H. SPIESBERGER¹⁾

Physikalisches Institut, Universität Würzburg, FRG,

W. HOLLIK

II. Institut für Theoretische Physik, Universität Hamburg, FRG

Abstract

A renormalization scheme for the electroweak standard model is presented in which the electric charge and the masses of the gauge bosons, Higgs particle and fermions are used as physical parameters. The photon is treated such that quantum electrodynamics is contained as a simple substructure. Field renormalization respecting the gauge symmetry gives finite propagators and vertex functions. The Ward identities between the Green functions of the unphysical sector allow a renormalization that maintains the simple pole structure of the propagators in the t'Hooft-Feynman gauge. We give a complete list of self energies and all renormalization constants also in the unphysical Higgs and ghost sector. Explicit results are given for the renormalized self energies, vertex functions and boxes that enter the evaluation of 1-loop radiative corrections to fermionic processes.

We calculate the 1-loop radiative corrections to purely leptonic reactions like μ decay, $\nu_\mu e$ scattering and μ pair production in e^+e^- annihilation. A test of the standard model is performed by comparing these low energy data with the results of the $P\bar{P}$ collider experiments for the W and Z boson masses.

I. Introduction

The recent discovery of the W and Z bosons at the $P\bar{P}$ collider at CERN [1] with values for the masses of these particles very close to those predicted by the GLASHOW-SALAM-WEINBERG model [2] was an important step in establishing this model as a good candidate for the gauge theory of the electroweak interaction. But also the experiments with low momentum transfers ($|q^2| \ll M_W^2$) [3] and at e^+e^- storage rings [4] contribute to a steady improvement of the determination of the structure and parameters of the electromagnetic and weak interaction. The accuracy of these experiments has reached a level which requires the inclusion of radiative corrections for an adequate theoretical discussion. This will be even more the case when the e^+e^- machines with energies up to 100 GeV, which are dedicated for the investigation of the detailed properties of the electroweak bosons, go into operation [5].

The standard model is a non-Abelian gauge theory of the electroweak interaction where the masses of the particles are generated with help of the Higgs mechanism. The

¹⁾ supported by the Deutsche Forschungsgemeinschaft.

renormalizability of quantum field theories of this class was proved already in 1971 by 't HOOFT [6]. This means that those parts occurring in the evaluation of Feynman diagrams of higher order which without regularization would become ultraviolet divergent can be absorbed by renormalization of the fields and couplings. The importance of the renormalization constants is not only to absorb divergences but also to complete the definition of the quantized field theory. The finite parts of the renormalization constants — fixed by the renormalization conditions — influence the results of the calculation of radiative corrections and therefore of physically observable effects.

Electroweak theories contain much more fields and parameters than quantum electrodynamics, moreover their structure is more complicated because of their non-Abelian, non-simple, spontaneously broken gauge symmetry. The choice of the renormalized parameters and their definition via measurable quantities as well as the definition of the weak mixing angle is not unique beyond the tree level.

Consequently several different schemes have been proposed in the literature [7–17]. The greater part [10, 12–55] deals with processes where $|q^2| \ll M_W^2$, like μ decay and ν scattering; refs. [9, 11, 16, 17] consider high q^2 e^+e^- annihilation. An attempt for their characterization can be made using the following criteria:

- Schemes with and without field renormalization; in the latter case S -matrix elements but not the Green functions such as self energies and 3-point vertex functions are finite.
- Field renormalization respecting the original gauge symmetry or not; Green functions are finite but have complicated properties under gauge transformations in the latter case.
- Determination of the parameters from low energy experiments like μ decay and $\nu_\mu e$ scattering or from high energy experiments i.e. measurements of the W, Z masses.

Of course, not all papers on electroweak radiative corrections fit simply into one of these categories.

In this paper we present a renormalization scheme for the standard electroweak model which is defined by the following conditions:

- i) The physical parameters are the electric charge e , the masses of the W and Z bosons, the Higgs mass and the fermion masses. This set was introduced by SIRLIN [10] and later used also by other authors [11, 15]. e is defined as the strength of the electromagnetic coupling in the Thomson limit, the masses as the position of the poles of the renormalized propagators. These parameters are directly accessible to experiment, since only the measurement of the fine structure constant α and of masses is required. The determination of masses in direct resonance production experiments is only very little influenced by radiative corrections. Bare masses and couplings do not occur; this avoids possible confusions in calculating cross sections in higher orders. The weak mixing angle θ_W and the Fermi constant G_F are no fundamental parameters. $c_W = \cos \theta_W = M_W/M_Z$, $s_W = \sqrt{1 - c_W^2}$ are only shorthand notations to simplify the formulas.
- ii) Real photons couple to the electron without any admixture of Z^0 contributions. Therefore the QED subpart of the model is realized in a simple way. Consequently photonic radiative corrections can be treated separately; especially for $e^+e^- \rightarrow f\bar{f}$ they can be taken over from pure QED calculations [18, 19].
- iii) Complete field renormalization respecting gauge invariance and the use of the 't Hooft-Feynman gauge lead to UV finite renormalized Green functions reflecting the gauge symmetry structure. We investigate the restrictions of the Slavnov-Taylor identities for the renormalization of the unphysical Green functions. Especially we

perform a renormalization of the gauge fixing parameters in such a way that their poles are situated at M_Z^2 , M_W^2 , 0.

We add some comments on the relation of this scheme to previous work by other authors.

The on-shell scheme (i) with e and the particle masses as parameters has been widely used for various applications in the last years [8–12, 15]. Counter terms in the physical sector and amplitudes for scattering between spin 1/2 particles are presented in ref. [8] in a unitary gauge calculation.

A vanishing renormalized photon- Z^0 mixing for on-shell photons (ii), which allows to be as close as possible to QED, has also been used by the authors of refs [8, 11, 12, 15]. The treatment of field renormalization in [11, 15] differs from [8, 12] and ours, since more renormalization constants than symmetry multiplets are introduced. For physical S -matrix elements the results should be equivalent. This is also the case for the scheme without field renormalization [10].

The method of SAKAKIBARA [12] to generate counter terms and his renormalization conditions are nearly identical to ours in the physical sector; for the unphysical gauge boson, Higgs and ghost parts ref. [12] contains less counter terms since the gauge fixing part is not renormalized, according to ROSS and TAYLOR [12]. One consequence of Sakakibara's procedure is that the relation $\sin^2 \theta_W = 1 - M_W^2/M_Z^2$ is no longer valid in higher order. This should not affect physical results if M_W , M_Z are rigorously used and auxiliary quantities avoided in final results. Since the evaluation and renormalization of all longitudinal gauge boson, Higgs and ghost self energies is not performed in [12] an explicit check of the equivalence of the pole structure also in the unphysical sector is not possible so far. However, ROSS and TAYLOR [12] claim that in this scheme which has no gauge parameter renormalization the poles of the individual unphysical propagators are not the corresponding tree levels poles.

The intention of this paper is to give a self contained and elaborate discussion of the standard model renormalization and to provide the basis for the calculations of radiative corrections, in particular to e^+e^- annihilation, deep inelastic scattering and $P\bar{P}$ annihilation with $|q^2| \cong M_W^2$. The paper is organized as follows:

Sect. 2 of this paper contains the definition of the complete Lagrangian and its parameters, sect. 3 the discussion of the Slavnov-Taylor resp. Ward identities, sect. 4 the renormalization conditions. The complete list of the Feynman rules including the counter terms can be found in the appendix A. In sect. 5 we list the 1-loop formulas for the unrenormalized self energies, the fermion gauge boson vertex functions and the renormalization constants. We give also all the unphysical Higgs and ghost self energies together with the renormalization constants which have not yet been presented so far. Sect. 6 contains the renormalized boson self and mixing energies and simple formulas for the renormalized gauge boson fermion vertices for arbitrary momentum transfer. Numerical results are shown for those self energies, vertices and box diagrams that enter the radiative corrections to electroweak processes between fermions. In the last section 7 we apply this renormalization scheme to the purely leptonic reactions μ decay, $\nu_\mu e$ scattering and lepton pair production in e^+e^- -annihilation. A test of the standard model is performed using as input the experimental data for these processes together with the measured values for M_W and M_Z [1].

2. The Renormalized Lagrangian and the Feynman Rules of the Standard Electroweak Model

2.1 The classical Lagrangian, parameter and fields

Gauge theories of the electroweak interaction are constructed in such a way that at low energies and in lowest order the experimentally successful Fermi model is recovered. In the case of the standard model [2] the universality of the weak interaction is realized in the form of the gauge group $SU(2) \times U(1)$. The gauge symmetry is spontaneously broken with help of a minimal Higgs mechanism with a $SU(2)$ doublet of scalar fields such that the electromagnetic gauge invariance $U(1)^{em}$ is maintained. The standard model allows to predict from low energy experiments the masses M_W, M_Z of the heavy gauge bosons W^\pm, Z . The existence and main properties of these particles have recently been confirmed by experiments at the $P\bar{P}$ collider [1].

The classical Lagrangian of the standard model \mathcal{L}_C is composed of the gauge, Higgs and fermion part:

$$\mathcal{L}_C = \mathcal{L}_{YM} + \mathcal{L}_H + \mathcal{L}_F. \tag{2.1}$$

According to the gauge group $SU(2) \times U(1)$ we have an isotriplet $W_\mu^a(x)$ and an isosinglet $B_\mu(x)$ of gauge fields with gauge coupling constants g_2 and g_1 leading to the Yang-Mills Lagrangian:

$$\mathcal{L}_{YM} = -\frac{1}{4} (\partial_\mu W_\nu^a - \partial_\nu W_\mu^a + g_2 \varepsilon^{abc} W_\mu^b W_\nu^c)^2 - \frac{1}{4} (\partial_\mu B_\nu - \partial_\nu B_\mu)^2. \tag{2.2}$$

The complex Higgs doublet $\varphi(x)$

$$\varphi(x) = \begin{pmatrix} \varphi^+(x) \\ \varphi^0(x) \end{pmatrix} = \begin{pmatrix} \varphi^+(x) \\ (v + \eta(x) + i\chi(x))/\sqrt{2} \end{pmatrix}$$

with hypercharge $Y = 1$ is coupled to the gauge bosons and has a self coupling:

$$\mathcal{L}_H = (D_\mu \varphi)^\dagger (D^\mu \varphi) - \frac{\lambda}{4} (|\varphi|^2)^2 + \mu^2 |\varphi|^2 \tag{2.3}$$

with the covariant derivative:

$$D_\mu = \partial_\mu - ig_2 I^a W_\mu^a + ig_1 \frac{Y}{2} B_\mu. \tag{2.4}$$

The left-handed fermion fields $\psi_{i\sigma}^L(x)$ are grouped into doublets ($i =$ doublet index, $\sigma =$ component of the doublet) of the weak isospin, the right-handed fields $\psi_{i\sigma}^R(x)$ into singlets, the hypercharges respecting the Gell-Mann Nishijima relation $Q = I^3 + Y/2$. The Lagrangian \mathcal{L}_F which describes the interaction between the fermions, the gauge fields and the scalars then has the form²⁾:

$$\begin{aligned} \mathcal{L}_F = \sum_i \{ & \bar{\psi}_{i\sigma}^L i \gamma^\mu D_\mu^{\sigma\sigma'} \psi_{i\sigma'}^L + \bar{\psi}_{i\sigma}^R i \gamma^\mu D_\mu^{\sigma\sigma'} \psi_{i\sigma'}^R \\ & + (-g_{i+} \bar{\psi}_{i+}^R \varphi^0 \psi_{i+}^L - g_{i-} \bar{\psi}_{i-}^R \varphi^{0*} \psi_{i-}^L + g_{i+} \bar{\psi}_{i+}^R \varphi^+ \psi_{i-}^L - g_{i-} \bar{\psi}_{i-}^R \varphi^- \psi_{i+}^L + \text{h.c.}) \}. \end{aligned} \tag{2.5}$$

²⁾ We do not write explicitly colour indices and the Cabbibo transformation of the quark fields i.e. we assume the coupling matrix $g_{ij} = g_i \delta_{ij}$ to be diagonal.

This completes the construction of \mathcal{L}_C in terms of the fields $W_\mu^a, B_\mu, \varphi, \psi^L, \psi^R$ and the parameters

$$g_2, g_1, \lambda, \mu^2, g_{i\sigma}. \tag{2.6}$$

\mathcal{L}_C is invariant under local transformations of the group $SU(2) \times U(1)$:

$$g = \exp \left[ig_2 I^a \theta_a(x) - i \frac{g_1}{2} Y \theta_Y(x) \right],$$

namely

$$\frac{\delta \mathcal{L}_C}{\delta \theta^a(x)} = 0, \quad \alpha = \{a, Y\}. \tag{2.7}$$

A formulation where the physical content of the theory is more — but the symmetry less — transparent can be obtained by performing the following transformation of the gauge fields:

$$\begin{aligned} W_\mu^\pm &= (W_\mu^1 \mp iW_\mu^2) / \sqrt{2}, \\ Z_\mu &= \frac{M_W}{M_Z} W_\mu^3 + \left(1 - \frac{M_W^2}{M_Z^2} \right)^{1/2} B_\mu, \\ A_\mu &= - \left(1 - \frac{M_W^2}{M_Z^2} \right)^{1/2} W_\mu^3 + \frac{M_W}{M_Z} B_\mu \end{aligned} \tag{2.8}$$

and using the following parameters:

$$e, M_W, M_Z, M_H, m_{i\sigma} \tag{2.9}$$

with

$$\begin{aligned} e &= \frac{g_1 g_2}{(g_1^2 + g_2^2)^{1/2}}, \quad M_W = g_2 \mu / \sqrt{\lambda}, \quad M_Z = (g_1^2 + g_2^2)^{1/2} \mu / \sqrt{\lambda}, \\ M_H &= \sqrt{2} \mu, \quad m_{i\sigma} = g_{i\sigma} \mu \sqrt{2/\lambda}. \end{aligned} \tag{2.10}$$

Each of the parameters (2.9) is directly accessible to experiments since for their determination measurements of the Thomson scattering cross section (for the electric charge e) and of the masses of the W boson, Z boson, Higgs boson and the fermions are required. This is the reason why we prefer the set of more physical fields (2.8) and parameters (2.9) as the basis for the formulation of the electroweak Lagrangian \mathcal{L}_C . It may be that for low energy processes the use of other parameters like the Fermi constant G_F and the weak mixing angle θ_W is more convenient [10, 12, 13]. The relation between M_W, M_Z and G_F, θ_W to lowest order is:

$$\begin{aligned} G_F / \sqrt{2} &= \pi \alpha / 2 M_W^2 (1 - M_W^2 / M_Z^2), \\ \cos \theta_W &= M_W / M_Z. \end{aligned} \tag{2.11}$$

Depending on the specific renormalization scheme some of the relations (2.8)–(2.11) get corrections from higher order contributions.

2.2 Gauge fixing and ghost fields

For the systematic treatment of the quantization of \mathcal{L}_C and higher order calculations it is convenient to choose a renormalizable gauge. We introduce linear gauge fixings $F^\alpha(W, B, \varphi)$ of the 't Hooft type:

$$\begin{aligned} F^\pm &= (\xi_1^W)^{-1/2} \partial^\mu W_\mu^\pm \mp iM_W(\xi_2^W)^{1/2} \varphi^\pm, \\ F^3 &= (\xi_1^3)^{-1/2} \partial^\mu W_\mu^3 - M_W(\xi_2^3)^{1/2} \chi, \\ F^B &= (\xi_1^B)^{-1/2} \partial^\mu B_\mu - (M_Z^2 - M_W^2)^{1/2} (\xi_2^B)^{1/2} \chi. \end{aligned} \tag{2.12}$$

Then we add to \mathcal{L}_C the term

$$\mathcal{L}_{\text{fix}} = -\frac{1}{2} \sum_\alpha (F^\alpha)^2 \tag{2.13}$$

and introduce the Faddeev-Popov ghost fields $u^\alpha(x)$ resp. $u^\pm(x), u^Z(x), u^B(x)$ with the Lagrangian [21]:

$$\mathcal{L}_{FP} = \bar{u}^\alpha(x) \frac{\delta F^\alpha}{\delta \theta^\beta(x)} u^\beta(x) = \bar{u}^\alpha K^{\alpha\beta} u^\beta. \tag{2.14}$$

A particular choice of the gauge parameters ξ is:

$$\xi_1^W = \xi_2^W = \xi_1^3 = \xi_2^3 = \xi_1^B = \xi_2^B = 1. \tag{2.15}$$

This 't Hooft-Feynman gauge has the advantage that at least to lowest order the poles of the longitudinal parts of the gauge boson propagators, the unphysical Higgs fields φ^\pm, χ and the ghost fields are situated at M_W^2 or M_Z^2 and that no gauge field – Higgs field mixing occurs.

With \mathcal{L}_{fix} and \mathcal{L}_{FP} we have completed the construction of a renormalizable Lagrangian

$$\mathcal{L} = \mathcal{L}_C + \mathcal{L}_{\text{fix}} + \mathcal{L}_{FP} \tag{2.16}$$

for the standard electroweak model.

2.3 Multiplicative Renormalization

The Lagrangian (2.16) is the starting point for the calculation of Green functions and S matrix elements including radiative corrections. We renormalize not only the physical parameters but also the fields in order to arrive at Green functions that are finite. For S -matrix elements the results should of course be equivalent to those obtained without field renormalization (see e.g. Sirlin [10]). Since symmetry arguments were important in the construction of \mathcal{L}_C we perform the multiplicative renormalization of \mathcal{L} in such a way that the gauge symmetry is respected:

$$\begin{aligned} W_\mu^a &\rightarrow (Z_2^W)^{1/2} W_\mu^a, & B_\mu &\rightarrow (Z_2^B)^{1/2} B_\mu, \\ \varphi &\rightarrow (Z^\varphi)^{1/2} \varphi, \\ \psi_{i\sigma}^L &\rightarrow (Z_L^i)^{1/2} \psi_{i\sigma}^L, & \psi_{i\sigma}^R &\rightarrow (Z_R^{i\sigma})^{1/2} \psi_{i\sigma}^R, \\ g_2 &\rightarrow Z_1^W (Z_2^W)^{-3/2} g_2, & g_1 &\rightarrow Z_1^B (Z_2^B)^{-3/2} g_1, \end{aligned} \tag{2.17}$$

$$\begin{aligned}
 \lambda &\rightarrow Z^\lambda (Z^\varphi)^{-2} \lambda, & \mu^2 &\rightarrow (\mu^2 - \delta\mu^2) (Z^\varphi)^{-1}, \\
 v &\rightarrow (Z^\varphi)^{1/2} (v - \delta v), \\
 g_{i\sigma} &\rightarrow (Z^\varphi)^{-1/2} Z_1^{i\sigma} g_{i\sigma}, \\
 \xi_{1,2}^\alpha &\rightarrow 1 + \delta_{\xi_{1,2}}^\alpha, & u^a &\rightarrow \tilde{Z}^W u^a, & u^B &\rightarrow \tilde{Z}^B u^B, & \bar{u}^\alpha &\rightarrow \bar{u}^\alpha.
 \end{aligned}
 \tag{2.17}$$

These definitions of renormalized fields and parameters induce corresponding expressions for the fields (2.8) i.e. W_μ^\pm, Z_μ, A_μ and the parameters (2.9). Writing

$$Z_i = 1 + \delta Z_i \tag{2.18}$$

we obtain $\mathcal{L} \rightarrow \mathcal{L} + \delta\mathcal{L}$ where the expression for \mathcal{L} in the renormalized quantities is identical with the original one, but now contains the renormalized physical parameters and fields. The quantities $\delta Z_i, \delta v, \delta\mu^2, \delta\xi_i^\alpha$ occur in the counter term Lagrangian $\delta\mathcal{L}$. Their finite parts have to be fixed by the explicit renormalization conditions. Before doing this we study the restrictions which are imposed on the renormalization procedure by the Slavnov-Taylor identities of the theory.

The Feynman rules belonging to \mathcal{L} and the counter terms from $\delta\mathcal{L}$ are listed in app. A.

3. Slavnov-Taylor Identities

3.1 The Becchi-Rouet-Stora transformation

The original gauge invariance of \mathcal{L}_C is lost after the introduction of \mathcal{L}_{fix} and \mathcal{L}_{FP} but the complete Lagrangian \mathcal{L} is invariant under gauge transformations involving also ghost fields $u^\alpha(x)$. In order to discuss this point we use the following condensed notation for the fields and their transformations:

$$\Phi_s = \{W_\mu^a(x), B_\mu(x), \varphi(x), \psi_{i\sigma}^L(x), \psi_{i\sigma}^R(x)\}, \tag{3.1}$$

$$\delta\Phi_s = (\Delta_s^\alpha + g^\alpha T_{st}^\alpha \Phi_t) \delta\theta^\alpha. \tag{3.2}$$

The inhomogeneous term Δ_s^α acts only on the gauge field part of Φ , T^α denotes the representation matrices of the $SU(2) \times U(1)$ generators. The transformation under which \mathcal{L} is invariant — the Becchi-Rouet-Stora transformation [22] — is constructed in such a way that the parameters of the infinitesimal gauge transformation $\delta\theta^\alpha$ contain the ghost fields:

$$\delta\theta^\alpha(x) = u^\alpha(x) \cdot \bar{\lambda}. \tag{3.3}$$

($\bar{\lambda}$ is independent of α and has ghost number -1). Since (3.2) together with (3.3) defines a gauge transformation \mathcal{L}_C is still invariant. The transformation of the ghost fields u^α, \bar{u}^α is defined in such a way that $\mathcal{L}_{\text{fix}} + \mathcal{L}_{FP}$ is also invariant:

$$\delta\bar{u}^\alpha = F^\alpha \cdot \bar{\lambda}, \tag{3.4}$$

$$\delta u^\alpha = -(K^{-1})^{\alpha\beta} \delta K^{\beta\gamma} u^\gamma = -\frac{1}{2} C^{\alpha\beta\gamma} u^\beta u^\gamma \bar{\lambda}, \tag{3.5}$$

where F^α is the linear gauge fixing operator (2.12), K the Faddeev-Popov kernel (2.14) and $C^{\alpha\beta\gamma}$ the structure constant of the gauge group.

3.2 The Slavnov-Taylor identities

The BRS symmetry of \mathcal{L} induces symmetry relations between the Green functions of the theory. They can be derived in a compact form with the help of the path integral formalism. The generating functional W of the Green functions $\tau_{s_1 \dots s_n} = \langle 0 | T \Phi_{s_1} \dots \Phi_{s_n} | 0 \rangle$:

$$\tau_{s_1 \dots s_n} = i^{-n} \left. \frac{\delta^n W}{\delta j_{s_1} \dots \delta j_{s_n}} \right|_{j=0} \tag{3.6}$$

is defined by:

$$W[j, \omega, \bar{\omega}] = \int D\Phi_s D\bar{u} Du \exp \left\{ i \int d^4x [\mathcal{L} + \Phi_s j_s + \bar{u}^a \omega^a + \bar{\omega}^a u^a] \right\}. \tag{3.7}$$

Here we have introduced sources j_s for the fields Φ_s and sources $\omega^a, \bar{\omega}^a$ for the (anti)-ghost fields. From the invariance of $\mathcal{L}, D\Phi_s$ and $D\bar{u} Du$ under BRS transformations one obtains for W the identity:

$$\left\{ i F^\alpha \left[\frac{\delta}{i \delta j} \right] + j_t \left(\Delta_t^\beta + g T_{uv}^\beta \frac{\delta}{i \delta j_{t'}} \right) \frac{\delta^2}{i \delta \omega^a i \delta \bar{\omega}^\beta} \right\} W[j, \omega, \bar{\omega}]|_{\omega=\bar{\omega}=0} = 0. \tag{3.8}$$

From this Slavnov-Taylor identity [23] follow the desired relations between the Green functions τ by taking suitable derivatives with respect to the sources j_s and putting afterwards all $j_s = 0$.

A special class of relations, those which do not directly contain Green functions of ghost fields, results if the gauge fixing operator F^α is applied to eq. (3.8):

$$F^\alpha \left[\frac{1}{i} \frac{\delta}{\delta j} \right] F^\beta \left[\frac{1}{i} \frac{\delta}{\delta j} \right] W[j]|_{j=0} = i \delta^{\alpha\beta} W[0]. \tag{3.9}$$

This equation relates the gauge boson propagators $\Delta_{\mu\nu}^{\alpha\beta}(k)$ to the gauge boson Higgs mixing propagators $\Delta_{\mu}^{\alpha i}(k)$ and the unphysical Higgs propagators $\Delta^{ij}(k)$:

$$\begin{aligned} k^\mu k^\nu \Delta_{\mu\nu}^W(k) + 2M_W k^\mu \Delta_{\mu}^{W\varphi}(k) + M_W^2 \Delta^\varphi(k) &= -i, \\ k^\mu k^\nu \Delta_{\mu\nu}^Z(k) - 2iM_Z k^\mu \Delta_{\mu}^{Z\chi}(k) + M_Z^2 \Delta^\chi(k) &= -i, \\ k^\mu k^\nu \Delta_{\mu\nu}^\gamma(k) &= -i, \\ k^\mu k^\nu \Delta_{\mu\nu}^{\gamma Z}(k) - iM_Z k^\mu \Delta_{\mu}^{\gamma Z}(k) &= 0. \end{aligned} \tag{3.10}$$

In order to get relations between self energies Σ we decompose the gauge field propagators into their transverse and longitudinal parts

$$\Delta_{\mu\nu}^{\alpha\beta}(k) = \left(-g_{\mu\nu} + \frac{k_\mu k_\nu}{k^2} \right) \Delta_T^{\alpha\beta}(k^2) - \frac{k_\mu k_\nu}{k^2} \Delta_L^{\alpha\beta}(k^2), \tag{3.11}$$

make use of the Lorentz covariance of the gauge Higgs mixing propagators

$$\Delta_{\mu}^{\alpha i}(k) = ik_\mu \Delta^{\alpha i}(k^2) = ik_\mu \frac{1}{k^2 - M_\alpha^2} \Sigma^{\alpha i}(k^2) \frac{1}{k^2 - M_i^2}, \tag{3.12}$$

split off the free parts of the propagators

$$\Delta_{T,L}^{\alpha\beta}(k^2) = \frac{i}{k^2 - M_\alpha^2} \left(\delta^{\alpha\beta} - \Sigma_{T,L}^{\alpha\beta}(k^2) \frac{1}{k^2 - M_\beta^2} \right) \tag{3.13}$$

and end with:

$$\begin{aligned}
 k^2(\Sigma_L^W + 2M_W \Sigma^{W\varphi}) - M_W^2 \Sigma^\varphi &= 0, \\
 k^2(\Sigma_L^Z - 2iM_Z \Sigma^{Z\chi}) - M_Z^2 \Sigma^\chi &= 0, \\
 k^2 \Sigma_L^\gamma &= 0, \\
 k^2(\Sigma_L^{\gamma Z} - iM_Z \Sigma^{\gamma\chi}) &= 0.
 \end{aligned}
 \tag{3.14}$$

As a consequence of $U(1)^{\text{em}}$ gauge invariance the longitudinal photon self energy vanishes identically as is the case in pure QED.

By adding the appropriate counter terms (app. A) we arrive at identities for the renormalized self energies $\hat{\Sigma}$:

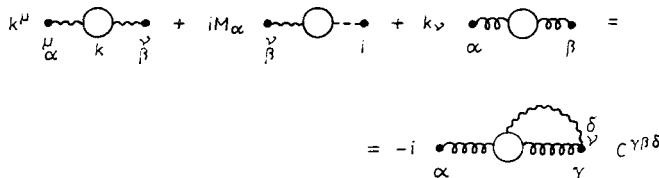
$$\begin{aligned}
 k^2(\hat{\Sigma}_L^W + 2M_W \hat{\Sigma}^{W\varphi}) - M_W^2 \hat{\Sigma}^\varphi &= (k^2 - M_W^2) [k^2(\delta Z_2^W - \delta \xi_1^W) \\
 &\quad - M_W^2(\delta \xi_2^W + \delta Z^\varphi) - \delta M_W^2], \\
 k^2(\hat{\Sigma}_L^Z - 2iM_Z \hat{\Sigma}^{Z\chi}) - M_Z^2 \hat{\Sigma}^\chi &= (k^2 - M_Z^2) [k^2(\delta Z_2^Z - \delta \xi_1^Z) \\
 &\quad - M_Z^2(\delta \xi_2^Z + \delta Z^\varphi) - \delta M_Z^2], \\
 \hat{\Sigma}_L^\gamma &= k^2(\delta Z_2^\gamma - \delta \xi_1^\gamma), \\
 (\hat{\Sigma}_L^{\gamma Z} - iM_Z \hat{\Sigma}^{\gamma\chi}) \\
 &= -k^2(\delta Z_2^{\gamma Z} - \delta \xi_1^{\gamma Z}) + M_Z^2 \left(\delta Z_1^{\gamma Z} - \delta Z_2^{\gamma Z} + \frac{1}{2} \delta \xi_2^{\gamma Z} - \frac{1}{2} \delta \xi_1^{\gamma Z} \right).
 \end{aligned}
 \tag{3.15}$$

As a consequence of these results the number of independent renormalization conditions for the unphysical propagators $\Delta_{\mu\nu}^{\alpha\beta}, \Delta_{\mu\nu}^{\alpha i}, \Delta^{ij}$ is reduced. But eq. (3.15) is compatible with a renormalization where the poles of these propagators are located at $M_W^2, M_Z^2, 0$. This means that the structure which is realized in lowest order in the Feynman gauge can be maintained in all orders by a suitable renormalization of the gauge fixing parameters $\xi_{1,2}^\alpha$.

We do not work out the relations like (3.9) between the ‘‘unphysical’’ parts of higher Green functions since we do not need them for the investigation of the restrictions on the renormalization constants in the unphysical sector.

Let us have a look now at the ghost propagators. Differentiation of eq. (3.8) with respect to the sources of the gauge fields yields:

$$\begin{aligned}
 [k^\mu \Delta_{\mu\nu}^{\alpha\beta}(k) + iM_\alpha \Delta_{\mu\nu}^{\beta i}(k) + k_\nu G^{\alpha\beta}(k)] \delta^{(4)}(k - k') \\
 = -iC^{\gamma\beta\delta} \int d^4q G^{\alpha\gamma,\delta}(k, -k' + q, -q),
 \end{aligned}
 \tag{3.16}$$



Here $G^{\alpha\beta}(k)$ denotes the ghost propagator and $G^{\alpha\beta,\delta} = \langle 0 | (T u^\alpha \bar{u}^\beta W_\nu^\delta) | 0 \rangle$ the gauge field – ghost three point function. Eq. (3.16) is in lowest order the usual relation between the longitudinal part of the gauge field propagator and the ghost propagators, in 1-loop

order it allows to determine the ghost self energies from $\Sigma_L^{\alpha\beta}$, $\Sigma^{\alpha i}$ and the diagram on the r.h.s. An important consequence of eq. (3.16) is that renormalization in the ghost sector can be performed in such a way that the poles of the ghost propagators remain at M_W^2 , M_Z^2 , 0.

The identities (3.16) read in 1-loop order for the self energies:

$$\begin{aligned} \Sigma_L^\gamma(k^2) - \tilde{\Sigma}^\gamma(k^2) &= \frac{\alpha}{4\pi} k^2 B_0(k^2; M_W, M_W), \\ \Sigma_L^{\gamma Z}(k^2) - \tilde{\Sigma}^{\gamma Z}(k^2) &= -\frac{\alpha}{4\pi} \frac{c_W}{s_W} (k^2 - M_Z^2) B_0(k^2; M_W, M_W), \\ \Sigma_L^{Z\gamma}(k^2) - iM_Z \Sigma^{\gamma Z}(k^2) - \tilde{\Sigma}^{\gamma Z}(k^2) &= -\frac{\alpha}{4\pi} \frac{c_W}{s_W} k^2 B_0(k^2; M_W, M_W), \\ \Sigma_L^Z(k^2) - iM_Z \Sigma^Z(k^2) - \tilde{\Sigma}^Z(k^2) &= \frac{\alpha}{4\pi} \frac{c_W^2}{s_W^2} (k^2 - M_Z^2) B_0(k^2; M_W, M_W), \\ \Sigma_L^W(k^2) + M_W \Sigma^{W\varphi}(k^2) - \tilde{\Sigma}^W(k^2) &= \frac{\alpha}{4\pi} (k^2 - M_W^2) \left[\frac{c_W^2}{s_W^2} B_0(k^2; M_W, M_Z) + B_0(k^2; M_W, 0) \right], \end{aligned} \tag{3.17}$$

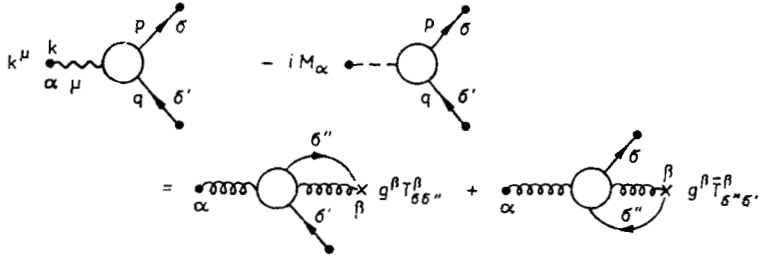
where the singular 1-loop integral B_0 is defined in eq. (5.4). Adding the appropriate counter terms of app. A we obtain the identities for the renormalized self energies:

$$\begin{aligned} \hat{\Sigma}_L^\gamma - \hat{\tilde{\Sigma}}^\gamma &= k^2 \left(\delta Z_2^\gamma - \delta \tilde{Z}^\gamma - \frac{1}{2} \delta \xi_1^\gamma + \frac{\alpha}{4\pi} B_0(k^2; M_W, M_W) \right), \\ \hat{\Sigma}_L^{\gamma Z} - \hat{\tilde{\Sigma}}^{\gamma Z} &= -k^2 \left(\delta Z_2^{\gamma Z} - \delta \tilde{Z}^{\gamma Z} - \frac{1}{2} \delta \xi_1^{\gamma Z} \right) + \frac{1}{2} M_Z^2 (\delta Z_2^{\gamma Z} - 2\delta \tilde{Z}^{\gamma Z}) \\ &\quad + \frac{\alpha}{4\pi} \frac{c_W}{s_W} (k^2 - M_Z^2) B_0(k^2; M_W, M_W), \\ \hat{\Sigma}_L^{\gamma Z} - iM_Z \hat{\Sigma}^{\gamma Z} - \hat{\tilde{\Sigma}}^{\gamma Z} &= -k^2 \left(\delta Z_2^{\gamma Z} - \delta \tilde{Z}^{\gamma Z} - \frac{1}{2} \delta \xi_1^{\gamma Z} \right) \\ &\quad + \frac{1}{2} M_Z^2 (\delta Z_2^{\gamma Z} - \delta \xi_1^{\gamma Z}) - \frac{\alpha}{4\pi} \frac{c_W}{s_W} k^2 B_0(k^2, M_W, M_W), \\ \hat{\Sigma}_L^Z - iM_Z \hat{\Sigma}^Z - \hat{\tilde{\Sigma}}^Z &= (k^2 - M_Z^2) \left(\delta Z_2^Z - \delta \tilde{Z}^Z - \frac{1}{2} \delta \xi_1^Z + \frac{\alpha}{4\pi} \frac{c_W^2}{s_W^2} B_0(k^2; M_W, M_W) \right), \\ \hat{\Sigma}_L^W + M_W \hat{\Sigma}^{W\varphi} - \hat{\tilde{\Sigma}}^W &= (k^2 - M_W^2) \left[\delta Z_2^W - \delta \tilde{Z}^W - \frac{1}{2} \delta \xi_1^W + \frac{\alpha}{4\pi} \left(\frac{c_W^2}{s_W^2} B_0(k^2; M_W, M_Z) \right. \right. \\ &\quad \left. \left. + B_0(k^2; M_W, 0) \right) \right]. \end{aligned} \tag{3.18}$$

$$\tag{3.18'}$$

3.3 Generalized Ward identities

The identities (3.10) and (3.16) relate unphysical parts of Green functions. In analogy to the QED-Ward identity [24] between the $e\bar{e}\gamma$ -vertex and the electron propagator we can derive from eq. (3.8) by differentiating twice with respect to the sources of the fermion fields identities relating fermion vertices to fermion propagators:



$$k^\mu \tau_\mu^{\alpha, \sigma\sigma'}(k, p, q) - iM_\alpha \tau^{\sigma\sigma'}(k, p, q) = iG^{\alpha\beta}(k) [g^\beta T_{\sigma\sigma''}^\beta S_F^{\sigma''\sigma'}(q) + S_F^{\sigma\sigma''}(p) g^\beta \bar{T}_{\sigma''\sigma'}^\beta] + ig^\beta T_{\sigma\sigma''}^\beta \int d^4r G_{\text{con}}^{\alpha\beta\sigma''\sigma'}(k, r - p, r, q) + i \int d^4r G_{\text{con}}^{\alpha\beta, \sigma\sigma''}(k, q - r, p, r) g^\beta \bar{T}_{\sigma''\sigma'}^\beta \quad (3.19)$$

with

$$\bar{T} = -\gamma_0 T^T \gamma_0.$$

The physical content of these identities can be seen by evaluating them in 1-loop approximation and inserting the results (3.17). Neglecting terms of order $\alpha \cdot m_{i\sigma} / (\sqrt{k^2}, M_W, M_Z)$ the following generalizations of the ordinary QED-Ward identity are valid:

$$k^\mu (A_\mu^{\gamma ee}(k, p, q) + A_\mu^{\gamma \nu\nu}(k, p, q)) = e[\Sigma^e(p) - \Sigma^e(q)], \quad (3.20)$$

$$k^\mu (A_\mu^{\gamma uu}(k, p, q) - A_\mu^{\gamma dd}(k, p, q)) = e \left[\frac{2}{3} (\Sigma^u(p) - \Sigma^u(q)) - \frac{1}{3} (\Sigma^d(p) - \Sigma^d(q)) \right]$$

and similar relations for the other fermion generations. The vertex functions $A_\mu^{\alpha\sigma\sigma'}$ are the 1-loop contributions to the amputated 3-point Green functions τ_μ . The fermion self energies $\Sigma^{i\sigma}$ follow from the propagators:

$$iS_F^{-1} = \not{p} - m_{i\sigma} + \Sigma^{i\sigma}(p) = \not{p} - m_{i\sigma} + \not{p} \Sigma_V^{i\sigma} + \not{p} \gamma_5 \Sigma_A^{i\sigma} + m_{i\sigma} \Sigma_S^{i\sigma}. \quad (3.21)$$

As a result the QED identities for each separate charged fermion are replaced by similar identities for the fermion doublets. In addition we have found analogous relations for the vertices of the fermions and the heavy gauge boson Z (written for the first fermion doublet):

$$k^\mu (A_\mu^{Z\nu\nu}(k, p, q) + A_\mu^{Zee}(k, p, q)) = \frac{e}{c_W s_W} \left[\Sigma^\nu(p) \frac{1}{2} \cdot \frac{1 - \gamma_5}{2} - \frac{1}{2} \cdot \frac{1 + \gamma_5}{2} \Sigma^\nu(q) + \Sigma^e(p) \left(-\frac{1}{2} \cdot \frac{1 - \gamma_5}{2} + s_W^2 \right) + \left(\frac{1}{2} \cdot \frac{1 + \gamma_5}{2} - s_W^2 \right) \Sigma^e(q) \right], \quad (3.22)$$

$$\begin{aligned}
 & k^\mu (A_\mu^{Zuu}(k, p, q) - A_\mu^{Zdd}(k, p, q)) \\
 &= \frac{e}{c_W s_W} \left[\Sigma^u(p) \left(\frac{1}{2} \cdot \frac{1 - \gamma_5}{2} - \frac{2}{3} s_W^2 \right) - \left(\frac{1}{2} \cdot \frac{1 + \gamma_5}{2} - \frac{2}{3} s_W^2 \right) \Sigma^u(q) \right. \\
 &\quad \left. + \Sigma^d(p) \left(-\frac{1}{2} \cdot \frac{1 - \gamma_5}{2} + \frac{1}{3} s_W^2 \right) + \left(\frac{1}{2} \cdot \frac{1 + \gamma_5}{2} - \frac{1}{3} s_W^2 \right) \Sigma^d(q) \right].
 \end{aligned}$$

4. Renormalization Conditions in the On-Shell Scheme

The study of the counter terms in the Lagrangian and of the detailed Slavnov-Taylor identities allows us to formulate explicitly the renormalization conditions. Thereby not only the ultraviolet divergencies occurring in the loop expansion are absorbed in the infinite parts of the renormalization constants but also the finite parts are fixed. These lead to physically observable consequences. As already mentioned in the introduction various more or less elaborate renormalizations for the standard model are used in the literature. They differ in the choice of the physical parameters and the prescriptions for the finite parts of the field renormalization constants. Although the results including radiative corrections obtained with different consistent renormalizations formally deviate from each other only on higher order terms it may be that the 1-loop corrections itself calculated with a low energy renormalization scheme and applied to high energy experiments differ from high energy renormalization calculations.

We present a renormalization scheme which is defined by the following conditions³⁾:

- The poles of the renormalized propagators lie at $M_W^2, M_Z^2, 0, M_H^2, m_{i\sigma}^2$. This implies for the renormalized self energies:

$$\hat{\Sigma}_T^W(M_W^2) = \hat{\Sigma}_T^Z(M_Z^2) = \hat{\Sigma}^\eta(M_H^2) = \hat{\Sigma}^{i\sigma}(m_{i\sigma}^2) = 0. \tag{4.1}$$

- According to the residual $U(1)^{em}$ symmetry it is possible to renormalize so that the properties of the photon and the electric charge are defined like in QED:

$$\frac{1}{k^2} \hat{\Sigma}_T^\gamma(k^2)|_{k^2=0} = 0, \quad \hat{\Sigma}_T^{\gamma Z}(0) = 0, \quad \hat{I}_\mu^{\gamma ee}(k^2 = 0, \not{p} = \not{q} = m_e) = ie\gamma_\mu^4. \tag{4.2}$$

- The residues of the propagators of fermions with $I^3 = -1/2$ and of the physical Higgs particle are one:

$$\left(\frac{1}{\not{p} - m_{i-}} \hat{\Sigma}^{-i}(p) \right) \Big|_{\not{p} = m_{i-}} = 0, \quad \left(\frac{\partial}{\partial p^2} \hat{\Sigma}^\eta(p^2) \right) \Big|_{p^2 = M_H^2} = 0. \tag{4.3}$$

- Vanishing tadpole:

$$\hat{T} = 0. \tag{4.4}$$

- The poles in the unphysical sector are at $M_W^2, M_Z^2, 0$:

$$\hat{\Sigma}_L^W(M_W^2) = \hat{\Sigma}_L^Z(M_Z^2) = \hat{\Sigma}^\varphi(M_W^2) = \hat{\Sigma}^\chi(M_Z^2) = \hat{\Sigma}^{\nu\chi}(0) = 0, \tag{4.5}$$

$$\frac{1}{k^2} \hat{\Sigma}_L^\gamma|_{k^2=0} = 0.$$

³⁾ In the following equations only real parts of self energies enter. The imaginary parts are finite by themselves and we define the mass as the real part of the pole position in the propagator.

⁴⁾ This is a condition for the vector part of the photon vertex $\hat{I}_\mu^{\gamma ee}$, only. For the axial vector part no separate condition has to be imposed since $\hat{I}_{\mu,A}^{ee}(k^2 = 0) = 0$ is automatically fulfilled.

- The residue of the photon ghost propagator is one and the photon-ghost Z -ghost mixing propagator vanishes at $k^2 = 0$:

$$\frac{1}{k^2} \hat{\Sigma}^\gamma(k^2)|_{k^2=0}, \quad \hat{\Sigma}^{Z\gamma}(0) = 0. \tag{4.6}$$

The conditions (4.1)–(4.6) fix all the renormalization constants of eq. (2.17).

We have chosen our scheme in such a way that the following properties hold:

- We use as physical renormalized parameters e, M_W, M_Z, M_H, m_f . The question from which processes an optimal determination of the standard model parameters should be performed depends on the experimental accuracy. At present the best choice is the Josephson effect for the determination of α , the $P\bar{P}$ collider experiments and the μ decay for M_W and M_Z (resp. M_W and s_W^2), but with experimental progress this may change. Especially a more accurate measurement of the W, Z masses seems to be very desirable, leaving e.g. μ decay and neutrino scattering as low energy tests for the standard model.
- Eqs. (4.2) characterize our procedure as a natural extension of the QED renormalization. This means in practice that existing results on photonic corrections [18, 19] can be taken over directly. Especially 1-loop calculations can be divided into real and virtual photonic corrections (the sum of their contributions in physical cross sections is infrared finite) and weak corrections (IR finite by themselves). We use $e^2/16\pi^2 = \alpha/4\pi = 1/(4\pi \cdot 137.036)$ as the effective expansion parameter.
- We work with only one field renormalization constant for a symmetry multiplet. Therefore renormalization conserves the gauge transformation properties of the fields and the Green functions. But as a consequence of the use of the minimal number of field renormalization constants not all the residues of the renormalized propagators are one. This is the case for the W, Z and the $I^3 = +1/2$ fermions and wave function renormalization for their in- and outgoing particles is needed. These do not occur in the complete amplitudes for physical S matrix elements.
- In $\mathcal{L}_{\text{fix}} + \mathcal{L}_{FP}$ we have built in the renormalization constants $\delta\xi_{1,2}^\alpha$ and fixed them in such a way that the simple pole structure of the 't Hooft-Feynman gauge survives renormalization. The Slavnov-Taylor identities (3.15) and (3.18) guarantee that with the conditions (4.5) also the poles in the other unphysical propagators $\Delta^{W\varphi}; \dots; G^W; \dots$ are at the same positions. This simplifies considerably the evaluation of Feynman diagrams.
- We have checked that the Ward identities for the fermion gauge boson vertices (3.19) are compatible with our renormalization prescription.

Finally we translate the conditions (4.1)–(4.6) into prescriptions for the singular and finite parts of the renormalization constants (2.17) resp. their combinations (app. A):

$$\begin{aligned} \Sigma_T^W(M_W^2) &= \delta\bar{M}_W^2 = \delta M_W^2 + 2M_W^2 \frac{\delta t}{t} \\ &= M_W^2 \left(-2 \frac{\delta v}{v} + 2\delta Z_1^W - 3\delta Z_2^W + \delta Z^\varphi + 2 \frac{\delta t}{t} \right), \\ \Sigma_T^Z(M_Z^2) &= \delta\bar{M}_Z^2 = \delta M_Z^2 + 2M_Z^2 \frac{\delta t}{t} \\ &= M_Z^2 \left(-2 \frac{\delta v}{v} + 2\delta Z_1^Z - 3\delta Z_2^Z + \delta Z^\varphi + 2 \frac{\delta t}{t} \right), \end{aligned} \tag{4.1'}$$

$$\begin{aligned}\Sigma^{\eta}(M_H^2) &= \delta\bar{M}_H^2 = \delta M_H^2 + 3M_H^2 \frac{\delta t}{t} \\ &= M_H^2 \left(-3 \frac{\delta v}{v} + \frac{3}{2} \delta Z^{\lambda} - \delta Z^{\nu} + 3 \frac{\delta t}{t} \right) + \delta\mu^2,\end{aligned}\tag{4.1'}$$

$$\Sigma_V^{i\sigma}(m_{i\sigma}) + \Sigma_S^{i\sigma}(m_{i\sigma}) = \frac{\delta\bar{m}_{i\sigma}}{m_{i\sigma}} = \frac{\delta m_{i\sigma}}{m_{i\sigma}} + \frac{\delta t}{t} = \delta Z_1^{i\sigma} - \frac{\delta v}{v} + \frac{\delta t}{t};$$

$$\frac{1}{k^2} \Sigma_T^{\gamma}(k^2)|_{k^2=0} = -\delta Z_2^{\gamma},$$

$$\Sigma_{\tau}^{\gamma Z}(0) = -M_Z^2(\delta Z_1^{\gamma Z} - \delta Z_2^{\gamma Z}),\tag{4.2'}$$

$$\frac{\delta e}{e} = \delta Z_1^{\gamma} - \frac{3}{2} \delta Z_2^{\gamma};$$

$$\Sigma_L^e(m_e) + m_e^2(\Sigma_L^{e'}(m_e) + \Sigma_R^{e'}(m_e) + 2\Sigma_s^{e'}(m_e)) = -\delta Z_L^{(e,e)},$$

$$\Sigma_R^e(m_e) + m_e^2(\Sigma_L^{e'}(m_e) + \Sigma_R^{e'}(m_e) + 2\Sigma_s^{e'}(m_e)) = -\delta Z_R^e,\tag{4.3'}$$

$$\Sigma'(M_H^2) = -\delta Z^{\nu};$$

$$\frac{\delta t}{t} = \frac{\delta v}{v} - \frac{\delta\mu^2}{M_H^2} - \frac{1}{2} \delta Z^{\lambda}, \quad t = M_W M_H^2 \cdot \frac{2s_W}{e};\tag{4.4'}$$

$$\Sigma_L^W(M_W^2) = \delta\bar{M}_W^2 + M_W^2 \delta\xi_1^W,$$

$$\Sigma_L^Z(M_Z^2) = \delta\bar{M}_Z^2 + M_Z^2 \delta\xi_1^Z,$$

$$\Sigma^{\nu}(M_W^2) = \delta M_W^2 + M_W^2 \delta\xi_2^W,$$

$$\Sigma^{\lambda}(M_Z^2) = \delta M_Z^2 + M_Z^2 \delta\xi_2^Z,$$

$$\frac{1}{k^2} \Sigma_L^{\gamma}(k^2)|_{k^2=0} = \delta\xi_1^{\gamma} - \delta Z_2^{\gamma},\tag{4.5'}$$

$$\Sigma^{\gamma Z}(0) = -\frac{1}{2} M_Z(\delta\xi_1^{\gamma Z} - \delta\xi_2^{\gamma Z}),$$

$$\frac{1}{k^2} \tilde{\Sigma}^{\gamma}(k^2)|_{k^2=0} = -\delta\tilde{Z}_2^{\gamma} + \frac{1}{2} \delta\xi_1^{\gamma},\tag{4.6'}$$

$$\tilde{\Sigma}^{Z\gamma}(0) = M_Z^2 \left(\delta Z_1^{\gamma Z} - \frac{3}{2} \delta Z_2^{\gamma Z} + \delta\tilde{Z}^{\gamma Z} \right).$$

5. Explicit Results in 1-Loop Approximation

The intention of this section is to provide the building blocks needed to compute radiative electroweak corrections to e^+e^- annihilation, deep inelastic scattering and other processes. We do this by evaluating the explicit 1-loop expressions for the renormalization

constants, renormalized self energies and fermion gauge boson vertices. The calculations are performed analytically, thereby neglecting terms which are of the order of magnitude $\chi m_f^2/(M_w^2, s)$ in the final results. The ultraviolet divergences are treated with the method of dimensional regularization [25]. This is possible since the standard model is free of γ_5 -anomalies. The 4-dimensional integration and the Dirac and tensor structures are replaced by D -dimensional ones:

$$\int \frac{d^4q}{(2\pi)^4} \rightarrow \mu^{4-D} \int \frac{d^Dq}{(2\pi)^D} \tag{5.1}$$

(μ is introduced for dimensional reasons).

In order to explain our notation we give the results for the scalar tadpole integral:

$$\begin{aligned} \text{Diagram} &\rightarrow \mu^{4-D} \int \frac{d^Dq}{(2\pi)^D} \frac{1}{q^2 - M^2 + i\epsilon} = \frac{-i}{16\pi^2} A(M) \\ A(M) &= -M^2(\Delta_M + 1). \end{aligned} \tag{5.2}$$

The UV divergent part Δ_M contains the Euler-Mascheroni constant γ and has the form:

$$\Delta_M = \frac{2}{4 - D} - \gamma - \ln \frac{M^2}{4\pi\mu^2}. \tag{5.3}$$

The scalar 1-loop self energy integral defines the function $B_0(k^2; M_1, M_2)$:

$$\begin{aligned} q + k \text{ Diagram} q &\rightarrow \mu^{4-D} \int \frac{d^Dq}{(2\pi)^D} \frac{1}{(q^2 - M_1^2 + i\epsilon)((q+k)^2 - M_2^2 + i\epsilon)} \\ &= \frac{i}{16\pi^2} B_0(k^2; M_1, M_2) \end{aligned}$$

with:

$$\begin{aligned} B_0(k^2; M_1, M_2) &= \frac{1}{2} \Delta_{M_1} + \frac{1}{2} \Delta_{M_2} + 1 - \frac{M_1^2 + M_2^2}{M_1^2 - M_2^2} \ln \frac{M_1}{M_2} + F(k^2; M_1, M_2) \\ &= \frac{1}{2} \Delta_{M_1} + \frac{1}{2} \Delta_{M_2} \\ &\quad - \int_0^1 dx \ln \frac{x^2 k^2 - x(k^2 + M_1^2 - M_2^2) + M_1^2 - i\epsilon}{M_1 M_2}. \end{aligned} \tag{5.4}$$

The function $F(k^2; M_1, M_2) = F(k^2; M_2, M_1)$ is finite and vanishes for $k^2 = 0$. Its explicit form is written in app. B.1.

5.1 The tadpole

The vacuum expectation value v of the Higgs field, which in lowest order is given by $v^2 = \mu^2/\lambda$ gets 1-loop contributions from the diagrams of fig. 1. They lead in the 't Hooft-

Feynman gauge to the expressions:

$$\begin{aligned}
 T &= \frac{1}{16\pi^2} \frac{e}{s_W} \cdot \frac{1}{2M_W} \left\{ -M_H^2 \left(A(M_W) + \frac{1}{2} A(M_Z) + \frac{3}{2} A(M_H) \right) \right. \\
 &\quad \left. - 6M_W^2 A(M_W) - 4M_W^4 - 3M_Z^2 A(M_Z) - 2M_Z^4 + 4 \sum_{i\sigma} m_{i\sigma}^2 A(m_{i\sigma}) \right\} \\
 &= -\delta t = -\frac{2s_W}{e} M_W M_H^2 \frac{\delta t}{t}.
 \end{aligned}
 \tag{5.5}$$

The tadpole diagrams of fig. 1 give for example contributions to the self energies. These are absorbed by mass renormalization rendering the $\delta\bar{M}_i^2$ gauge independent.

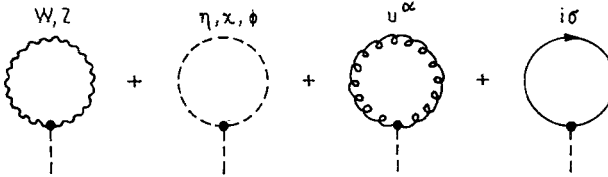


Fig. 1. 1-loop tadpole diagrams

5.2 Unrenormalized self energies and vertex functions

a) Gauge boson self energies

The contributions of the diagrams of fig. 2 to the longitudinal and transverse unrenormalized self energies have been computed by [9]. We present them decomposed into the singular parts (defined to be proportional to Δ) and finite parts:

$$\Sigma(k^2) = \Sigma_{\text{sing}}(k^2, \Delta) + \Sigma_{\text{fin}}(k^2).
 \tag{5.6}$$

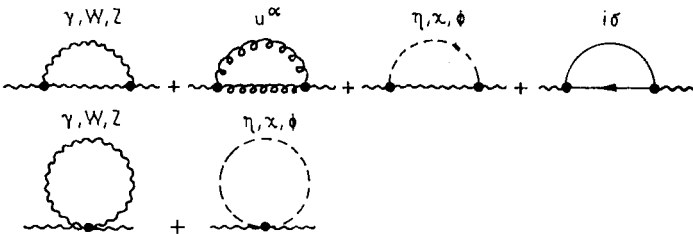


Fig. 2. 1-loop gauge boson self energy diagrams*).

The explicit expressions are (the index f denotes any fermion $i\sigma$; $v_f = v_{i\sigma}$, $a_f = a_{i\sigma}$ are defined in app. A. We also omit in sects. 5 and 6 the index W at s_W , c_W):

$$\begin{aligned}
 \Sigma_{T,\text{sing}}^\gamma &= \frac{\alpha}{4\pi} k^2 \left\{ \frac{4}{3} \sum_f Q_f^2 \Delta_f - 3\Delta_W \right\}, \\
 \Sigma_{T,\text{fin}}^\gamma &= \frac{\alpha}{4\pi} \left\{ \frac{4}{3} \sum_f Q_f^2 \left[(k^2 + 2m_f^2) F(k^2; m_f, m_f) - \frac{k^2}{3} \right] \right. \\
 &\quad \left. - (3k^2 + 4M_W^2) F(k^2; M_W, M_W) \right\},
 \end{aligned}
 \tag{5.7}$$

*) In figs. 2–7 tadpole diagrams are omitted.

$$\Sigma_{T,\text{sing}}^{YZ} = \frac{\alpha}{4\pi} \left\{ -\frac{4}{3} \sum_f Q_f v_f k^2 \Delta_f + \frac{1}{cs} \left[k^2 \left(3c^2 + \frac{1}{6} \right) + 2M_W^2 \right] \Delta_W \right\}, \tag{5.8}$$

$$\Sigma_{T,\text{fin}}^{YZ} = \frac{\alpha}{4\pi} \left\{ -\frac{4}{3} \sum_f Q_f v_f \left[(k^2 + 2m_f^2) F(k^2; m_f, m_f) - \frac{k^2}{3} \right] + \frac{1}{cs} \left[k^2 \left(3c^2 + \frac{1}{6} \right) + M_W^2 \left(4c^2 + \frac{4}{3} \right) \right] F(k^2; M_W, M_W) + \frac{k^2}{9cs} \right\};$$

$$\Sigma_{T,\text{sing}}^Z = \frac{\alpha}{4\pi} \left\{ \frac{4}{3} \sum_f \left[(v_f^2 + a_f^2) k^2 - \frac{3m_f^2}{8c^2 s^2} \right] \Delta_{\bar{f}} + \left[k^2 \left(3 - \frac{19}{6s^2} + \frac{1}{6c^2} \right) + M_Z^2 \left(4 + \frac{1}{c^2} - \frac{1}{s^2} \right) \right] \Delta_W \right\} - 2M_Z^2 \frac{T}{t}, \tag{5.9}$$

$$\begin{aligned} \Sigma_{T,\text{fin}}^Z &= \frac{\alpha}{4\pi} \left\{ \frac{4}{3} \sum_f \left[(v_f^2 + a_f^2) \left((k^2 + 2m_f^2) F(k^2; m_{\bar{f}}, m_{\bar{f}}) - \frac{k^2}{3} \right) - \frac{3}{8c^2 s^2} m_f^2 F(k^2; m_f, m_f) \right] \right. \\ &\quad - \frac{c^2}{3s^2} \left[\frac{2}{3} k^2 + (10k^2 + 20M_W^2) F(k^2; M_W, M_W) \right] \\ &\quad + \frac{1}{3s^2 c^2} \left[3M_W^2 F(k^2; M_W, M_W) + \frac{1}{4} (10M_Z^2 - 2M_H^2 + k^2) \right. \\ &\quad \times \left(1 - \frac{M_H^2 + M_Z^2}{M_H^2 - M_Z^2} \ln \frac{M_H}{M_Z} - \ln \frac{M_H M_Z}{M_W^2} + F(k^2; M_H, M_Z) \right) \\ &\quad - \frac{1}{2} M_H^2 \ln \frac{M_H^2}{M_W^2} - \frac{1}{2} M_Z^2 \ln \frac{M_Z^2}{M_W^2} + \frac{k^2}{6} \\ &\quad \left. + (M_H^2 - M_Z^2)^2 F(k^2; M_Z, M_H) / 4k^2 \right] + \frac{(c^2 - s^2)^2}{3s^2 c^2} \\ &\quad \left. \times \left[\frac{k^2}{6} + \left(2M_W^2 + \frac{k^2}{4} \right) F(k^2; M_W, M_W) \right] \right\}; \end{aligned}$$

$$\Sigma_{T,\text{sing}}^W = \frac{\alpha}{4\pi} \cdot \frac{1}{s^2} \left\{ \frac{1}{6} \sum_i \left[\Delta_{i+} \left(k^2 - \frac{5}{2} m_{i+}^2 - \frac{1}{2} m_{i-}^2 \right) + \Delta_{i-} \left(k^2 - \frac{5}{2} m_{i-}^2 - \frac{1}{2} m_{i+}^2 \right) \right] - \left[M_W^2 \left(1 - \frac{s^2}{c^2} \right) + \frac{19}{6} k^2 \right] \Delta_W \right\} - 2M_W^2 T/t, \tag{5.10}$$

$$\Sigma_{T,\text{fin}}^W = \frac{\alpha}{4\pi} \left\{ \frac{1}{3s^2} \sum_i \left[\left(k^2 - \frac{m_{i+}^2 + m_{i-}^2}{2} \right) \left(1 - \frac{m_{i+}^2 + m_{i-}^2}{m_{i+}^2 - m_{i-}^2} \ln \frac{m_{i+}}{m_{i-}} + F(k^2; m_{i+}, m_{i-}) \right) - \frac{k^2}{3} - \frac{(m_{i+}^2 - m_{i-}^2)^2}{2k^2} F(k^2; m_{i+}, m_{i-}) \right] \right\}$$

⁵⁾ $\bar{f} = f$ for $f \neq \nu_l$ and $\bar{f} = l$ for $f = \nu_l$.

⁶⁾ For lepton doublets with $m_{i+} = 0$ replace $\Delta_{i+} \rightarrow \Delta_{i-}$ and drop the log term in $\Sigma_{T,\text{fin}}^W$.

$$\begin{aligned}
& - \frac{c^2}{3s^2} \left[(7M_Z^2 + 7M_W^2 + 10k^2) \left(1 - \frac{M_Z^2}{M_Z^2 - M_W^2} \ln \frac{M_Z^2}{M_W^2} \right. \right. \\
& \left. \left. + F(k^2; M_Z, M_W) \right) + 4M_Z^2 \ln \frac{M_Z^2}{M_W^2} + \frac{2}{3} k^2 - \frac{2}{k^2} (M_Z^2 - M_W^2)^2 \right. \\
& \left. \times F(k^2; M_Z, M_W) \right] - \frac{4}{3} M_W^2 - \frac{32}{9} k^2 - \frac{1}{3} (4M_W^2 + 10k^2) \\
& \times F(k^2; 0, M_W) + \frac{2}{3} \frac{M_W^4}{k^2} F(k^2; 0, M_W) \\
& + \frac{s^2}{c^2} \left[1 - \frac{M_Z^2}{M_Z^2 - M_W^2} \ln \frac{M_Z^2}{M_W^2} + F(k^2; M_Z, M_W) \right] M_W^2 \\
& + \frac{1}{s^2} \left[1 - \frac{M_H^2}{M_H^2 - M_W^2} \ln \frac{M_H^2}{M_W^2} + F(k^2; M_H, M_W) \right] M_W^2 \\
& + \frac{1}{s^2} \left[\frac{5}{18} k^2 - \frac{1}{3} M_W^2 - \frac{1}{6} M_Z^2 - \frac{1}{6} M_H^2 \right. \\
& \left. + \frac{1}{6} \left(2M_W^2 - \frac{1}{2} k^2 \right) \frac{M_Z^2}{M_Z^2 - M_W^2} \ln \frac{M_Z^2}{M_W^2} \right. \\
& \left. - \frac{1}{6} \left(M_W^2 + M_Z^2 - \frac{k^2}{2} \right) F(k^2; M_Z, M_W) \right. \\
& \left. + (M_Z^2 - M_W^2)^2 F(k^2; M_Z, M_W)/12k^2 \right. \\
& \left. + \frac{1}{6} \left(2M_W^2 - \frac{1}{2} k^2 \right) \frac{M_H^2}{M_H^2 - M_W^2} \ln \frac{M_H^2}{M_W^2} \right. \\
& \left. - \frac{1}{6} \left(M_W^2 + M_H^2 - \frac{k^2}{2} \right) F(k^2; M_H, M_W) \right. \\
& \left. + (M_H^2 - M_W^2)^2 F(k^2; M_H, M_W)/12k^2 \right] \Bigg\};
\end{aligned}$$

$$\Sigma_{L,\text{sing}}^{\gamma} = \Sigma_{L,\text{fin}}^{\gamma} = 0; \quad (5.11)$$

$$\Sigma_{L,\text{sing}}^Z = - \frac{\alpha}{4\pi} \left\{ M_Z^2 \left(2 \frac{c^2}{s^2} - \frac{1}{c^2 s^2} - 2 \right) \Delta_W \right\} - 2M_Z^2 T/t, \quad (5.12)$$

$$\begin{aligned}
\Sigma_{L,\text{fin}}^Z &= \frac{\alpha}{4\pi} \left\{ \frac{1}{c^2 s^2} \left[M_Z^2 - \frac{M_Z^2}{M_H^2 - M_Z^2} \left(M_H^2 \ln \frac{M_H^2}{M_W^2} - M_Z^2 \ln \frac{M_Z^2}{M_W^2} \right) \right. \right. \\
& \left. \left. + \left(M_Z^2 - \frac{(M_H^2 - M_Z^2)^2}{4k^2} \right) F(k^2; M_H, M_Z) \right] \right. \\
& \left. - 2 \frac{c^2 - s^2}{s^2} M_Z^2 F(k^2; M_W, M_W) \right\};
\end{aligned}$$

$$\Sigma_{L,\text{sing}}^{\gamma Z} = \frac{\alpha}{4\pi} \left\{ 2 \frac{c}{s} M_Z^2 \Delta_W \right\}, \quad (5.13)$$

$$\Sigma_{L,\text{fin}}^{\gamma Z} = \frac{\alpha}{4\pi} \left\{ 2 \frac{c}{s} M_Z^2 F(k^2; M_W, M_W) \right\};$$

$$\Sigma_{L,\text{sing}}^W = -\frac{\alpha}{4\pi} \left\{ \frac{c^2 - s^2}{c^2 s^2} M_W^2 \Delta_W \right\} - 2M_W^2 T/t, \tag{5.14}$$

$$\Sigma_{L,\text{fin}}^W = -\frac{\alpha}{4\pi} \left\{ \frac{c^2 - s^2}{c^2 s^2} M_W^2 + \frac{3s^2 - 2}{s^4} M_Z^2 \ln \frac{M_Z^2}{M_W^2} \right.$$

$$+ \frac{1}{s^2} \frac{M_W^2}{M_H^2 - M_W^2} M_H^2 \ln \frac{M_H^2}{M_W^2} + 2 \frac{M_W^4}{k^2} F(k^2; 0, M_W)$$

$$+ \left[\frac{3c^2 - 1}{c^2 s^2} M_W^2 + \left(2 \frac{c^2}{s^2} + \frac{1}{4s^2} \right) \frac{(M_W^2 - M_Z^2)^2}{k^2} \right] F(k^2; M_W, M_Z)$$

$$\left. - \frac{1}{s^2} \left(M_W^2 - \frac{(M_H^2 - M_W^2)^2}{4k^2} \right) F(k^2; M_W, M_H) \right\}.$$

b) Gauge boson Higgs boson mixing

The diagrams of fig. 3 contribute to the gauge boson Higgs boson mixing energies defined in eq. (3.12). Their singular and finite parts are



Fig. 3. Diagrams for gauge boson Higgs boson mixing

$$i\Sigma_{\text{sing}}^{\gamma Z} = \frac{\alpha}{4\pi} \left\{ 2 \frac{c}{s} M_Z \Delta_W \right\}, \tag{5.15}$$

$$i\Sigma_{\text{fin}}^{\gamma Z} = \frac{\alpha}{4\pi} \left\{ 2 \frac{c}{s} M_Z F(k^2; M_W, M_W) \right\};$$

$$i\Sigma_{\text{sing}}^{ZZ} = \frac{\alpha}{4\pi} \left\{ 2 + \frac{1}{2c^2} + \frac{1}{4c^2 s^2} \right\} M_Z \Delta_W - M_Z T/t, \tag{5.16}$$

$$i\Sigma_{\text{fin}}^{ZZ} = \frac{\alpha}{4\pi} M_Z \left\{ \frac{3}{4c^2 s^2} \left[1 - \frac{1}{M_H^2 - M_Z^2} \left(M_H^2 \ln \frac{M_H^2}{M_W^2} - M_Z^2 \ln \frac{M_Z^2}{M_W^2} \right) \right. \right.$$

$$\left. + \left(1 - \frac{(M_Z^2 - M_H^2)^2}{3k^2 M_Z^2} \right) F(k^2; M_H, M_Z) \right] + \frac{4s^2 - 1}{2s^2} F(k^2; M_W, M_W) \right\};$$

$$\Sigma_{\text{sing}}^{W\phi} = \frac{\alpha}{4\pi} M_W \left\{ \frac{1}{2s^2} - \frac{3}{4c^2 s^2} \right\} \Delta_W + M_W T/t, \tag{5.17}$$

$$\Sigma_{\text{fin}}^{W\phi} = \frac{\alpha}{4\pi} M_W \left\{ -\frac{1}{4s^2} - \frac{3}{4c^2 s^2} \right.$$

$$+ \frac{3}{4s^2} \left[1 - \frac{M_H^2}{M_W^2 - M_H^2} \ln \frac{M_H^2}{M_W^2} \right.$$

$$\left. \left. - \left(1 - \frac{(M_H^2 - M_W^2)^2}{3k^2 M_W^2} \right) F(k^2; M_W, M_H) \right] \right\}$$

$$\begin{aligned}
& + \frac{4c^2s^2 + 5c^2 - 3}{4c^2s^2} \left[\frac{M_Z^2}{M_W^2 - M_Z^2} \ln \frac{M_Z^2}{M_W^2} + F(k^2; M_W, M_Z) \right] \\
& - \frac{8c^2 + 1}{4c^2} \frac{M_W^2 - M_Z^2}{k^2} F(k^2; M_W, M_Z) + \left(2 \frac{M_W^2}{k^2} - 1 \right) F(k^2; 0, M_W) \}.
\end{aligned}$$

c) Higgs boson self energies

The self energies of the Higgs bosons are needed to calculate the full set of renormalization constants. The diagrams of fig. 4 give

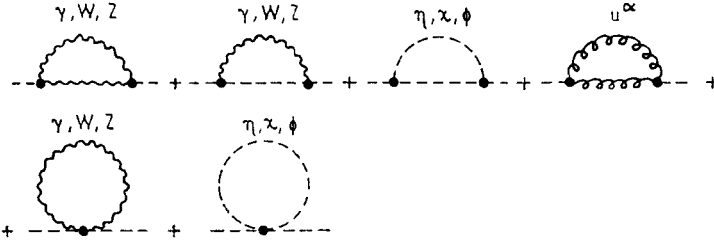


Fig. 4. 1-loop Higgs boson self energy diagrams

$$\begin{aligned}
\Sigma_{\text{sing}}^{\eta} = & -\frac{\alpha}{4\pi} \left\{ \frac{2c^2 + 1}{2c^2s^2} k^2 - \frac{17}{4c^2s^2} M_Z^2 - \frac{17}{2s^2} M_W^2 - \frac{2c^2 + 1}{8c^2s^2} M_H^2 \right. \\
& \left. - \frac{27}{8s^2} \frac{M_H^4}{M_W^2} \right\} \Delta_W - 3M_H^2 T/t,
\end{aligned} \tag{5.18}$$

$$\begin{aligned}
\Sigma_{\text{fin}}^{\eta} = & -\frac{\alpha}{4\pi} \left\{ \frac{7}{4c^2s^2} (M_Z^2 + 2c^2M_W^2) - \frac{2c^2 + 1}{8c^2s^2} M_H^2 - \frac{3}{8s^2} \frac{M_H^4}{M_W^2} \right. \\
& + \frac{1}{4c^2s^2} \left[-2k^2 + 17M_Z^2 + \frac{1}{2} M_H^2 + \frac{M_H^4}{M_Z^2} \right] \ln \frac{M_Z^2}{M_W^2} \\
& + \frac{21}{8s^2} \frac{M_H^4}{M_W^2} \ln \frac{M_H^2}{M_W^2} - \frac{9}{4s^2} \frac{M_H^4}{M_W^2} F(k^2; M_H, M_H) \\
& + \frac{1}{s^2} \left[k^2 - 7M_W^2 - \frac{M_H^4}{2M_W^2} \right] F(k^2; M_W, M_W) \\
& \left. + \frac{1}{2c^2s^2} \left[k^2 - 7M_Z^2 - \frac{M_H^4}{2M_W^2} \right] F(k^2; M_Z, M_Z) \right\};
\end{aligned}$$

$$\Sigma_{\text{sing}}^{\chi} = -\frac{\alpha}{4\pi} \frac{2c^2 + 1}{2c^2s^2} k^2 \Delta_W, \tag{5.19}$$

$$\begin{aligned}
\Sigma_{\text{fin}}^{\chi} = & -\frac{\alpha}{4\pi} \left\{ \frac{1}{2c^2s^2} k^2 \left[1 - \frac{1}{M_H^2 - M_Z^2} \left(M_H^2 \ln \frac{M_H^2}{M_W^2} - M_Z^2 \ln \frac{M_Z^2}{M_W^2} \right) \right. \right. \\
& \left. \left. + \left(1 - \frac{(M_H^2 - M_Z^2)^2}{2k^2 M_Z^2} \right) F(k^2; M_H, M_Z) \right] + \frac{1}{s^2} k^2 F(k^2; M_W, M_W) \right\};
\end{aligned}$$

$$\Sigma_{\text{sing}}^{\varphi} = -\frac{\alpha}{4\pi} \frac{2c^2 + 1}{2c^2s^2} k^2 \Delta_W, \tag{5.20}$$

$$\begin{aligned} \Sigma_{\text{fin}}^{\varphi} = & -\frac{\alpha}{4\pi} \left\{ \frac{2c^2 + 1}{2c^2s^2} k^2 + \frac{1 + c^2 - 4c^2s^2}{2c^2s^2} k^2 \right. \\ & \times \left[\frac{M_Z^2}{M_W^2 - M_Z^2} \ln \frac{M_Z^2}{M_W^2} + F(k^2; M_W, M_Z) \right] \\ & + \frac{k^2 M_H^2}{2s^2(M_W^2 - M_H^2)} \ln \frac{M_H^2}{M_W^2} - \frac{(8c^2 + 1)s^2}{4c^2} M_Z^2 F(k^2; M_W, M_Z) \\ & + \frac{1}{4s^2} \left(2k^2 - \frac{(M_W^2 - M_H^2)^2}{M_W^2} \right) F(k^2; M_W, M_H) \\ & \left. + 2(k^2 - M_W^2) F(k^2; 0, M_W) \right\}. \end{aligned}$$

d) Ghost self energies

The results of the diagrams of fig. 5 for the ghost self energies are:

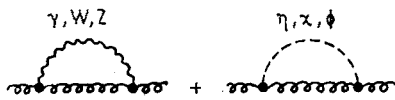


Fig. 5. 1-loop ghost self energy diagrams

$$\tilde{\Sigma}_{\text{sing}}^{\gamma} = -\frac{\alpha}{4\pi} k^2 \Delta_W, \quad \tilde{\Sigma}_{\text{fin}}^{\gamma} = -\frac{\alpha}{4\pi} k^2 F(k^2; M_W, M_W); \tag{5.21}$$

$$\tilde{\Sigma}_{\text{sing}}^{\gamma Z} = \frac{\alpha}{4\pi} \left\{ \frac{c}{s} (k^2 + M_Z^2) \Delta_W \right\}, \tag{5.22}$$

$$\tilde{\Sigma}_{\text{fin}}^{\gamma Z} = \frac{\alpha}{4\pi} \left\{ \frac{c}{s} (k^2 + M_Z^2) F(k^2; M_W, M_W) \right\}; \tag{5.23}$$

$$\tilde{\Sigma}_{\text{sing}}^{\gamma Z} = \frac{\alpha}{4\pi} \left\{ \frac{c}{s} k^2 \Delta_W \right\}, \quad \tilde{\Sigma}_{\text{fin}}^{\gamma Z} = \frac{\alpha}{4\pi} \left\{ \frac{c}{s} k^2 F(k^2; M_W, M_W) \right\};$$

$$\tilde{\Sigma}_{\text{sing}}^Z = -\frac{\alpha}{4\pi} \left\{ \frac{c^2}{s^2} k^2 - \left(1 + \frac{1}{4c^2s^2} - \frac{1}{2s^2} \right) M_Z^2 \right\} \Delta_W - M_Z^2 T/t, \tag{5.24}$$

$$\begin{aligned} \tilde{\Sigma}_{\text{fin}}^Z = & -\frac{\alpha}{4\pi} \left\{ -\frac{M_Z^2}{4c^2s^2} \left[1 - \frac{1}{M_H^2 - M_Z^2} \left(M_H^2 \ln \frac{M_H^2}{M_W^2} - M_Z^2 \ln \frac{M_Z^2}{M_W^2} \right) \right. \right. \\ & \left. \left. + F(k^2; M_H, M_Z) \right] + \frac{c^2}{s^2} \left(k^2 - \frac{2s^2 - 1}{2c^2} M_Z^2 \right) F(k^2; M_W, M_W) \right\}; \end{aligned}$$

$$\tilde{\Sigma}_{\text{sing}}^W = -\frac{\alpha}{4\pi} \left\{ \frac{1}{s^2} k^2 + \frac{2c^2 - 1}{4c^2s^2} M_W^2 \right\} \Delta_W - M_W^2 T/t, \tag{5.25}$$

$$\begin{aligned} \tilde{\Sigma}_{\text{fin}}^W = & -\frac{\alpha}{4\pi} \left\{ \frac{1}{s^2} k^2 + \frac{2c^2 - 1}{4c^2s^2} M_W^2 - \frac{1}{s^2} \left(\frac{c^2}{s^2} k^2 + \frac{3c^2 - 1}{4c^2s^2} M_W^2 \right) \ln \frac{M_Z^2}{M_W^2} \right. \\ & + \frac{1}{4s^2} \frac{M_H^2 M_W^2}{M_H^2 - M_W^2} \ln \frac{M_H^2}{M_W^2} + k^2 F(k^2; M_W, 0) \\ & \left. + \left(\frac{c^2}{s^2} k^2 + \frac{3c^2 - 1}{4c^2s^2} M_W^2 \right) F(k^2; M_W, M_Z) - \frac{1}{4s^2} M_W^2 F(k^2; M_W, M_H) \right\}. \end{aligned}$$

e) Fermion self energies

Because of Lorentz covariance we can decompose the self energies $\Sigma^{i\sigma}(k)$ of the fermions:

$$\Sigma^{i\sigma}(k) = \not{k}\Sigma_V^{i\sigma}(k^2) + \not{k}\gamma_5\Sigma_A^{i\sigma}(k^2) + m_{i\sigma}\Sigma_S^{i\sigma}(k^2). \tag{5.26}$$

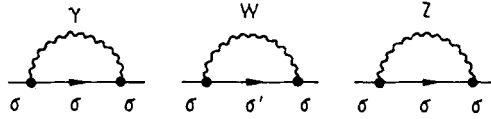


Fig. 6. 1-loop fermion self energy diagrams

The diagrams of fig. 6 give the following contributions to the invariant functions $\Sigma_{V,A,S}^{i\sigma}$:

$$\begin{aligned} \Sigma_V^{i\sigma} = & -\frac{\alpha}{4\pi} \left[Q_{i\sigma}^2 (2B_1(k^2; m_{i\sigma}, \lambda) + 1) + (v_{i\sigma}^2 + a_{i\sigma}^2) (2B_1(k^2; m_{i\sigma}, M_Z) + 1) \right. \\ & \left. + \frac{1}{4s^2} (2B_1(k^2; m_{i\sigma}, M_W) + 1) \right], \end{aligned} \tag{5.27}$$

$$\Sigma_A^{i\sigma} = -\frac{\alpha}{4\pi} \left[2v_{i\sigma}a_{i\sigma} (2B_1(k^2; m_{i\sigma}, M_Z) + 1) - \frac{1}{4s^2} (2B_1(k^2; m_{i\sigma'}, M_W) + 1) \right],$$

$$\Sigma_S^{i\sigma} = -\frac{\alpha}{4\pi} \left[Q_{i\sigma}^2 (4B_0(k^2; m_{i\sigma}, \lambda) - 2) + (v_{i\sigma}^2 - a_{i\sigma}^2) (4B_0(k^2; m_{i\sigma}, M_Z) - 2) \right].$$

The photon contribution was calculated with a small photon mass λ in order to regularize possible infrared divergencies. The functions B_0 and B_1 are defined in eqs. (5.4) and (B.2). Instead of the vector and axial vector parts of the self energies $\Sigma_{V,A}$ it may be more convenient to use the right- and left-handed parts:

$$\Sigma_R = (\Sigma_V + \Sigma_A), \quad \Sigma_L = (\Sigma_V - \Sigma_A). \tag{5.27'}$$

f) Fermion gauge boson vertex functions

The vertex functions⁷⁾ $\Gamma_\mu^{\sigma\sigma'}(k^2, p, q)$ contain for $|k^2| \gg m_{\sigma\sigma'}^2$ and $p^2 = m_\sigma^2, q^2 = m_{\sigma'}^2$, only vector and axial vector parts. The Feynman diagrams of fig. 7 yield (diagrams containing Higgs exchanges can be neglected):

$$\begin{aligned} \Gamma_\mu^{\gamma\sigma\sigma}(k^2) = & -ieQ_\sigma\gamma_\mu \\ & - ieQ_\sigma\gamma'_\mu \frac{\alpha}{4\pi} Q_\sigma^2 \left[\Delta_\sigma - 2 \ln \frac{m_\sigma^2}{\lambda^2} + 4 + \Delta_1(k^2, m_\sigma) \right] \\ & - ieQ_\sigma [(v_\sigma^2 + a_\sigma^2) \gamma_\mu - 2v_\sigma a_\sigma \gamma_\mu \gamma_5] \frac{\alpha}{4\pi} \left[\Delta_Z - \frac{1}{2} + \Delta_2(k^2, M_Z) \right] \\ & - ieQ_{\sigma'} \gamma_\mu (1 - \gamma_5) \frac{\alpha}{4\pi} \frac{1}{4s^2} \left[\Delta_W - \frac{1}{2} + \Delta_2(k^2, M_W) \right] \\ & - ieI_\sigma^3 \gamma_\mu (1 - \gamma_5) \frac{\alpha}{4\pi} \frac{3}{2s^2} \left[\Delta_W - \frac{1}{6} + \Delta_3(k^2, M_W) \right]^8, \end{aligned} \tag{5.28}$$

⁷⁾ In the following we drop the fermion family index i since Cabbibo rotation is not involved.

⁸⁾ In eqs. (5.28, 30) σ' denotes the isospin partner of the fermion σ .

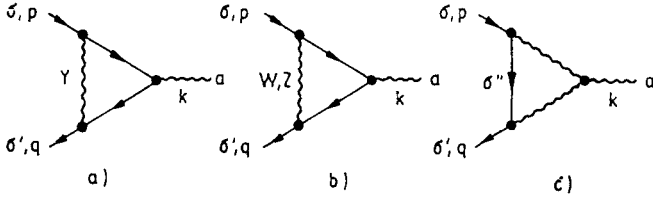


Fig. 7. 1-loop gauge boson fermion vertex diagrams

$$\Gamma_\mu^{\gamma\gamma}(k^2) = ie\gamma_\mu(1 - \gamma_5) \frac{\alpha}{4\pi} \frac{1}{4s^2} \left[\Delta_W - \frac{1}{2} + \Delta_2(k^2, M_W) \right] - ie\gamma_\mu(1 - \gamma_5) \frac{\alpha}{4\pi} \frac{3}{4s^2} \left[\Delta_W - \frac{1}{6} + \Delta_3(k^2, M_W) \right], \quad (5.29)$$

$$\Gamma_\mu^{Z\sigma\sigma}(k^2) = ie\gamma_\mu(v_\sigma^- a_\sigma \gamma_5) + ie\gamma_\mu(v_\sigma^- a_\sigma \gamma_5) \times \frac{\alpha}{4\pi} Q_\sigma^2 \left[\Delta_0 - 2 \ln \frac{m_\sigma^2}{\lambda^2} + 4 + \Delta_1(k^2, m_\sigma) \right] + ie[v_\sigma(v_\sigma^2 + 3a_\sigma^2) \gamma_\mu - a_\sigma(3v_\sigma^2 + a_\sigma^2) \gamma_\mu \gamma_5] \frac{\alpha}{4\pi} \left[\Delta_Z - \frac{1}{2} + \Delta_2(k^2, M_Z) \right] + ie\gamma_\mu(1 - \gamma_5) \frac{\alpha}{4\pi} \frac{v_{\sigma'} + a_{\sigma'}}{4s^2} \left[\Delta_W - \frac{1}{2} + \Delta_2(k^2, M_W) \right] + ieI_\sigma^3 \gamma_\mu(1 - \gamma_5) \frac{\alpha}{4\pi} \frac{3c}{2s^3} \left[\Delta_W - \frac{1}{6} + \Delta_3(k^2, M_W) \right], \quad (5.30)$$

$$\Gamma_\mu^{Z\nu\nu}(k^2) = i \frac{e}{2sc} \gamma_\mu \frac{1 - \gamma_5}{2} \left\{ 1 + \frac{\alpha}{4\pi} \frac{1}{4s^2 c^2} \left[\Delta_Z - \frac{1}{2} + \Delta_2(k^2, M_Z) \right] + \frac{\alpha}{4\pi} \frac{2s^2 - 1}{2s^2} \left[\Delta_W - \frac{1}{2} + \Delta_2(k^2, M_W) \right] + \frac{\alpha}{4\pi} \frac{3c^2}{5^2} \left[\Delta_W - \frac{1}{6} + \Delta_3(k^2, M_W) \right] \right\}, \quad (5.31)$$

$$\Gamma_\mu^{W\bar{e}e}(k^2) = i \frac{e}{\sqrt{2}s} \gamma_\mu \frac{1 - \gamma_5}{2} \left\{ 1 + \frac{\alpha}{4\pi} \frac{2s^2 - 1}{4s^2 c^2} \left[\Delta_Z - \frac{1}{2} + \Delta_2(k^2, M_Z) \right] + \frac{\alpha}{4\pi} \cdot 3 \left[\Delta_W + \frac{5}{6} + \Delta_4^{m_e}(k^2; M_W, 0) \right] + \frac{\alpha}{4\pi} \cdot \frac{3c^2}{s^2} \left[\Delta_W + \frac{5}{6} + \frac{M_Z^2}{M_Z^2 - M_W^2} \ln \frac{M_W^2}{M_Z^2} + \Delta_4(k^2; M_Z, M_W) \right] \right\}, \quad (5.32)$$

$$\Gamma_\mu^{Wdu}(k^2) = \frac{ie}{2\sqrt{2}s} \gamma_\mu(1 - \gamma_5) \cdot \left\{ 1 + \frac{\alpha}{4\pi} Q_u Q_d \left[\Delta_d - 2 \ln \frac{m_d^2}{\lambda^2} + 4 + 3 \ln \frac{m_d}{m_u} + \frac{1}{2} \Delta_1(k^2, m_d) + \frac{1}{2} \Delta_1(k^2, m_u) \right] \right\}$$

$$\begin{aligned}
& + \frac{\alpha}{4\pi} (v_u + a_u) (v_d + a_d) \left[\Delta_Z - \frac{1}{2} + \Lambda_2(k^2, M_Z) \right] \\
& + \frac{\alpha}{4\pi} 3Q_u \left[\Delta_W + \frac{5}{6} + \Lambda_4^{m_u}(k^2; M_W, 0) \right] \\
& - \frac{\alpha}{4\pi} 3Q_d \left[\Delta_W + \frac{5}{6} + \Lambda_4^{m_d}(k^2, M_W, 0) \right] \\
& + \frac{\alpha}{4\pi} \frac{3c^2}{s^2} \left[\Delta_W + \frac{5}{6} + \frac{M_Z^2}{M_Z^2 - M_W^2} \ln \frac{M_W^2}{M_Z^2} + \Lambda_4(k^2; M_Z, M_W) \right] \Big\}.
\end{aligned}$$

The invariant functions $\Lambda_{1,\dots,4}$ together with some of their properties are presented in app. B.3.

For the renormalization of the electric charge we need the γee -vertex at $k^2 = 0$, $p^2 = q^2 = m_e^2$. Its explicit form is:

$$\begin{aligned}
\Gamma_\mu^{\gamma ee}(0) &= ie\gamma_\mu + ie\gamma_\mu \frac{\alpha}{4\pi} \left[\Delta_e - 2 \ln \frac{m_e^2}{\lambda^2} + 4 \right] \\
&+ ie \frac{\alpha}{4\pi} [(v_e^2 + a_e^2) \gamma_\mu - 2v_e a_e \gamma_\mu \gamma_5] \left[\Delta_Z - \frac{1}{2} \right] \\
&+ ie\gamma_\mu \frac{1 - \gamma_5}{2} \frac{\alpha}{4\pi} \frac{3}{2s^2} \left[\Delta_W - \frac{1}{6} \right].
\end{aligned} \tag{5.33}$$

For later use we give also the neutrino-photon vertex at $k^2 = 0$:

$$\Gamma_\mu^{\gamma\nu\nu} = -ie\gamma_\mu \frac{1 - \gamma_5}{2} \frac{\alpha}{4\pi} \frac{1}{s^2} \Delta_W. \tag{5.34}$$

5.3 Renormalization constants

The prescriptions for the calculation of the renormalization constants from the unrenormalized self energies and vertex functions have been defined in eq.s (4.1') to (4.6'). We find for the mass renormalization $\delta\overline{M}_W^2$, $\delta\overline{M}_Z^2$ of the heavy gauge bosons

$$\delta\overline{M}_W^2 = \delta\overline{M}_{W,\text{sing}}^2 + \delta\overline{M}_{W,\text{fin}}^2 = \Sigma_{T,\text{sing}}^W(M_W^2) + \text{Re} \Sigma_{T,\text{fin}}^W(M_W^2), \tag{5.35}$$

$$\delta\overline{M}_Z^2 = \delta\overline{M}_{Z,\text{sing}}^2 + \delta\overline{M}_{Z,\text{fin}}^2 = \Sigma_{T,\text{sing}}^Z(M_Z^2) + \text{Re} \Sigma_{T,\text{fin}}^Z(M_Z^2) \tag{5.36}$$

explicit expressions by using eq.s (5.9) and (5.10). Eq.s (4.1') tell us that with $\delta\overline{M}_W^2$, $\delta\overline{M}_Z^2$ also the following combination of δe , δZ_1^Z , δZ_2^Z is determined:

$$\frac{\delta\overline{M}_Z^2}{M_Z^2} - \frac{\delta\overline{M}_W^2}{M_W^2} = \frac{s^2}{c^2 - s^2} \left(2 \frac{\delta e}{e} - 2\delta Z_1^Z + 3\delta Z_2^Z \right). \tag{5.37}$$

Eq.s (4.2') together with (5.7), (5.8), (5.33) give for the photon field renormalization constant

$$\delta Z_2^\gamma = \frac{\alpha}{4\pi} \left[-\frac{4}{3} \sum_{i\sigma} (Q_{i\sigma}^2 \Lambda_{i\sigma}) + 3\Delta_W + \frac{2}{3} \right], \tag{5.38}$$

a combination of the (γ, Z) renormalization constants

$$\delta Z_{1^{\gamma Z}} - \delta Z_{2^{\gamma Z}} = \frac{sc}{c^2 - s^2} (\delta Z_{1^Z} - \delta Z_{2^Z} - \delta Z_{1^{\gamma}} + \delta Z_{2^{\gamma}}) = -\frac{\alpha}{4\pi} \frac{2c}{s} \Delta_W \quad (5.39)$$

and the charge renormalization

$$\frac{\delta e}{e} = \delta Z_{1^{\gamma}} - \frac{3}{2} \delta Z_{2^{\gamma}} = \frac{\alpha}{4\pi} \left[\frac{2}{3} \sum_{i\sigma} (Q_{i\sigma}^2 \Delta_{i\sigma}) - \frac{7}{2} \Delta_W - \frac{1}{3} \right]. \quad (5.40)$$

A comparison of eq. (5.40) with (5.38) shows that

$$\frac{\delta e}{e} = -\frac{1}{2} \delta Z_{2^{\gamma}} - \frac{\alpha}{4\pi} \cdot 2\Delta_W. \quad (5.41)$$

This means that the familiar QED relation is modified by the non-Abelian couplings of the gauge bosons.

The four eq.s (5.37) to (5.40) allow the separate determination of $\delta Z_{1^{\gamma}}$, $\delta Z_{2^{\gamma}}$, δZ_{1^Z} , δZ_{2^Z} :

$$\begin{aligned} \delta Z_{1^{\gamma}} &= \frac{\alpha}{4\pi} \left[-\frac{4}{3} \sum_{i\sigma} (Q_{i\sigma}^2 \Delta_{i\sigma}) + \Delta_W + \frac{2}{3} \right], \\ \delta Z_{2^{\gamma}} &= \frac{\alpha}{4\pi} \left[-\frac{4}{3} \sum_{i\sigma} (Q_{i\sigma}^2 \Delta_{i\sigma}) + 3\Delta_W + \frac{2}{3} \right], \\ \delta Z_{1^Z} &= \frac{\alpha}{4\pi} \left[-\frac{4}{3} \sum_{i\sigma} (Q_{i\sigma}^2 \Delta_{i\sigma}) + \left(7 - 6 \frac{c^2}{s^2} \right) \Delta_W + \frac{2}{3} \right] \\ &\quad + \frac{c^2 - s^2}{s^2} \left(\frac{\delta M_Z^2}{M_Z^2} - \frac{\delta M_W^2}{M_W^2} \right), \\ \delta Z_{2^Z} &= \frac{\alpha}{4\pi} \left[-\frac{4}{3} \sum_{i\sigma} (Q_{i\sigma}^2 \Delta_{i\sigma}) + \left(7 - 4 \frac{c^2}{s^2} \right) \Delta_W + \frac{2}{3} \right] \\ &\quad + \frac{c^2 - s^2}{s^2} \left(\frac{\delta M_Z^2}{M_Z^2} - \frac{\delta M_W^2}{M_W^2} \right). \end{aligned} \quad (5.42)$$

Together with these constants also δZ_{1^W} , δZ_{2^W} , $\delta Z_{1^{\gamma Z}}$, $\delta Z_{2^{\gamma Z}}$ are determined. Explicit expressions may be obtained with help of eq. (A.1).

The mass and field renormalization of the leptons according to eq.s (4.1') and (4.3') treats the charged, massive leptons and the neutral, massless neutrinos in an unsymmetric way. This is a consequence of spontaneous breaking of $SU(2) \times U(1)$ and of chiral symmetry. As a result the neutrinos remain massless and left-handed after renormalization, whereas the charged leptons suffer mass renormalization:

$$\begin{aligned} \frac{\delta m_{i\sigma}}{m_{i\sigma}} &= \frac{\alpha}{4\pi} \left\{ \frac{1}{4s^2} \left(\Delta_W - \frac{1}{2} \right) + 2(v_{i\sigma}^2 + a_{i\sigma}^2) \left(\Delta_Z - \frac{1}{2} \right) \right. \\ &\quad \left. - 4(v_{i\sigma}^2 - a_{i\sigma}^2) \left(\Delta_Z + \frac{1}{2} \right) - 3 \left(\Delta_{i\sigma} + \frac{4}{3} \right) \right\} = -\frac{\delta v}{v} + \delta Z_{1^{i\sigma}}. \end{aligned} \quad (5.43)$$

The residue of the electron propagator was put equal to one for both the L and R parts. This gives:

$$\begin{aligned} \delta Z_L^{(e,\nu)} &= -\frac{\alpha}{4\pi} \left\{ \Delta_e - 2 \ln \frac{m_e^2}{\lambda^2} + 4 + (v_e + a_e)^2 \left(\Delta_Z - \frac{1}{2} \right) + \frac{1}{2s^2} \left(\Delta_W - \frac{1}{2} \right) \right\}, \\ \delta Z_R^e &= -\frac{\alpha}{4\pi} \left\{ \Delta_e - 2 \ln \frac{m_e^2}{\lambda^2} + 4 + (v_e - a_e)^2 \left(\Delta_Z - \frac{1}{2} \right) \right\}. \end{aligned} \tag{5.44}$$

SAKAKIBARA [12] applies the condition $\text{Res} = 1$ to the ν propagator which consequently does not get an artificial IR singularity. But in this scheme the electronfield is not treated like in QED.

In the case of quarks we have two right-handed singlets associated with one left-handed doublet. The two mass renormalization constants are determined by eq. (5.43). The doublet renormalization constant $\delta Z_L^{(d,u)}$ and the singlet renormalization constant δZ_R^d for the $I_3 = -1/2$ members are fixed as in the lepton case: L and R residues in the d -propagator are put equal to one.

δZ_R^u is determined such that the residues of the L and R parts in the u -propagator are still equal (but $\neq 1$). This yields:

$$\begin{aligned} \delta Z_L^{(d,u)} &= -\frac{\alpha}{4\pi} \left\{ Q_d^2 \left(\Delta_d - 2 \ln \frac{m_d^2}{\lambda^2} + 4 \right) + (v_d + a_d)^2 \left(\Delta_Z - \frac{1}{2} \right) + \frac{1}{2s^2} \left(\Delta_W - \frac{1}{2} \right) \right\}, \\ \delta Z_R^d &= -\frac{\alpha}{4\pi} \left\{ Q_d^2 \left(\Delta_d - 2 \ln \frac{m_d^2}{\lambda^2} + 4 \right) + (v_d - a_d)^2 \left(\Delta_Z - \frac{1}{2} \right) \right\}, \\ \delta Z_R^u &= -\frac{\alpha}{4\pi} \left\{ Q_u^2 \left(\Delta_u - 2 \ln \frac{m_u^2}{\lambda^2} + 4 \right) + (v_u - a_u)^2 \left(\Delta_Z - \frac{1}{2} \right) - \delta(u, d) \right\}, \end{aligned} \tag{5.45}$$

with

$$\delta(u, d) = Q_u^2 \left(\ln \frac{M_Z^2}{m_u^2} - 2 \ln \frac{m_u^2}{\lambda^2} \right) - Q_d^2 \left(\ln \frac{M_Z^2}{m_d^2} - 2 \ln \frac{m_d^2}{\lambda^2} \right) + \frac{3}{2}. \tag{5.46}$$

Since the propagators of the u -type fermions have a residue different from 1 a wave function renormalization factor $1 - \alpha/4\pi \cdot \delta(u, d)/2$ has to be assigned to each external line.

The Higgs mass M_H and the Higgs field are renormalized using the prescriptions (4.1') and (4.3') for δM_H^2 and δZ^H together with the expression (5.18) for the unrenormalized Higgs self energy. This gives:

$$\begin{aligned} \frac{\delta M_H^2}{M_H^2} \Big|_{\text{sing}} &= \frac{\alpha}{4\pi} \Delta_W \left(\frac{3 + 6c^2}{8c^2s^2} - \frac{17}{4c^2s^2} \frac{M_Z^2 + 2c^2M_W^2}{M_H^2} - \frac{27}{8s^2} \frac{M_H^2}{M_W^2} \right), \\ \frac{\delta M_H^2}{M_H^2} \Big|_{\text{fin}} &= \frac{\alpha}{4\pi} \left\{ -\frac{2c^2 + 1}{8c^2s^2} + \frac{7}{4c^2s^2} \frac{M_Z^2 + 2c^2M_W^2}{M_H^2} - \frac{3}{8s^2} \frac{M_H^2}{M_W^2} \right. \\ &\quad \left. + \frac{1}{4c^2s^2} \left(-\frac{3}{2} + 17 \frac{M_Z^2}{M_H^2} + \frac{M_H^2}{M_Z^2} \right) \ln \frac{M_Z^2}{M_W^2} + \frac{21}{8s^2} \frac{M_H^2}{M_W^2} \ln \frac{M_H^2}{M_W^2} \right\}, \end{aligned} \tag{5.47}$$

$$\begin{aligned}
 & + \frac{1}{s^2} \left(1 - 7 \frac{M_W^2}{M_H^2} - \frac{M_H^2}{2M_W^2} \right) \operatorname{Re} F(M_H^2; M_W, M_W) \\
 & + \frac{1}{2c^2s^2} \left(1 - 7 \frac{M_Z^2}{M_H^2} - \frac{M_H^2}{2M_W^2} \right) \operatorname{Re} F(M_H^2; M_Z, M_Z) - \frac{9}{4s^2} \frac{M_H^2}{M_W^2} \Big\}; \\
 \delta Z_{\text{sing}}^\varphi & = \frac{\alpha}{4\pi} \Delta_W \frac{2c^2 + 1}{2c^2s^2},
 \end{aligned} \tag{5.48}$$

$$\begin{aligned}
 \delta Z_{\text{fin}}^\varphi & = -\frac{\alpha}{4\pi} \operatorname{Re} \left\{ \frac{1}{2c^2s^2} \ln \frac{M_Z^2}{M_W^2} - \frac{1}{s^2} F(M_H^2; M_W, M_W) \right. \\
 & - \frac{1}{2c^2s^2} F(M_H^2; M_Z, M_Z) + \frac{1}{s^2} \left(7M_W^2 - M_H^2 + \frac{M_H^4}{2M_W^2} \right) \\
 & \times F'(M_H^2; M_W, M_W) + \frac{1}{2c^2s^2} \left(7M_Z^2 - M_H^2 + \frac{M_H^4}{2M_Z^2} \right) F'(M_H^2; M_Z, M_Z) \\
 & \left. + \frac{9}{4s^2} \frac{M_H^4}{M_W^2} F'(M_H^2; M_H, M_H) \right\}.
 \end{aligned}$$

The renormalization of the gauge fixing parameters ξ follows from eq. (4.5') together with the expressions (5.11–14), (5.19, 20) for the longitudinal parts of the gauge boson self energies and the self energies of the unphysical Higgs fields:

$$\delta \xi_1^\gamma = \delta Z_2^\gamma, \tag{5.49}$$

$$\begin{aligned}
 \delta \xi_1^Z & = -\frac{\alpha}{4\pi} \frac{1}{c^2s^2} \operatorname{Re} \left\{ (2c^2 - 4c^2s^2 - 1) \Delta_W - 1 \right. \\
 & + \frac{1}{M_H^2 - M_Z^2} \left(M_H^2 \ln \frac{M_H^2}{M_W^2} - M_Z^2 \ln \frac{M_Z^2}{M_W^2} \right) \\
 & + 2c^2(c^2 - s^2) F(M_Z^2; M_W, M_W) \\
 & \left. - \left(1 - \frac{(M_H^2 - M_Z^2)^2}{4M_Z^4} F(M_Z^2; M_H, M_Z) \right) - \frac{\delta M_Z^2}{M_Z^2} \right\},
 \end{aligned} \tag{5.50}$$

$$\begin{aligned}
 \delta \xi_1^W & = -\frac{\alpha}{4\pi} \frac{1}{c^2s^2} \operatorname{Re} \left\{ (c^2 - s^2) (\Delta_W + 1) \right. \\
 & + \left(3 - \frac{2}{s^2} \right) \ln \frac{M_Z^2}{M_W^2} + c^2 \frac{M_H^2}{(M_H^2 - M_W^2)} \ln \frac{M_H^2}{M_W^2} \\
 & + 2c^2s^2 F(M_W^2; 0, M_W) + \left(2s^4c^2 + 3c^2 - 1 + \frac{s^4}{4} \right) F(M_W^2; M_W, M_Z) \\
 & \left. + c^2 \left(\frac{(M_H^2 - M_W^2)^2}{4M_W^4} - 1 \right) F(M_W^2; M_W, M_H) \right\} - \frac{\delta M_W^2}{M_W^2},
 \end{aligned} \tag{5.51}$$

$$\delta \xi_2^{\gamma Z} = \frac{cs}{c^2 - s^2} (\delta \xi_1^Z - \delta \xi_1^\gamma) + \frac{\alpha}{4\pi} \cdot 4 \frac{c}{s} \Delta_W,$$

$$\begin{aligned} \delta\xi_2^Z &= -\frac{\alpha}{4\pi} \frac{1}{2c^2s^2} \operatorname{Re} \left\{ (2c^2 + 1) \Delta_W + 1 - \frac{M_H^2}{M_H^2 - M_Z^2} \ln \frac{M_H^2}{M_W^2} \right. \\ &\quad + \frac{M_Z^2}{M_H^2 - M_Z^2} \ln \frac{M_Z^2}{M_W^2} + 2c^2 F(M_Z^2; M_W, M_W) \\ &\quad \left. + \left(1 - \frac{(M_H^2 - M_Z^2)^2}{2M_Z^4} F(M_Z^2; M_H, M_Z) \right) \right\} - \frac{\delta M_Z^2}{M_Z^2}, \end{aligned} \tag{5.52}$$

$$\begin{aligned} \delta\xi_2^W &= -\frac{\alpha}{4\pi} \frac{1}{2c^2s^2} \operatorname{Re} \left\{ (2c^2 + 1) \Delta_W + 2c^2 + 1 + \left(4c^2 - \frac{1 + c^2}{s^2} \right) \ln \frac{M_Z^2}{M_W^2} \right. \\ &\quad + c^2 \frac{M_H^2}{M_W^2 - M_H^2} \ln \frac{M_H^2}{M_W^2} + \frac{1}{2} \left(5 - 9s^2 - \frac{1}{s^2} \right) F(M_W^2; M_W, M_Z) \\ &\quad \left. + c^2 \left(1 - \frac{(M_W^2 - M_H^2)^2}{2M_W^4} \right) F(M_W^2; M_W, M_H) \right\} - \frac{\delta M_W^2}{M_W^2}. \end{aligned} \tag{5.53}$$

Finally we have to renormalize the ghost fields. Eq.s (4.6') and (5.21, 22) give:

$$\delta\tilde{Z}^\gamma = s^2 \delta\tilde{Z}^W + c^2 \delta\tilde{Z}^B = \frac{1}{2} \delta Z_2^\gamma + \frac{\alpha}{4\pi} \Delta_W, \tag{5.54}$$

$$\delta\tilde{Z}^{\gamma Z} = cs(\delta\tilde{Z}^W - \delta\tilde{Z}^B) = -\delta Z_1^{\gamma Z} + \frac{3}{2} \delta Z_2^{\gamma Z} - \frac{\alpha}{4\pi} \frac{c}{s} \Delta_W. \tag{5.55}$$

With these expressions we have determined all the renormalization constants of our renormalization scheme of the standard model. They can be used together with the counterterms to derive the finite renormalized Green functions of the model in 1-loop order. In the next section we present the results for the self energies of the gauge bosons and the fermions as well as the fermion gauge boson vertices and box diagrams.

6. Renormalized Self Energies and Vertex Functions

6.1 Gauge boson self energies

In order to give an impression of the influence of the 1-loop contributions on the magnitude of radiative corrections we present in this section the formulas for the renormalized self energies and vertex functions and numerical results for these quantities. From the expressions (5.7–14) for the unrenormalized self energies and the renormalization constants (5.35–42) together with the prescriptions for the renormalization we obtain for the renormalized transverse parts of the gauge boson self energies the following formulas:

$$\begin{aligned} \hat{\Sigma}_T^\gamma(k^2) &= \Sigma_T^\gamma(k^2) - k^2 \frac{\partial}{\partial k^2} \Sigma_T^\gamma(k^2)|_{k^2=0}, \\ \hat{\Sigma}_T^{\gamma Z}(k^2) &= \Sigma_T^{\gamma Z}(k^2)|_{\text{fin}} \\ &\quad - k^2 \frac{c}{s} \operatorname{Re} \left(\frac{\Sigma_T^Z(M_Z^2)}{M_Z^2} - \frac{\Sigma_T^W(M_W^2)}{M_W^2} + \frac{\alpha}{4\pi} \frac{m_t^2 - m_b^2}{4s^2 M_W^2} \ln \frac{m_t^2}{m_b^2} \right) \Big|_{\text{fin}} \\ &\quad - k^2 \frac{1}{6cs} \delta_q, \end{aligned} \tag{6.1}$$

$$\begin{aligned} \hat{\Sigma}_T^Z(k^2) &= (\Sigma_T^Z(k^2) - \text{Re } \Sigma_T^Z(M_Z^2))|_{\text{fin}} \\ &+ (k^2 - M_Z^2) \left(\frac{\alpha}{6\pi} + \frac{c^2 - s^2}{s^2} \text{Re} \left(\frac{\Sigma_T^Z(M_Z^2)}{M_Z^2} - \frac{\Sigma_T^W(M_W^2)}{M_W^2} \right) \right. \\ &\left. + \frac{\alpha}{4\pi} \frac{m_t^2 - m_b^2}{4s^2 M_W^2} \ln \frac{m_t^2}{m_b^2} \right)|_{\text{fin}} + \frac{1}{3s^2} \delta_q, \\ \hat{\Sigma}_T^W(k^2) &= (\Sigma_T^W(k^2) - \text{Re } \Sigma_T^W(M_W^2))|_{\text{fin}} \\ &+ (k^2 - M_W^2) \left(\frac{\alpha}{6\pi} + \frac{c^2}{s^2} \text{Re} \left(\frac{\Sigma_T^Z(M_Z^2)}{M_Z^2} - \frac{\Sigma_T^W(M_W^2)}{M_W^2} \right) \right. \\ &\left. + \frac{\alpha}{4\pi} \frac{m_t^2 - m_b^2}{4s^2 M_W^2} \ln \frac{m_t^2}{m_b^2} \right)|_{\text{fin}} + \frac{1}{3s^2} \delta_q, \end{aligned}$$

with

$$\delta_q = \frac{\alpha}{4\pi} \left(\ln \frac{m_u^2}{m_d^2} + \ln \frac{m_c^2}{m_s^2} + \ln \frac{m_t^2}{m_b^2} \right).$$

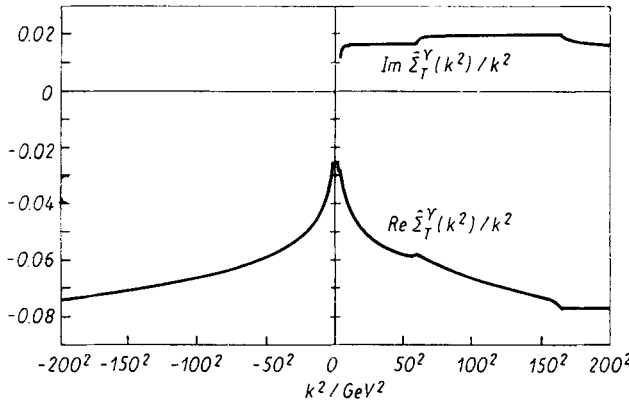


Fig. 8. Real and imaginary parts of the renormalized transverse photon self energy $\hat{\Sigma}_T^\nu(k^2)$. The curve shows $\hat{\Sigma}_T^\nu(k^2)/k^2$

The numerical results in figs. 8–11 for $|k^2| < (200 \text{ GeV})^2$ have been calculated with the following standard set of parameters (if possible taken from [26]):

$$\begin{aligned} \alpha &= (137.036)^{-1}, \\ M_W &= 82 \text{ GeV}, & M_Z &= 93 \text{ GeV}, & M_H &= 100 \text{ GeV}, \\ m_e &= 0.511 \text{ MeV}, & m_\mu &= 105.66 \text{ MeV}, & m_\tau &= 1784 \text{ MeV}, \\ m_u &= 5 \text{ MeV}, & m_d &= 7 \text{ MeV}, & m_s &= 150 \text{ MeV} [27], \\ m_c &= 1.5 \text{ GeV}, & m_b &= 4.5 \text{ GeV}, & m_t &= 30 \text{ GeV}. \end{aligned} \tag{6.2}$$

The real parts of the diagonal self energies $\hat{\Sigma}_T^\nu$, $\hat{\Sigma}_T^Z$, $\hat{\Sigma}_T^W$ are, compared to the free inverse propagators, not small but yield 10% as typical order of magnitude. The contributions to the imaginary parts from the fermion loops are positive but those from the gauge loops are negative. Both the real and imaginary parts of the W and Z self energy

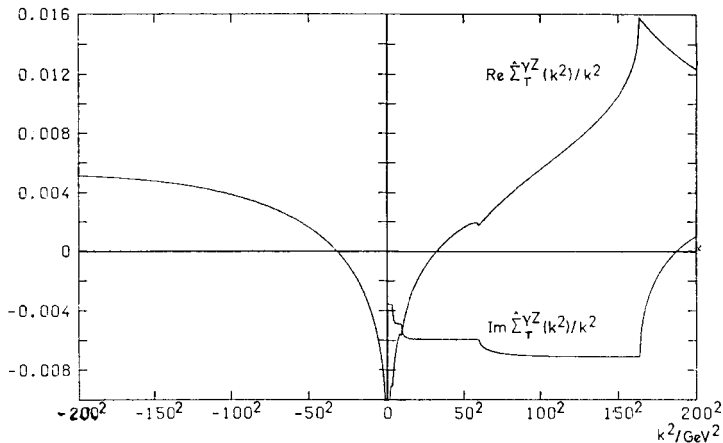


Fig. 9. Photon Z boson mixing. Presented is $\hat{\Sigma}_T^{\gamma Z}(k^2)/k^2$

depend strongly on the energy. The approximation using a constant imaginary part in the vicinity of the resonance leading to the usual Breit-Wigner type form of the modulus square of the propagator is thus not really justified. In fig. 12, 13 we show a comparison between a Breit-Wigner distribution using M_W and $\text{Im } \hat{\Sigma}_T^W(M_W^2)$ resp. M_Z and $\text{Im } \hat{\Sigma}_T^Z(M_Z^2)$ and the corresponding quantities resulting from (6.1). We find for the W and Z FWHM values which are 10% bigger than $\text{Im } \hat{\Sigma}_T(M^2)/M = \Gamma$. This means that for the determination of the width of the W and Z a careful analysis of the experimental distributions is necessary.

In the case of the W self energy we have contributions of loops containing photons. The physical channel $W \rightarrow W + \gamma$ has its threshold at $k^2 = M_W^2$. Consequently we observe in fig. 11 the peak in the real part and the structure in the imaginary part. The magnitudes of these effects depend on the details of the $WW\gamma$ coupling. In a model

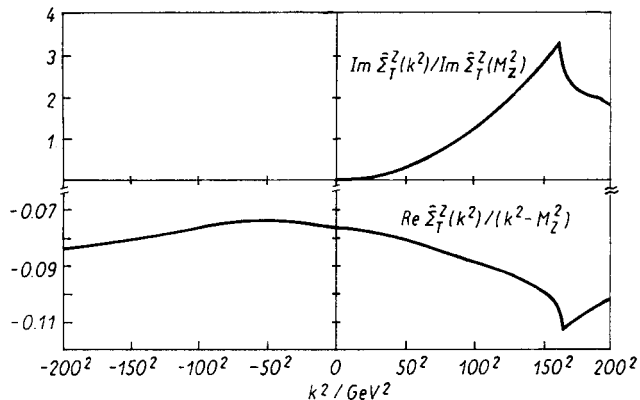


Fig. 10

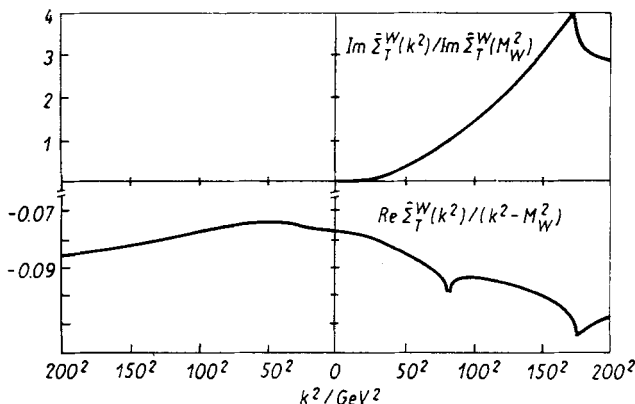


Fig. 11

Fig. 10, 11. Renormalized W, Z self energy. The curves are $\text{Re } \hat{\Sigma}_T^{W,Z}(k^2)/(k^2 - M_{W,Z}^2)$ and $\text{Im } \hat{\Sigma}_T^{W,Z}(k^2)/\text{Im } \Sigma_T^{W,Z}(M_{W,Z}^2)$ (Read $-0.06, -0.08, -0.10$ instead of $-0.07, -0.09, -0.11$, resp.)

where the W is coupled to the photon in the form of a minimal substitution it would be different from that of the standard model.

The diagonal gauge boson self energies are very large compared to α/π and therefore will give the main contributions besides bremsstrahlung to the radiative corrections in e^+e^- annihilation. Compared to these the γZ mixing is much smaller and in our renormalization scheme typically of the order of magnitude of 1%. In our scheme we do not use the weak mixing angle θ_w as a fundamental parameter but as a short hand for $\sin^2 \theta_w = (1 - M_W^2/M_Z^2)$. The results shown in fig. 9 might be interpreted as contributions to an effective running i.e. energy depending mixing angle.

The residue of the renormalized Z propagator is different from 1. We obtain:

$$\frac{\partial}{\partial k^2} \hat{\Sigma}_T^Z(k^2)|_{k^2=M_Z^2} = -0.080 + i 0.029. \tag{6.3}$$

For comparison with other renormalization schemes we present also $\hat{\Sigma}_T^W(0)$ and $\hat{\Sigma}_T^Z(0)$:

$$\begin{aligned} \frac{\partial}{\partial k^2} \hat{\Sigma}_T^{\gamma Z}(k^2)|_{k^2=0} &= \Pi^{\gamma Z}(0) = -0.021 \\ \hat{\Sigma}_T^W(0)/M_W^2 &= -\Pi^W(0) = 0.069, \quad \hat{\Sigma}_T^Z(0)/M_Z^2 = -\Pi^Z(0) = 0.069. \end{aligned} \tag{6.4}$$

These values enter into the calculation of radiative corrections to low energy processes.

The parameters (6.2) which we used for the numerical discussion of the self energies are only partly known from experiment. The W and Z masses have been chosen in agreement with the $P\bar{P}$ -collider results [1] but since they still have rather large errors we have investigated the dependence of the self energies on the masses M_W, M_Z of the gauge bosons. We find that it is determined mainly through the ratio M_W/M_Z . Therefore we present as an example in Figs 14 and 15 $\Pi^W(0), \Pi^{\gamma Z}(0)$ as functions of $s_w^2 = 1 - M_W^2/M_Z^2$ and M_W .

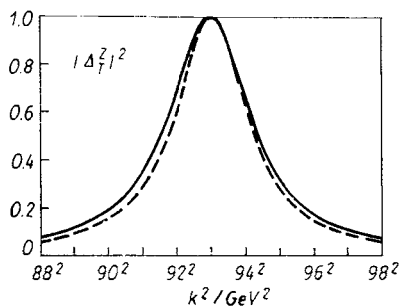
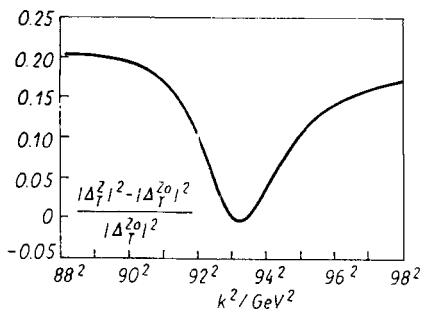


Fig. 12

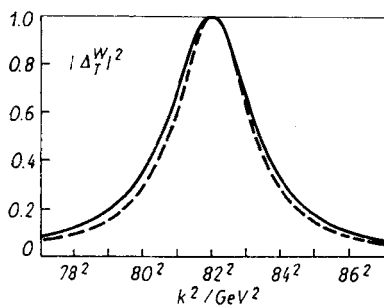
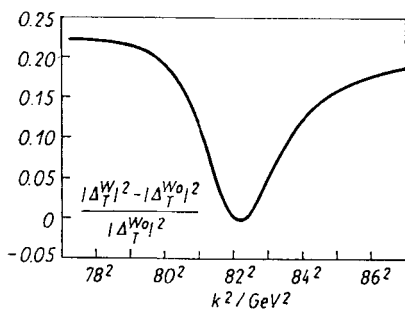


Fig. 13

Fig. 12, 13. Comparison between a Breit-Wigner distribution with $M_{W,Z}$ and $\text{Im} \hat{\Sigma}_T^{W,Z} \times (M_{W,Z}^2)$ as parameters (-----) and the square of the modulus of the renormalized W, Z propagators (—)

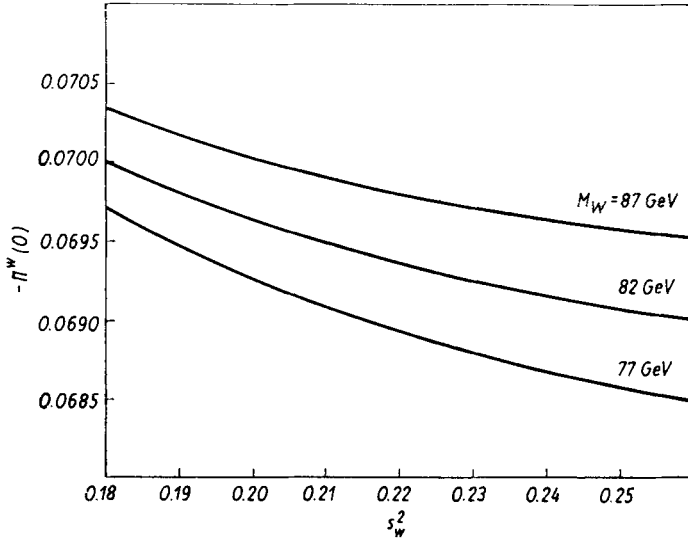


Fig. 14. The W self energy $-\Pi^W(0) = \hat{\Sigma}_T^W(0)/M_W^2$ as function of s_W^2, M_W for the standard set of parameters (6.2)

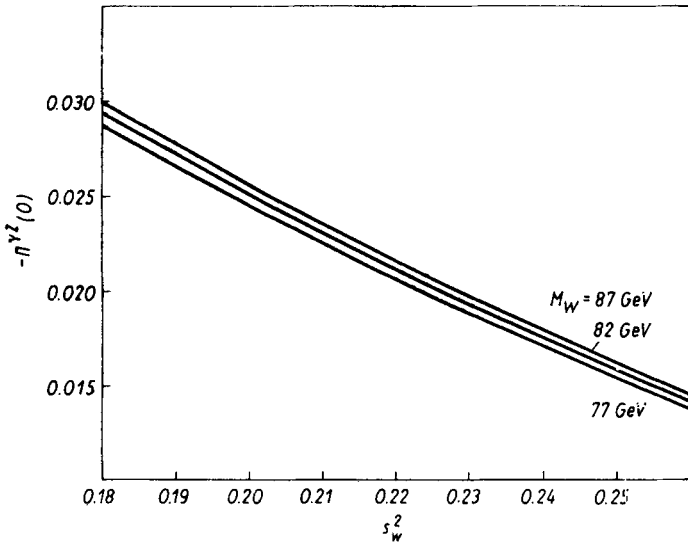


Fig. 15. The γZ mixing $\Pi^{\gamma Z}(0)$ as function of s_W^2, M_W (other parameters like in fig. 14)

The masses for the u, d, s quarks used above correspond to the values obtained by GASSER and LEUTWYLER [27]. The evaluation of the hadronic contribution to the photon self energy using quark loops with these values of the quark masses leads to energies between 10 and 100 GeV to numerical results which are in agreement with a determination [28] of these contribution using dispersion theory and experimental data from e^+e^- -annihilation. However, since the quark masses are not known very precisely and since in

the literature calculations of radiative corrections using much bigger values for these masses can be found, we have studied the dependence of Π^W , $\Pi^{\nu Z}$, Π^Z on $m_i = \{m_u, m_d, m_s\}$. Defining $\delta_q \Pi = \Pi(m_{i_1}) - \Pi(m_{i_2})$ we find :

$$\delta_q \Pi^W = \delta_q \Pi^Z = -\frac{2\alpha}{\pi} \sum_i Q_i^2 \ln \frac{m_{i_1}}{m_{i_2}}, \tag{6.5}$$

$$\delta_q \Pi^{\nu Z} = \frac{\alpha}{4\pi c_W s_W} \sum_i Q_i (I_i^3 - 2Q_i) \ln \frac{m_{i_1}}{m_{i_2}}.$$

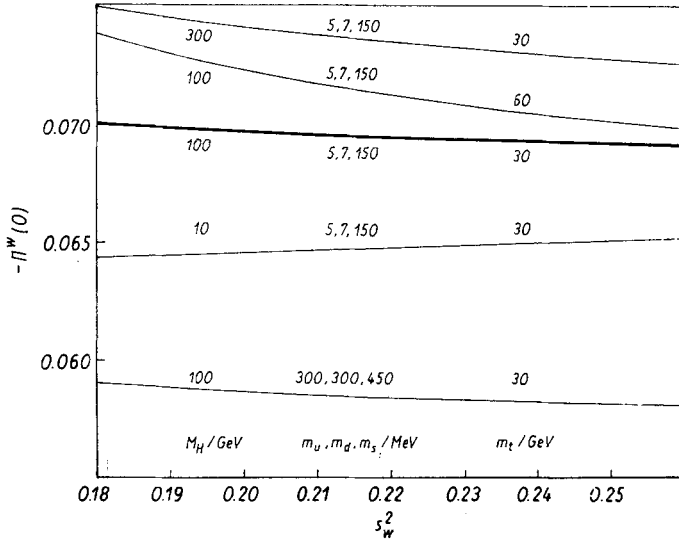


Fig. 16 a

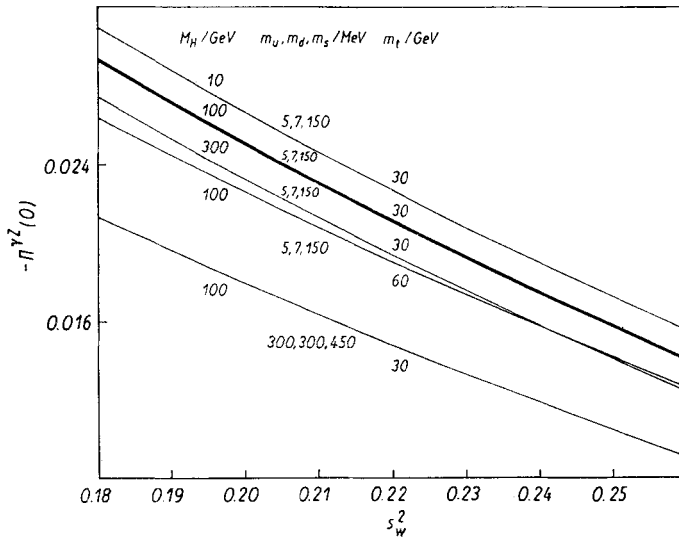


Fig. 16 b

Fig. 16 a, b. $\Pi^W(0)$ (a), $\Pi^{\nu Z}(0)$ (b), as functions of s_W^2 with $M_W = 82$ GeV fixed. Shown are the variations with the Higgs mass, top quark mass and the masses of the light quarks

The extreme choice $m_u = m_d = 300$ MeV, $m_s = 450$ MeV leads to the curve for $\Pi^W(0)$, $\Pi^Z(0)$ shown in fig. 16a, b. $|\Pi^W(0)|$ is lowered by $\simeq 0.011$. In figs. 16a, b we present also the variation of $\Pi^W(0)$ and $\Pi^Z(0)$ with the mass of the top quark. A change from $m_t = 30$ GeV to e.g. $m_t = 60$ GeV increases $|\Pi^W(0)|$ for $s_W^2 = 0.221$ by 0.002.

Finally we do not know the Higgs mass M_H . Therefore we have displayed $\Pi^W(0)$, $\Pi^Z(0)$ also for $M_H = 10$ GeV and $M_H = 300$ GeV in figs. 16. A light Higgs mass decreases $|\Pi^W(0)|$, a heavy one increases it. The conclusion of this discussion is that our ignorance of the mass parameters give uncertainties in the calculation of Π^W , Π^Z and the other self energies amounting to ± 0.01 which might be of the same order of magnitude as 2-loop effects.

6.2 Fermion self energies

We described the renormalization prescription for the lepton and quark self energies in sect. 5.3. Together with the unrenormalized expressions (5.27) and the renormalization constants (5.43–46) we obtain the renormalized self energies from the equations:

$$\begin{aligned} \hat{\Sigma}^{i\sigma}(k) = & \not{k} \frac{1 - \gamma_5}{2} (\Sigma_L^{i\sigma}(k^2) + \delta Z_L^i) + \not{k} \frac{1 + \gamma_5}{2} (\Sigma_R^{i\sigma}(k) + \delta Z_R^{i\sigma}) \\ & + m_{i\sigma} \Sigma_S^{i\sigma}(k^2) - m_{i\sigma} (\delta Z_R^{i\sigma} + \delta Z_L^i) / 2 - \delta m_{i\sigma}. \end{aligned} \tag{6.6}$$

We illustrate the results with help of the ν_e self energy and the electron self energy. The corresponding invariant functions are shown in figs. 17 and 18. For the neutrinos only left-handed contributions exist. They are in our renormalization scheme infrared divergent. Therefore in fig. 17 the IR finite quantity $\hat{\Sigma}_L^{\nu}(p^2) - \hat{\Sigma}_L^{\nu}(0)$ is drawn for time-like momenta p^2 . It depends only weakly on p^2 .

The real and imaginary parts of the invariant functions $\hat{\Sigma}_V^e$, $\hat{\Sigma}_A^e$, $\hat{\Sigma}_S^e$ of the electron self energy are presented in figs. 18. In the case of $\text{Re } \hat{\Sigma}_V^e$ and $\text{Re } \hat{\Sigma}_S^e$ we have subtracted the IR divergent part $\alpha/4\pi (2 \ln(m_e^2/\lambda^2) - 4)$. We find that $\hat{\Sigma}_A$ and $\hat{\Sigma}_V$ are small, only $\text{Re } \hat{\Sigma}_S^e(p^2)$ reaches a level of several percent.

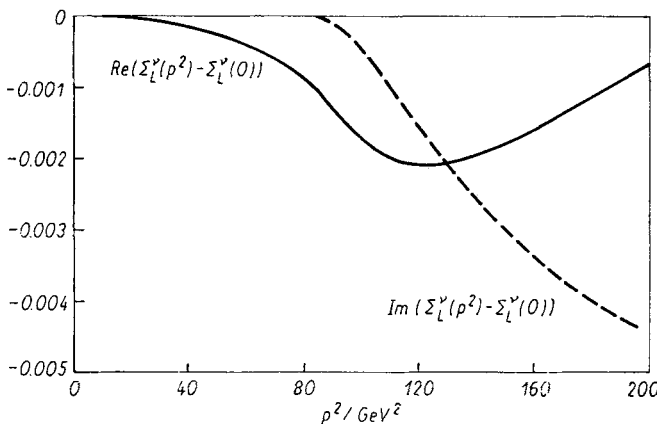


Fig. 17. Real (—) and imaginary (---) parts of the neutrino self energy subtracted at $p^2 = 0$ (Read 40², 80², ... instead of 40, 80, ... resp.)

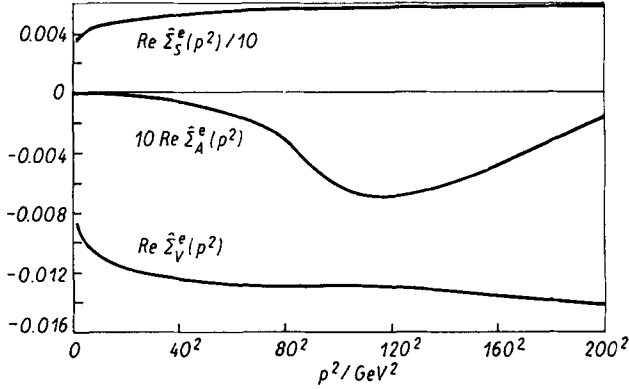


Fig. 18 a

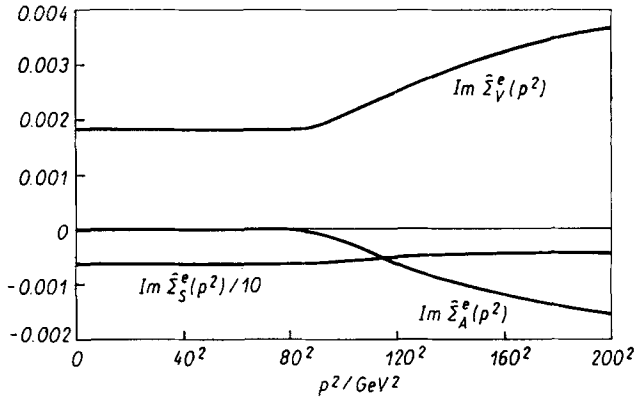


Fig. 18 b

Fig. 18 a, b. Real (a) and imaginary (b) parts of the electron self energy. Presented are the infrared finite parts of the invariant functions $\hat{\Sigma}_S^e$, $\hat{\Sigma}_A^e$, $\hat{\Sigma}_V^e$

6.3 Renormalized gauge boson fermion vertices

The following list of the renormalized vertex functions contains vector and axial vector couplings only and is valid for on shell fermions and $|k^2| \gg m_f^2$. As in sect. 5.2 we write down the formulas only for the first lepton and quark multiplet.

a) Electromagnetic current :

$$\begin{aligned}
 \hat{\Gamma}_\mu^{\gamma ee}(k^2) &= ie\gamma_\mu(F_V\gamma^e - \gamma_5 F\gamma^e), \\
 \hat{\Gamma}_\mu^{\gamma rr}(k^2) &= ie\gamma_\mu(1 - \gamma_5) F\gamma^r, \\
 \hat{\Gamma}_\mu^{\gamma dd}(k^2) &= -ieQ_d\gamma_\mu(F_V\gamma^d - \gamma_5 F_A\gamma^d), \\
 \hat{\Gamma}_\mu^{\gamma uu}(k^2) &= -ieQ_u\gamma_\mu(F_V\gamma^u - \gamma_5 F\gamma^u).
 \end{aligned} \tag{6.7}$$

The form factors contain the functions A_1, \dots, A_4 given in Appendix B.3 :

$$F_{1,\gamma^e} = 1 + \frac{\alpha}{4\pi} \left[A_1(k^2, m_e) + (v_e^2 + a_e^2) A_2(k^2, M_Z) + \frac{3}{4s^2} A_3(k^2, M_W) \right],$$

$$F_{A^{\prime e}} = \frac{\alpha}{4\pi} \left[2v_e a_e A_2(k^2, M_Z) + \frac{3}{4s^2} A_3(k^2, M_W) \right], \quad (6.8)$$

$$F^{rv} = \frac{\alpha}{4\pi} \frac{1}{4s^2} [A_2(k^2, M_W) - 3A_3(k^2, M_W)];$$

$$F_{V^{\prime d}} = 1 + \frac{\alpha}{4\pi} \left[Q_d^2 A_1(k^2, m_d) + (v_d^2 + a_d^2) A_2(k^2, M_Z) - \frac{1}{2s^2} A_2(k^2, M_W) + \frac{9}{4s^2} A_3(k^2, M_W) \right],$$

$$F_{A^{\prime d}} = \frac{\alpha}{4\pi} \left[2v_d a_d A_2(k^2, M_Z) - \frac{1}{2s^2} A_2(k^2, M_W) + \frac{9}{4s^2} A_3(k^2, M_W) \right], \quad (6.9)$$

$$F_{V^{\prime u}} = 1 + \frac{\alpha}{4\pi} \left[Q_u^2 A_1(k^2, m_u) + (v_u^2 + a_u^2) A_2(k^2, M_Z) - \frac{1}{8s^2} A_2(k^2, M_W) + \frac{9}{8s^2} A_3(k^2, M_W) + \delta(u, d) \right]^9,$$

$$F_{A^{\prime u}} = \frac{\alpha}{4\pi} \left[2v_u a_u A_2(k^2, M_Z) - \frac{1}{8s^2} A_2(k^2, M_W) + \frac{9}{8s^2} A_3(k^2, M_W) \right].$$

b) Weak neutral current:

$$\begin{aligned} \hat{F}_\mu^{zee}(k^2) &= ie\gamma_\mu(F_V^{ze} - \gamma_5 F_A^{ze}), \\ \hat{F}_\mu^{z\nu\nu}(k^2) &= ie\gamma_\mu(1 - \gamma_5) F^{z\nu}, \\ \hat{F}_\mu^{z\bar{d}d}(k^2) &= ie\gamma_\mu(F_V^{zd} - \gamma_5 F_A^{zd}), \\ \hat{F}_\mu^{z\bar{u}u}(k^2) &= ie\gamma_\mu(F_V^{zu} - \gamma_5 F_A^{zu}) \end{aligned} \quad (6.10)$$

with the form factors:

$$\begin{aligned} F_V^{ze} &= v_e + \frac{\alpha}{4\pi} \left[v_e A_1(k^2, m_e) + v_e(v_e^2 + 3a_e^2) A_2(k^2, M_Z) + \frac{1}{8s^2 c} A_2(k^2, M_W) - \frac{3c}{4s^3} A_3(k^2, M_W) \right], \\ F_A^{ze} &= a_e + \frac{\alpha}{4\pi} \left[a_e A_1(k^2, m_e) + a_e(3v_e^2 + a_e^2) A_2(k^2, M_Z) + \frac{1}{8s^2 c} A_2(k^2, M_W) - \frac{3c}{4s^3} A_3(k^2, M_W) \right], \\ F^{z\nu} &= \frac{1}{4sc} \left\{ 1 + \frac{\alpha}{4\pi} \left[-\ln \frac{M_Z^2}{m_e^2} - \frac{9}{2} + 2 \ln \frac{m_e^2}{\lambda^2} + \frac{1}{4s^2 c^2} A_2(k^2, M_Z) + \frac{2s^2 - 1}{2s^2} A_2(k^2, M_W) + \frac{3c^2}{s^2} A_3(k^2, M_W) \right] \right\}; \end{aligned} \quad (6.11)$$

⁹⁾ $\delta(u, d)$ is defined in eq. (5.46).

$$\begin{aligned}
F_V^{zd} &= v_d + \frac{\alpha}{4\pi} \left[v_d Q_d^2 A_1(k^2, m_d) + v_d(v_d^2 + 3a_d^2) A_2(k^2, M_Z) \right. \\
&\quad \left. + \frac{1 - 2Q_u s^2}{8s^3 c} A_2(k^2, M_W) - \frac{3c}{4s^3} A_3(k^2, M_W) \right], \\
F_A^{zd} &= a_d + \frac{\alpha}{4\pi} \left[a_d Q_d^2 A_1(k^2, m_d) + a_d(3v_d^2 + a_d^2) A_2(k^2, M_Z) \right. \\
&\quad \left. + \frac{1 - 2Q_u s^2}{8s^3 c} A_2(k^2, M_W) - \frac{3c}{4s^3} A_3(k^2, M_W) \right], \\
F_V^{zu} &= v_u + \frac{\alpha}{4\pi} \left[v_u Q_u^2 A_1(k^2, m_u) + v_u(v_u^2 + 3a_u^2) A_2(k^2, M_Z) + v_u \delta(u, d) \right. \\
&\quad \left. - \frac{1 + 2Q_d s^2}{8s^3 c} A_2(k^2, M_W) + \frac{3c}{4s^3} A_3(k^2, M_W) \right], \\
F_A^{zu} &= a_u + \frac{\alpha}{4\pi} \left[a_u Q_u^2 A_1(k^2, m_u) + a_u(3v_u^2 + a_u^2) A_2(k^2, M_Z) + a_u \delta(u, d) \right. \\
&\quad \left. - \frac{1 + 2Q_d s^2}{8s^3 c} A_2(k^2, M_W) + \frac{3c}{4s^3} A_3(k^2, M_W) \right].
\end{aligned} \tag{6.12}$$

c) Weak charged current:

$$\begin{aligned}
\hat{F}_\mu^{W_{e\nu}}(k^2) &= i \frac{e}{2\sqrt{2}s} \gamma_\mu (1 - \gamma_5) F^{W_{e\nu}}, \\
\hat{F}_\mu^{W_{du}}(k^2) &= i \frac{e}{2\sqrt{2}s} \gamma_\mu (1 - \gamma_5) F^{W_{du}},
\end{aligned} \tag{6.13}$$

with the formfactors

$$\begin{aligned}
F^{W_{e\nu}} &= 1 + \frac{\alpha}{4\pi} \left\{ \frac{3(3c^2 - 1)}{2s^2} + \ln \frac{m_e^2}{M_W^2} + 2 \ln \frac{m_e^2}{\lambda^2} + \left(\frac{2s^2 - 1}{2s^2} + \frac{3c^2}{s^4} \right) \ln \frac{M_W^2}{M_Z^2} \right. \\
&\quad \left. + \frac{2s^2 - 1}{4s^2 c^2} A_2(k^2, M_Z) + 3A_4^{m_e}(k^2; M_W, 0) + \frac{3c^2}{s^2} A_4(k^2; M_Z, M_W) \right\}, \\
F^{W_{du}} &= 1 + \frac{\alpha}{4\pi} \left\{ Q_u Q_d \left[3 \ln \frac{m_d}{m_u} + \frac{1}{2} A_1(k^2, m_d) + \frac{1}{2} A_1(k^2, m_u) \right. \right. \\
&\quad \left. \left. + \frac{s^2}{c^2} A_2(k^2, M_Z) \right] + \frac{2s^2 - 1}{4s^2 c^2} A_2(k^2, M_Z) + 3Q_u A_4^{m_u}(k^2, M_W, 0) \right. \\
&\quad \left. - 3Q_d A_4^{m_d}(k^2, M_W, 0) + \frac{3c^2}{s^2} A_4(k^2, M_Z, M_W) \right. \\
&\quad \left. - \frac{1}{3} \left(\ln \frac{M_Z^2}{m_d^2} - 2 \ln \frac{m_d^2}{\lambda^2} + \frac{9}{2} \right) + \frac{3}{s^2} + \left(\frac{1}{2s^2} - \frac{3c^2}{s^4} \right) \ln \frac{M_Z^2}{M_W^2} \right\}.
\end{aligned} \tag{6.14}$$

d) Examples: The electron and ν photon formfactors, the electron Z boson formfactor, the $W_{\nu\nu}$ -formfactor

For illustration we present the weak contributions (the parts with $A_{2,3}$ in eq.s (6.7–13)) to the vector and axialvector photonic formfactor of the electron in fig. 19 for $|k^2| \leq (150 \text{ GeV})^2$. The vector part $F_{V,\text{weak}}^{\gamma e}$ vanishes at $k^2 = 0$ as a consequence of charge renormalization, the axial vector part $F_{A,\text{weak}}^{\gamma e}(0) = 0$ because of the Ward identity. For the k^2 values given above the real and imaginary parts of these formfactors are typically of the order of magnitude if $10^{-3}e$.

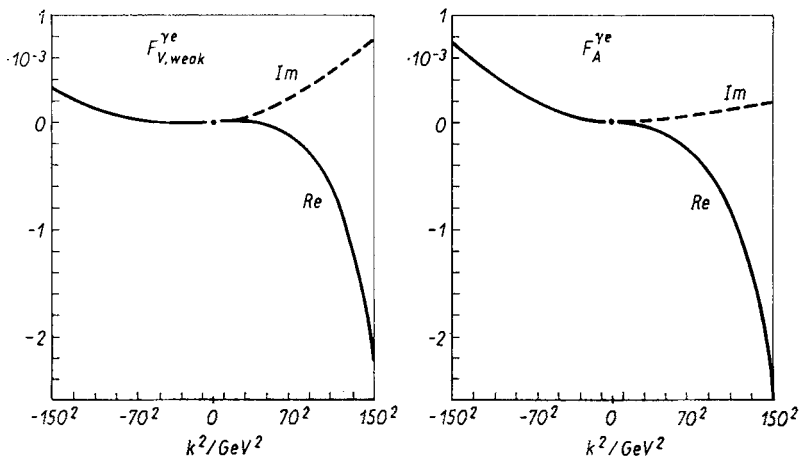


Fig. 19 a, b. Real (—) and imaginary (---) parts of the weak corrections to the vector (a) and axial vector (b) photon formfactor of the electron

The $\gamma\nu$ vertex vanishes in lowest order but gets contributions from 1-loop diagrams (b, c of fig. 7) containing the W exchange and the non-Abelian gauge boson coupling. The resulting formfactor $F^{\gamma\nu}(k^2)$ shown in fig. 20 grows for $|k^2| \leq (150 \text{ GeV})^2$ to $\sim 10^{-3}e$.

The non-photon contributions to the eZ boson formfactors are shown in fig. 21a, b. They have the same characteristics as the other formfactors. Compared to the self energy

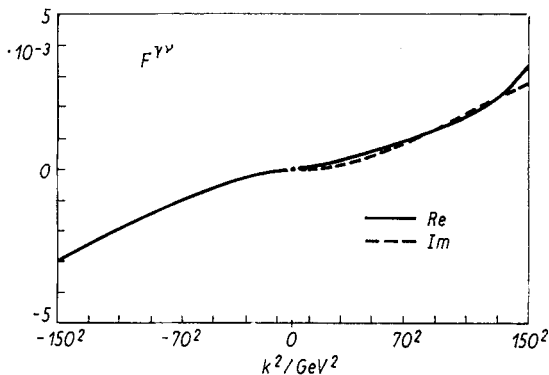


Fig. 20. Real (—) and imaginary (---) parts of the electromagnetic formfactor of the neutrino

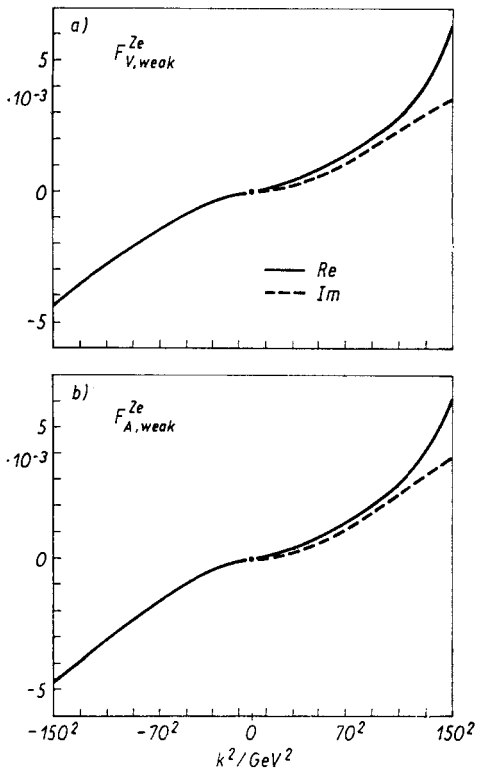


Fig. 21 a, b. Real (—) and imaginary (---) parts of the weak contributions to the vector (a) and axial vector (b) Z boson electron form-factor

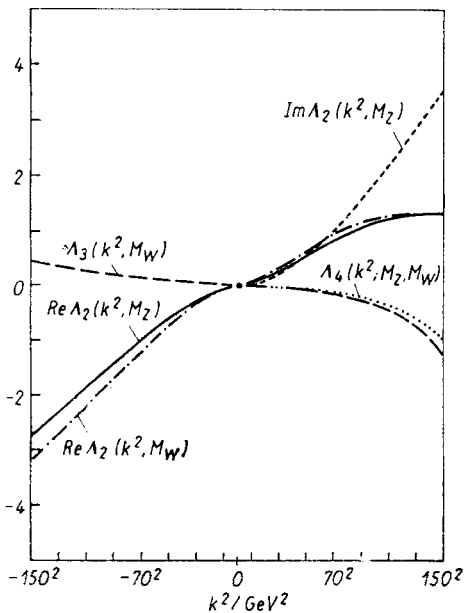


Fig. 22. Real and imaginary parts of the vertex integral $A_2(k^2, M)$ for $M = M_W, M_Z$ and $A_3(k^2, M_W), A_4(k^2, M_Z, M_W)$

effects of the weak bosons the weak contributions to the vertex corrections give effects in e^+e^- annihilation processes which are one order of magnitude smaller.

The $W_{e\nu}$ - and the corresponding quark formfactors obtain a contribution from the $WW\gamma$ -coupling (see fig. 7c). This shows a pronounced structure around $k^2 = M_W^2$ and reaches an order of magnitude of $-40 \cdot \alpha/4\pi$ for the real and imaginary part (see fig. 23).

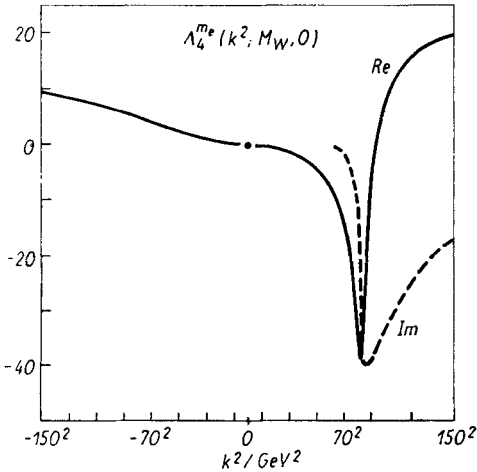


Fig. 23. Real (—) and imaginary (---) parts of the photonic invariant function $A_4^m(k^2, M_W, 0)$ for $m = m_e$

Together with the corresponding contribution (the $W\gamma$ -loop) to the W self energy it may lead to interesting effects in W exchange dominated reactions for timelike large momentum transfers.

We conclude this section with some remarks on the box diagrams with two weak bosons. In contrast to the self energy and vertex diagrams they are both UV and IR finite and consequently in the 1-loop approximation not directly influenced by the renormalization scheme. Their contribution to 1-loop radiative corrections to S matrix elements is in the energy range considered of the same order of magnitude as those of the vertex corrections. Explicit expressions are given in the appendix B.4 and numerical results presented in fig. 24a, b.

7. Application to Purely Leptonic Reactions

In this section we apply these 1-loop results to purely leptonic reactions like μ decay, $\nu_\mu e$ scattering and lepton pair production in e^+e^- annihilation [29]. Although the results from deep inelastic lepton scattering have now reached very good statistics, we have restricted our analysis to leptonic processes in this paper since these have smaller theoretical uncertainties from the strong interaction. Therefore these processes allow the cleanest tests of the electroweak interaction.

According to the choice of M_W, M_Z as parameters in the renormalization scheme used, the most direct way to compare the predictions of the electroweak standard theory with experimental data is to start with the measured values for M_W, M_Z (or equivalently M_W, s_W^2 resp. M_Z, s_W^2).

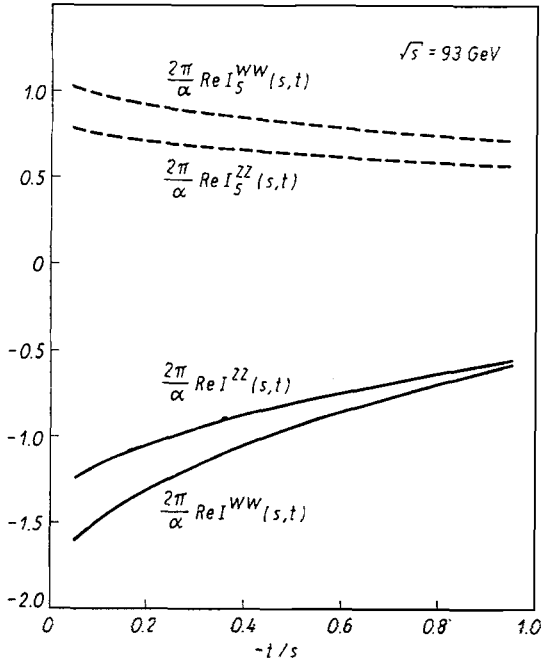


Fig. 24a. Real part of the s-channel box diagram form-factors $2\pi/\alpha \cdot I$ (—) and $2\pi/\alpha \cdot I_5$ (----) for the ZZ and WW box ($\sqrt{s} = 93 \text{ GeV}$)

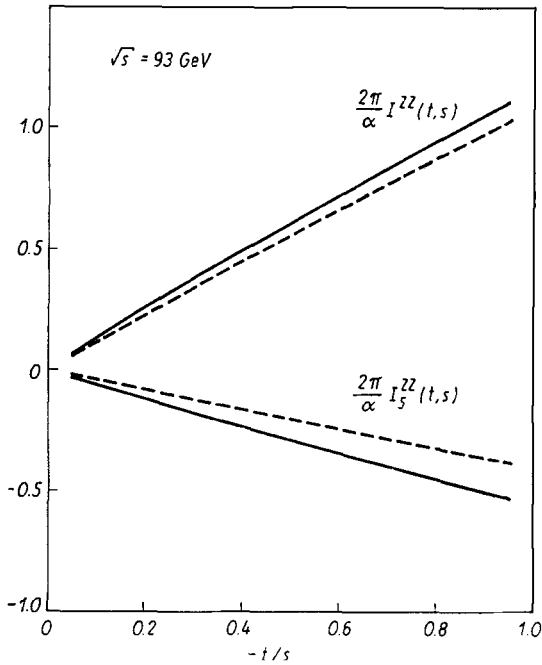


Fig. 24b. Real (—) and imaginary (----) parts of the t-channel box $2\pi/\alpha \cdot I^{ZZ}(t, s)$ and $2\pi/\alpha \cdot I_5^{ZZ}(t, s)$ with two Z bosons for $\sqrt{s} = 93 \text{ GeV}$

The UA 1 and UA 2 groups have determined

$$M_W = 82.2 \pm 1.1 \text{ GeV}, \quad M_Z = 92.7 \pm 1.0 \text{ GeV}. \tag{7.1}$$

A value for $\Delta M = M_Z - M_W$ can be deduced from experiment with an error smaller than that resulting from (7.1) because of a partial cancellation of the systematic uncertainties. Together with the definition of s_W^2 :

$$s_W^2 = 1 - \frac{M_W^2}{M_Z^2} = \frac{\Delta M}{M_Z} \left(2 - \frac{\Delta M}{M_Z} \right) \tag{7.2}$$

this gives for the mixing angle [1]:

$$s_W^2 = 0.218 \pm 0.023. \tag{7.3}$$

a) μ decay:

Neglecting terms of order $(m_e/m_\mu)^3$ and $(m_\mu/M_W)^2$ the lowest order expression for the decay width for $\mu^- \rightarrow \nu_\mu \bar{\nu}_e e^-$ is given by:

$$\begin{aligned} \Gamma_\mu^0 &= \frac{\alpha^2}{384\pi} m_\mu \left(1 - 8 \frac{m_e^2}{m_\mu^2} \right) \frac{m_\mu^4}{M_W^4} \frac{1}{(1 - M_W^2/M_Z^2)^2} \\ &= \frac{\alpha^2}{384\pi} m_\mu \left(1 - 8 \frac{m_e^2}{m_\mu^2} \right) \left(\frac{m_\mu}{M_W s_W} \right)^4. \end{aligned} \tag{7.4}$$

Putting together the 1-loop corrections yields the following results:

$$\begin{aligned} \Gamma_\mu &= \Gamma_\mu^0 \left\{ 1 + \frac{\alpha}{2\pi} \left(\frac{25}{4} - \pi^2 \right) - 2\Pi^W(0) + \frac{\alpha}{2\pi s_W^2} \left[6 + \frac{7 - 4s_W^2}{2s_W^2} \ln c_W^2 \right] \right\} \\ &= \Gamma_\mu^0 (1 + \delta\Gamma_\mu/\Gamma_\mu^0). \end{aligned} \tag{7.5}$$

The first correction term is the familiar QED correction in the Fermi model, the second the contribution of the transverse part of the W self energy, $\Pi^W(0)$ of eq. (6.4), the last term the sum of the vertex and box diagrams together with the ν_e, ν_μ wave function renormalization.

The decay width $\Gamma_\mu = \Gamma_\mu^0 + \delta\Gamma_\mu$ depends on both M_W and s_W^2 . Using the mean values of (7.1) and (7.3) the expressions (7.4–5) give:

$$\Gamma_\mu = 2.96 \cdot 10^{-16} \text{ MeV},$$

whereas the QED corrected Fermi model result is:

$$\Gamma_\mu^0 \left[1 + \frac{\alpha}{2\pi} \left(\frac{25}{4} - \pi^2 \right) \right] = 2.56 \cdot 10^{-16} \text{ MeV}.$$

This has to be compared with the measured value $\Gamma_\mu^{\text{exp}} = 2.9958 \cdot 10^{-16} \text{ MeV}$ [26]. With a fixed value of $M_W = 82.2 \text{ GeV}$ we obtain $2.42 \cdot 10^{-16} \leq \Gamma_\mu \leq 3.70 \cdot 10^{-16} \text{ MeV}$, corresponding to the variation of s_W^2 in (7.3).

The present accuracy of the direct M_W, M_Z measurements does not allow to predict Γ_μ with a precision that can compete with the accuracy of Γ_μ^{exp} . Instead, Γ_μ^{exp} can be used as an input quantity from which for a given s_W^2 (resp. M_W) the corresponding M_W and M_Z (resp. s_W^2, M_Z) is obtained. The result of this calculation is shown in figs. 25 and 26 for various values of the other parameters.

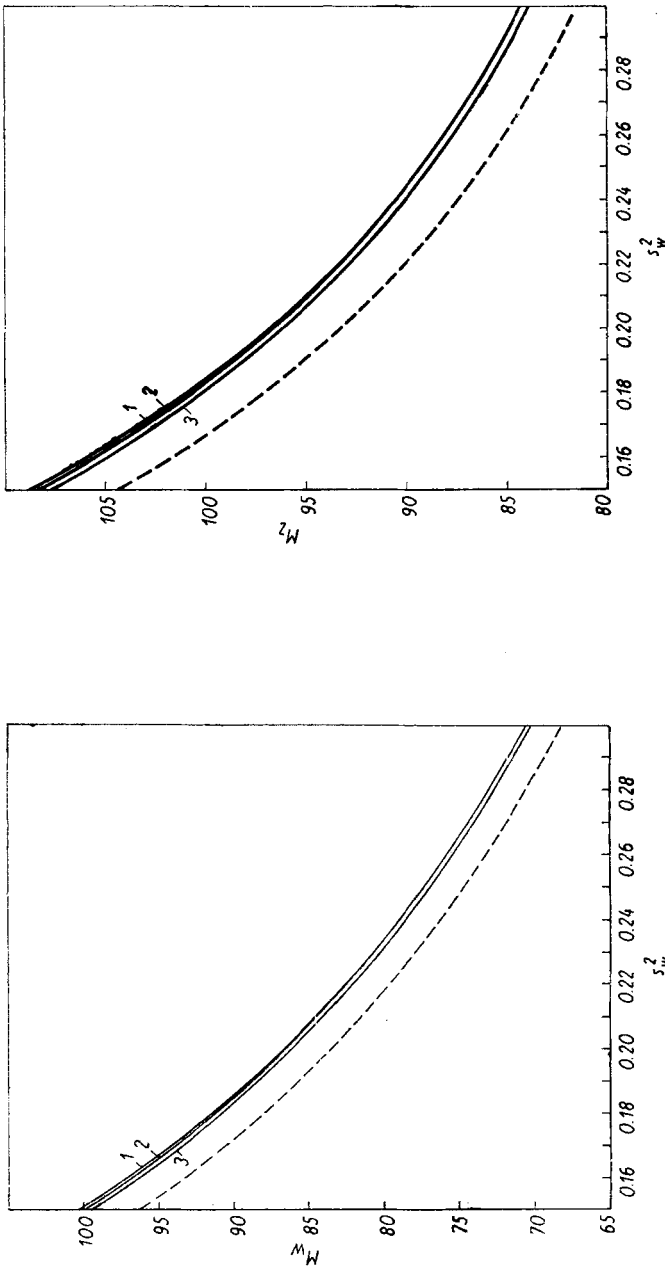


Fig. 25. M_W (a) and M_Z (b) as function of s_W^2 determined from the μ decay width in lowest order (---) and including 1-loop radiative corrections (—) for:

1: $(m_u, m_d, m_s) = (5, 7, 150)$ MeV, $m_t = 60$ GeV;
 2: $(m_u, m_d, m_s) = (5, 7, 150)$ MeV, $m_t = 30$ GeV;

3: $(m_u, m_d, m_s) = (300, 300, 450)$ MeV, $m_t = 30$ GeV;
 $M_H = 100$ GeV

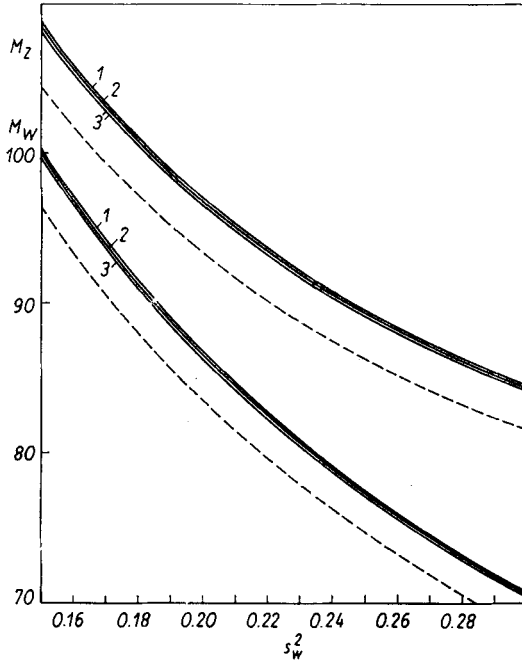


Fig. 26. Same as figs 25 a, b for several choices of M_H : 1: $M_H = 300$ GeV, 2: $M_H = 100$ GeV, 3: $M_H = 10$ GeV. Quark masses as in eq. (6.2)

b) $\nu_\mu e$ scattering:

The ratio

$$\Delta_\nu = \frac{\sigma(\nu_\mu e) - \sigma(\bar{\nu}_\mu e)}{\sigma(\nu_\mu e) + \sigma(\bar{\nu}_\mu e)} = \frac{\sigma(\nu_\mu e)/\sigma(\bar{\nu}_\mu e) - 1}{\sigma(\nu_\mu e)/\sigma(\bar{\nu}_\mu e) + 1} = \frac{R_\nu - 1}{R_\nu + 1} \tag{7.6}$$

is well-suited for our purpose since it is sensitive to the ratio M_W/M_Z resp. s_W^2 and less subject to systematic errors than the cross sections themselves; moreover it is free of electromagnetic higher order corrections.

With the ratio ξ of the vector and axial vector coupling constants of the electron to the Z :¹⁰⁾

$$\xi = v/a = 1 - 4s_W^2. \tag{7.7}$$

Δ_ν has in lowest order the simple form:

$$\Delta_\nu^0 = \frac{\xi}{1 + \xi^2} \quad \text{or} \quad R_\nu^0 = \frac{1 + \xi + \xi^2}{1 - \xi + \xi^2}. \tag{7.8}$$

The 1-loop corrected expression of Δ_ν can be written in the following way:

$$\Delta_\nu = \frac{\xi + \Delta\nu^Z - V + \xi A}{1 + \xi^2 + A\xi^2 + 2\xi(\Delta\nu^Z - V)} = \Delta_\nu^0 + \delta\Delta_\nu. \tag{7.9}$$

¹⁰⁾ In this section we omit the index e of the coupling constants v_e, a_e .

It gets contributions from the γZ mixing energy $\hat{\Sigma}_T^{\gamma Z}$ (6.1), the derivative of the $\gamma\nu\nu$ formfactor

$$\begin{aligned} \Delta^{\gamma Z} = & 4c_W s_W \frac{1}{s} \hat{\Sigma}_T^{\gamma Z}(s)|_{s=0} + \frac{2\alpha}{3\pi} \left(\ln \frac{M_W^2}{m_\mu^2} + 1 \right) = -4c_W^2 \left(\frac{\delta M_Z^2}{M_Z^2} - \frac{\delta M_W^2}{M_W^2} \right) \Big|_{\text{fin}} \\ & + \frac{\alpha}{3\pi} \left(3 + 2c_W^2 + 2 \ln \frac{M_W^2}{m_\mu^2} \right) - \frac{\alpha}{4\pi} \frac{2}{3} \left(\ln \frac{m_u^2}{m_d^2} + \ln \frac{m_c^2}{m_s^2} + \ln \frac{m_t^2}{m_b^2} \right) \\ & - \frac{\alpha}{4\pi} \frac{c^2}{s^2} \frac{m_t^2}{M_W^2} \ln \frac{m_t^2}{m_b^2} \end{aligned} \quad (7.10)$$

and of the box diagrams containing two massive gauge bosons:

$$V = +\frac{\alpha}{\pi} \left[\frac{1}{s_W^2} + 3va \right], \quad A = -\frac{\alpha}{\pi} \left[\frac{1}{s_W^2} + \frac{3}{2} (v^2 + a^2) \right]. \quad (7.11)$$

The weak contributions to the renormalized $\gamma\nu\nu$, $Z\nu\nu$ and Zee vertex functions vanish in our scheme at zero momentum transfer, yielding the simple expressions above.

The quantity R_ν , resp. Δ_ν , eq. (7.6), depends on M_W and M_Z mainly via the combination M_W/M_Z , because the variation of the γZ mixing energy with M_W (whence s_W^2 fixed) is small (see fig. 15). Therefore the value of s_W^2 from (7.3) can directly be converted into the observable R_ν (see also fig. 27):

$$R_\nu^0 = 1.29^{+0.24}_{-0.21}, \quad R_\nu = 1.28^{+0.23}_{-0.20}.$$

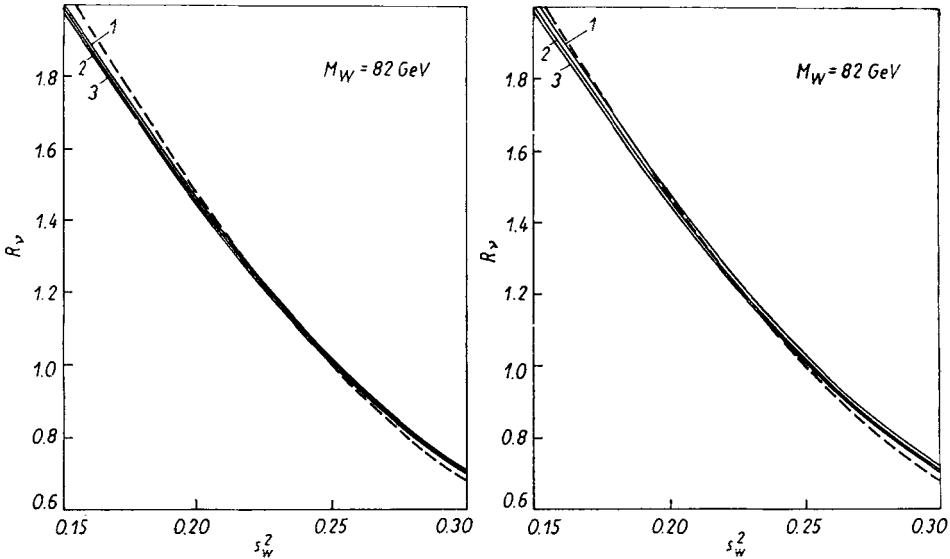


Fig. 27. R_ν as function of s_W^2 in lowest order (---) and including radiative corrections (—) for several choices of

a) M_H ; 1: $M_H = 300$ GeV, 2: $M_H = 100$ GeV, 3: $M_H = 10$ GeV and

b) quark masses:

1: $(m_u, m_d, m_s) = (300, 300, 450)$ MeV, $m_t = 30$ GeV;

2: $(m_u, m_d, m_s) = (5, 7, 150)$ MeV, $m_t = 60$ GeV;

3: $(m_u, m_d, m_s) = (5, 7, 150)$ MeV, $m_t = 30$ GeV; other parameters from (6.2)

The actual experimental value is [30]:

$$R_\nu = 1.38_{+0.40}^{-0.31}.$$

The measurement of R_ν together with that of Γ_μ can be used to determine the gauge boson masses by simultaneously solving the equations

$$R_\nu^{\text{exp}} = R_\nu^{\text{theor}}(M_W, M_Z), \quad \Gamma_\mu^{\text{exp}} = \Gamma_\mu^{\text{theor}}(M_W, M_Z).$$

This way to analyse the low energy data has been — until the experimental discovery of the W and Z — the only possibility to get information on the values of the gauge boson masses from purely leptonic reactions [31]. The results of our calculation are presented in fig. 28, where we have plotted the W and Z mass as a function of R_ν^{exp} .

c) Forward-backward asymmetry in $e^+e^- \rightarrow \mu^+\mu^-$:

The forward backward asymmetry $A_{FB}(x)$ in e^+e^- annihilation into μ pairs is defined as ($c = \cos \theta$):

$$A_{FB}(x) = \frac{\int_0^x dc \frac{d\sigma}{d\Omega} - \int_{-x}^0 dc \frac{d\sigma}{d\Omega}}{\int_0^x dc \frac{d\sigma}{d\Omega} + \int_{-x}^0 dc \frac{d\sigma}{d\Omega}}. \tag{7.12}$$

$d\sigma/d\Omega$ reads in Born approximation

$$\begin{aligned} \frac{4s}{\alpha^2} \cdot \frac{d\sigma^0}{d\Omega} &= 1 + c^2 + 2\chi(s) [v^2(1+c)^2 + 2a^2c] \\ &\quad + \chi(s)^2 [(v^2 + a^2)^2 (1+c^2) + 4v^2a^2 \cdot 2c] \end{aligned} \tag{7.13}$$

where:

$$\chi(s) = \frac{s}{s - M_Z^2}. \tag{7.14}$$

This gives:

$$A_{FB}^0(x, s) = \frac{x}{1+x^2/3} \cdot \frac{2a^2\chi(s)}{1+2v^2\chi(s) + (v^2+a^2)^2\chi(s)^2}. \tag{7.15}$$

At PETRA/PEP energies one is allowed to neglect the imaginary part $M_Z\Gamma_Z$ in the denominator of χ since $(\Gamma_Z/M_Z)^2 \ll 1$. Also we know that $v^2 \ll a^2$ and consequently may simplify (7.15):

$$A_{FB} = A_{FB}^0(1, s) \cong \frac{3}{2} a^2\chi/(1+a^4\chi^2) \tag{7.16}$$

with

$$a^2\chi = -\frac{s}{16M_W^2(1-M_W^2/M_Z^2)} \frac{M_Z^2}{M_Z^2 - s}. \tag{7.17}$$

The radiative corrections to $d\sigma/d\Omega$ can be divided into electromagnetic (real and virtual photonic corrections) and purely weak parts:

$$\frac{d\sigma}{d\Omega} = \frac{d\sigma^0}{d\Omega} (1 + C_{\text{em}} + C_W). \tag{7.18}$$

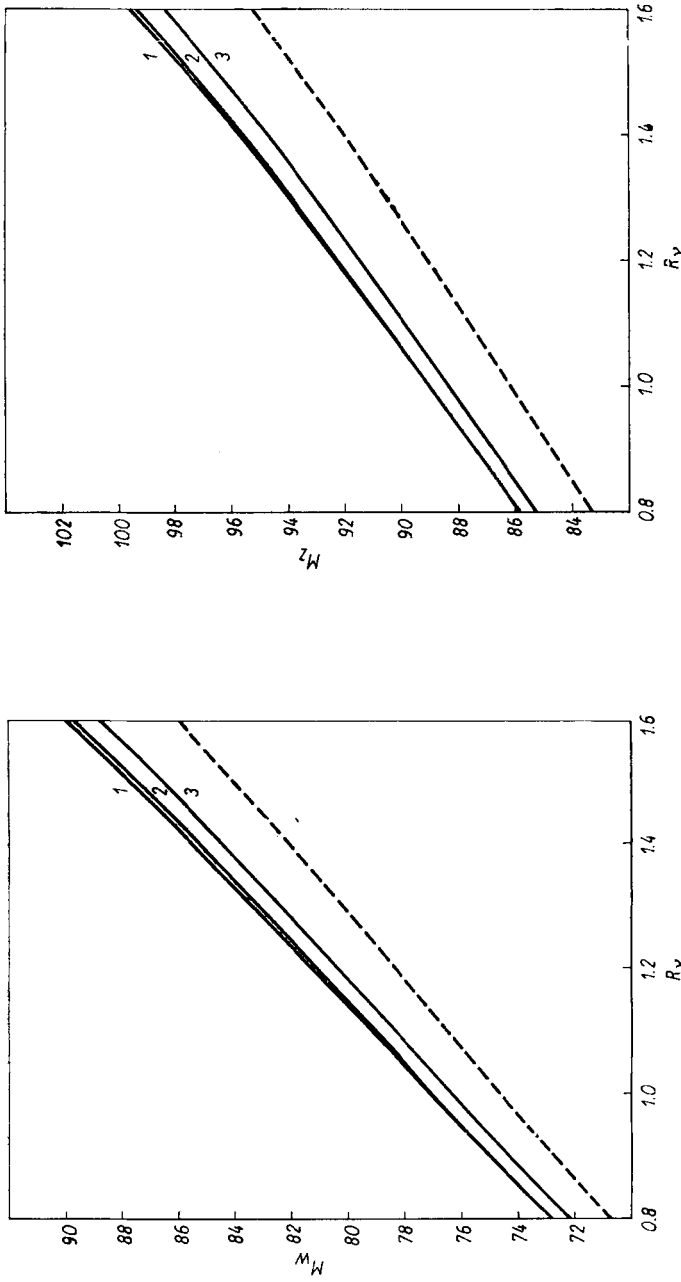


Fig. 28 a, b. M_W (a) and M_Z (b) determined from μ decay and $\nu_\mu e$ scattering as function of R_ν in lowest order (-----) and including radiative corrections (—) for:

1: $(m_u, m_d, m_s) = (5, 7, 150)$ MeV, $m_t = 30$ GeV;
 2: $(m_u, m_d, m_s) = (5, 7, 150)$ MeV, $m_t = 60$ GeV;

3: $(m_u, m_d, m_s) = (300, 300, 450)$ MeV, $m_t = 30$ GeV;
 $M_H = 100$ GeV

The electromagnetic corrections C_{em} and their influence on \mathcal{A}_{FB} have been treated in ref. [18] and especially in [19]. Therefore we do not reproduce the expressions for C_{em} in this paper but take the formulas of [19] for the numerical evaluation of their contribution to \mathcal{A}_{FB} .

The purely weak part C_w is built up from the Z self energy, the gauge part of the γ self energy, the γZ mixing energy, the weak contributions F_w to the e and μ photon and Z formfactors and the box graphs with two heavy bosons. For PETRA/PEP energies, neglecting terms of order $\alpha/2\pi \cdot (|t|/M_Z^2)$ these box contributions become independent of $c = \cos \theta$, and therefore the weak corrections can be written in the following way :

$$\frac{d\sigma^0}{d\Omega} \cdot C_w = (1 + c^2) [C_w^{\gamma^*+} + 2\chi C_w^{\gamma Z,+} + \chi^2 C_w^{Z,+}] + 2c[2\chi C_w^{\gamma Z,-} + \chi^2 C_w^{Z,-}]. \tag{7.19}$$

These terms modify the expression (7.16) for the forward-backward asymmetry \mathcal{A}_{FB} to become:

$$\mathcal{A}_{FB} = \frac{3}{4} \cdot \frac{2\chi(a^2 + C_w^{\gamma Z,-}) + \chi^2(4v^2a^2 + C_w^{Z,-})}{1 + C_w^{\gamma^*+} + 2\chi(v^2 + C_w^{\gamma Z,+}) + \chi^2((v^2 + a^2)^2 + C_w^{Z,+})}. \tag{7.20}$$

Now we write down the explicit form of the corrections C_w :

$$\begin{aligned} C_w^{\gamma^*+} &= -2\Pi_w^\gamma + 4F_{V,w}^{\gamma^*e}, \\ C_w^{\gamma Z,+} &= -v^2(\Pi_w^\gamma + \Pi^{\gamma Z}) - 2v\Pi^{\gamma Z} + 2vF_{V,w}^{Ze} + 2v(vF_{V,w}^{\gamma e} + aF_{A,w}^{\gamma e}) \\ &\quad + 4v^2a^2A_1^{ZZ} + (2s_W)^{-4} V_1^{WW}, \\ C_w^{\gamma Z,-} &= -a^2(\Pi_w^\gamma + \Pi^Z) + 2aF_{A,w}^{Ze} + 2a(vF_{A,w}^{\gamma e} + aF_{V,w}^{\gamma e}) \\ &\quad + (v^2 + a^2)^2 A_1^{ZZ} + (2s_W)^{-4} V_1^{WW}, \\ C_w^{Z,+} &= -2(v^2 + a^2)^2 \Pi^Z - 2v(v^2 + a^2) \cdot 2\Pi^{\gamma Z} + 4(v^2 + a^2) (vF_{V,w}^{Ze} + aF_{A,w}^{Ze}) \\ &\quad + (v \cdot 2va + a(v^2 + a^2))^2 A_1^{ZZ} + (v + a)^2 (2s_W)^{-4} V_1^{WW}, \\ C_w^{Z,-} &= -8v^2a^2\Pi^Z - 8a^2v\Pi^{\gamma Z} + 8va(vF_{A,w}^{Ze} + aF_{V,w}^{Ze}) \\ &\quad + (v(v^2 + a^2) + a \cdot 2va)^2 A_1^{ZZ} + (v + a)^2 (2s_W)^{-4} V_1^{WW}. \end{aligned} \tag{7.21}$$

The quantities Π are related to the renormalized transverse self energies $\hat{\Sigma}_T(s)$ (6.1):

$$\begin{aligned} \Pi_w^\gamma(s) &= \frac{1}{s} \text{Re } \hat{\Sigma}_{T,w}^\gamma(s) \text{ (non-fermionic part),} \\ \Pi^{\gamma Z}(s) &= \frac{1}{s} \text{Re } \hat{\Sigma}_T^{\gamma Z}(s), \\ \Pi^{Z,W}(s) &= \frac{1}{s - M_{Z,W}^2} \text{Re } \hat{\Sigma}_T^{Z,W}(s). \end{aligned} \tag{7.22}$$

The weak contributions $F_{V,w}^{Ze}, \dots, F_{A,w}^{\gamma e}$ to the formfactors are built from the functions $\Lambda_{2,3}(s, M^2)$ and coupling constants (comp. 6.8, 11) and app. B.3):

$$\begin{aligned} F_{V,w}^{Ze}(s) &= \frac{\alpha}{4\pi} \left[v(v^2 + a^2) \text{Re } \Lambda_2(s, M_Z^2) \right. \\ &\quad \left. + \frac{1}{8s_W^3 c_W} \text{Re } \Lambda_2(s, M_W^2) - \frac{3c_W}{4s_W^3} \Lambda_3(s, M_W^2) \right], \end{aligned} \tag{7.23}$$

$$\begin{aligned}
 F_{A,w}^{Ze}(s) &= \frac{\alpha}{4\pi} \left[a(3v^2 + a^2) \operatorname{Re} A_2(s, M_Z^2) \right. \\
 &\quad \left. + \frac{1}{8s_W^3 c_W} \operatorname{Re} A_2(s, M_W^2) - \frac{3c_W}{4s_W^3} A_2(s, M_W^2) \right], \\
 F_{V,w}^{\gamma e}(s) &= \frac{\alpha}{4\pi} \left[(v^2 + a^2) \operatorname{Re} A_2(s, M_Z^2) + \frac{3}{4s_W^2} A_3(s, M_W^2) \right], \\
 F_{A,w}^{\gamma e}(s) &= \frac{\alpha}{4\pi} \left[2va \cdot \operatorname{Re} A_2(s, M_Z^2) + \frac{3}{4s_W^2} A_3(s, M_W^2) \right].
 \end{aligned}
 \tag{7.23}$$

These expressions vanish for $s = 0$ and are for energies $\sqrt{s} < 45$ GeV smaller than 10^{-3} . Finally the low energy approximations of the ZZ , WW box diagrams have the simple form (coupling constants removed):

$$A_1^{ZZ} = -3 \frac{\alpha}{4\pi}, \quad V_1^{WW} = \frac{\alpha}{4\pi}
 \tag{7.24}$$

yielding terms of the order of magnitude of less than 10^{-3} .

If an accuracy of the relative corrections to \mathcal{A}_{FB} at PETRA/PEP energies of 10^{-3} is desired, one is allowed to neglect in the contributions to C_w all terms but the self energies. Then one gets for $\mathcal{A}_{FB}^{\text{Born+weak}}$ the following expression (using also $v^2 \ll a^2$):

$$\mathcal{A}_{FB}^{\text{Born+weak}} \simeq \frac{3}{2} \chi a^2 \cdot \frac{1 - \Pi_w^\gamma - \Pi^Z}{1 - 2\Pi_w^\gamma + \chi^2 a^4} \simeq \frac{3}{2} \frac{\chi a^2}{1 + \chi^2 a^4} (1 + \Pi_w^\gamma - \Pi^Z).
 \tag{7.25}$$

χ was defined in eq. (7.14) as the ratio of the free Z and γ propagators. Therefore the result (7.25) has the simple interpretation:

$$\mathcal{A}_{FB}^{\text{Born+weak}}(s) = \frac{3}{2} \frac{\chi(s)^{\text{Born+weak}}}{1 + \chi(s)^2 a^4} a^2, \quad \chi^{\text{Born+weak}} = \frac{s + \hat{\Sigma}_{T,w}^\gamma(s)}{s - M_Z^2 + \hat{\Sigma}_T^Z(s)}.
 \tag{7.26}$$

The lowest order expression for $\chi(s)$ has to be replaced by the renormalized one, the radiative corrections to a^2 can be neglected.

The weak i.e. non-Abelian gauge contribution to Π^γ , comes from vacuum polarization by W pairs, the corresponding ghosts and unphysical charged Higgses and results for small energies as can be seen from (6.1), (5.7) in:

$$\Pi_w^\gamma(s) = -\frac{\alpha}{4\pi} \cdot \frac{s}{2M_W^2} + O\left(\frac{\alpha}{4\pi} \left(\frac{s}{M_W^2}\right)^2\right).
 \tag{7.27}$$

Consequently this can also be neglected at the desired accuracy at PETRA/PEP energies, leaving the simple result suited for the practical calculations:

$$\mathcal{A}_{FB}^{\text{Born+weak}} = \frac{3}{2} \frac{\chi(s) a^2}{1 + \chi^2 a^4} (1 - \Pi^Z(s)).
 \tag{7.28}$$

We find — in agreement with [16] — that the weak radiative corrections to \mathcal{A}_{FB} at low energies are determined by the transverse Z boson self energy only, with an accuracy of $\delta\mathcal{A}^{\text{weak}}/\mathcal{A}^0 < 10^{-3}$.

On the basis of the formulas (7.18–23) we present in table 1 the weak corrections to A_{FB} for a large range of the Z mass and s_W^2 . The α^3 contribution to A_{FB} which is of pure QED origin is not included because it is model independent and already respected in the experimental data. The sum of the QED corrections to Z exchange and γZ interference and the purely weak corrections turn out to be very small over the parameter range considered for realistic cuts (≤ 0.001 in A_{FB}). Fig. 29 shows the predictions for $A_{FB}(|\cos \theta| \leq 0.8)$ for $\sqrt{s} = 34.5$ GeV with an acollinearity cut of 10^0 and an energy cut of $0.5E_{\text{beam}}$

Table 1

Purely weak corrections to $A_{FB}(|\cos \theta| < 1)$ in percent for $\sqrt{s} = 43$ GeV ($M_H = 100$ GeV, $m_t = 30$ GeV).

s_W^2	$M_Z(\text{GeV})$								
	89	90	91	92	93	94	95	96	97
0.15	-1.66	-1.62	-1.57	-1.53	-1.49	-1.45	-1.42	-1.38	-1.35
0.16	-1.57	-1.53	-1.48	-1.44	-1.41	-1.37	-1.34	-1.30	-1.27
0.17	-1.49	-1.45	-1.41	-1.37	-1.33	-1.30	-1.27	-1.23	-1.20
0.18	-1.41	-1.37	-1.34	-1.30	-1.27	-1.23	-1.20	-1.17	-1.14
0.19	-1.35	-1.31	-1.28	-1.24	-1.21	-1.18	-1.15	-1.12	-1.09
0.20	-1.29	-1.26	-1.22	-1.19	-1.16	-1.13	-1.10	-1.07	-1.05
0.21	-1.24	-1.21	-1.17	-1.14	-1.11	-1.08	-1.06	-1.03	-1.00
0.22	-1.19	-1.16	-1.13	-1.10	-1.07	-1.04	-1.02	-0.99	-0.97
0.23	-1.15	-1.12	-1.09	-1.06	-1.03	-1.01	-0.98	-0.96	-0.93
0.24	-1.12	-1.08	-1.06	-1.03	-1.00	-0.97	-0.95	-0.93	-0.90
0.25	-1.08	-1.05	-1.02	-1.00	-0.97	-0.94	-0.92	-0.90	-0.88
0.26	-1.05	-1.02	-0.99	-0.97	-0.94	-0.92	-0.89	-0.87	-0.85
0.27	-1.02	-0.99	-0.97	-0.94	-0.92	-0.89	-0.87	-0.85	-0.83
0.28	-1.00	-0.97	-0.94	-0.92	-0.89	-0.87	-0.85	-0.83	-0.81
0.29	-0.97	-0.95	-0.92	-0.90	-0.87	-0.85	-0.83	-0.81	-0.79
0.30	-0.95	-0.92	-0.90	-0.88	-0.85	-0.83	-0.81	-0.79	-0.77

for the bremsstrahlung part. These results are scaled up to $|\cos \theta| \leq 1$ according to the lowest order formula (7.15) in order to be directly comparable with the PETRA results [4] that are shown in the figure, too.

One can see from fig. 29 that the experimental result for A_{FB} at 34.5 GeV favours values of s_W^2 which are slightly smaller than those following from the M_W/M_Z ratio.

d) Tests of the standard model at the 1-loop level:

The most important parameters of the electroweak standard model are the masses of the intermediate bosons. Therefore, we have expressed every observable quantity with help of M_W and M_Z . Consequently each measured value R_{exp} of a quantity R

$$R^{\text{exp}} = R^{\text{theor}}(M_W, M_Z) \tag{7.29}$$

gives a relation between M_W and M_Z . This depends if one includes radiative corrections slightly on the other parameters of the model i.e. the fermion masses and the Higgs mass. In order to perform a test of the standard model using purely leptonic reactions we

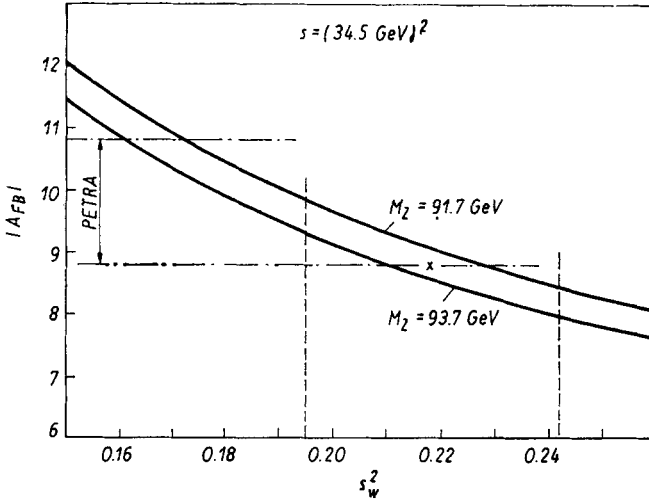


Fig. 29. A_{FB} (0.8) scaled up to $|\cos \theta| \leq 1$ according to eq. (7.15) at $\sqrt{s} = 34.5$ GeV as function of s_W^2 including complete electroweak radiative corrections. Shown are the curves resulting from the upper (93.7) and lower (91.7) bounds on M_Z from the $P\bar{P}$ collider experiment together with the upper and lower bounds on s_W^2 (dashed lines) from the same experiment. The cross marks the point corresponding to the mean values $M_Z = 92.7$ GeV, $s_W^2 = 0.218$. The dashed-dotted lines mark the PETRA results

present the experimental results in the (M_W, M_Z) plane. This is done in fig. 30 including 1-loop corrections (for our previously specified standard set of parameters (6.2)) for:

- μ decay, which gives a curve in the (M_W, M_Z) plane;
- $\nu_\mu e$ scattering, yielding relatively weak bounds on M_W, M_Z due to the present experimental errors [30];
- the lepton pair forward-backward asymmetry at $\sqrt{s} = 34.5$ GeV;
- the direct measurement of M_W and M_Z in the $P\bar{P}$ collider [1].

This picture represents a comprehensive test of the electroweak standard theory at the 1-loop level in the leptonic sector.

Clearly the low energy data (from Γ_μ, R, A_{FB}) and the high energy data (M_W, M_Z) are compatible with each other. The agreement would be worse if radiative corrections were not taken into account. But in order to become really sensitive to these corrections improvements in the experimental determination of M_W, M_Z and R , are necessary.

8. Conclusion and Outlook

In this paper we have worked out a renormalization scheme for the standard electroweak model characterized by the following properties: use of the electric charge e and particle masses as physical parameters; minimal number of field renormalization constants respecting the $SU(2) \times U(1)$ symmetry; the simple pole structure of the 't Hooft-Feynman gauge is maintained after renormalization in a way consistent with the Slavnov-Taylor identities. We have calculated all the physical and unphysical self and mixing energies together with the complete set of renormalization constants, and the fermion gauge boson vertices. We have presented also the renormalized results for the self energies, vertices and box diagrams. These are the building blocks needed for the calculation

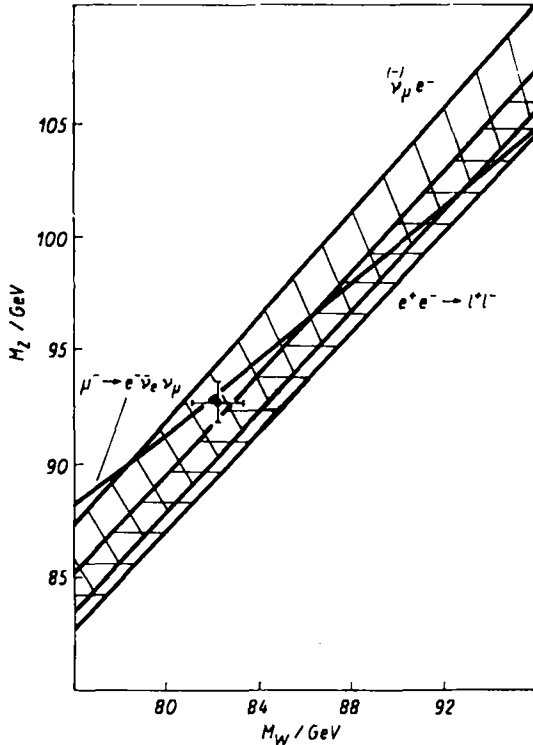


Fig. 30. Comparison of the results for the boson masses in the (M_W, M_Z) plane. Shown are: the curve resulting from μ decay (—), the 68% CL band determined from ν/e scattering (//////) and that from the forward-backward asymmetry in $e^+e^- \rightarrow \mu^+\mu^-$ (===). The blob with the error bars represents the combined UA 1 and UA 2 results

of electroweak radiative corrections to e^+e^- annihilation, deep inelastic lepton scattering and $P\bar{P}$ annihilation at high energies.

Finally we have performed a comparison between experiment and the results of the standard model including radiative corrections for μ -decay, $\nu_\mu e$ -scattering and e^-e^- -annihilation into lepton pairs. We find good agreement between theory and experiment if radiative corrections are included. But the accuracy of the experiment has not yet reached a level where radiative corrections can be conclusively tested. We expect this to be the case in the near future, when results of the next generation of the e^-e^- -machines and of the high precision experiments on lepton scattering are available. These then may also help to gather some information on the Higgs sector and finally will allow to discriminate between the minimal electroweak model and more extended versions.

References

- [1] UA 1 Collaboration, G. ARNISON et al., Phys. Lett. 126 B (1983) 398; UA 2 Collaboration, P. BAGNAIA et al., Phys. Lett. 129 B (1983) 130; UA 1 Collaboration, G. ARNISON et al., Phys. Lett. 129 B (1983) 273; E. RADERMACHER, CERN-EP/84-41; L. DiLELLA, HEP 85 Conference, Bari 1985.

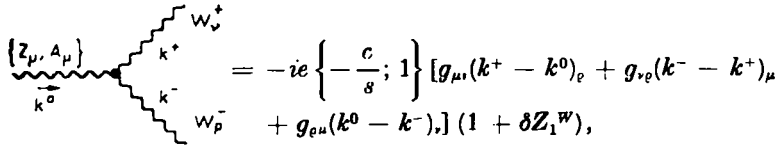
- [2] S. L. GLASHOW, Nucl. Phys. **22** (1961) 579; S. WEINBERG, Phys. Rev. Lett. **19** (1967) 1264; A. SALAM, in Elementary Particle Theory, ed. N. Svartholm (Almqvist and Wiksell, Stockholm 1968), p. 367; S. L. GLASHOW, J. ILLIOPOULOS, L. MAIANI, Phys. Rev. **D 2** (1970) 1285.
- [3] R. H. HEISTERBERG et al., Phys. Rev. Lett. **44** (1979) 635; CHARM Collaboration, F. BERGSMAN et al., Phys. Lett. **117 B** (1982) 272; W. KRENZ, Aachen PITHA 82/26 (1982); L. A. AHRENS et al., Phys. Rev. Lett. **51** (1983) 1514; CDHS Collaboration, CH. GEWENIGER, Brighton Conference 1983; CHARM Collaboration, M. JONKER et al., CERN-EP/82-207 (1982).
- [4] PLUTO Collaboration, CH. BERGER et al., DESY 83-084; P. GROSSE-WIESMANN, DESY 83-087; TASSO Collaboration, M. ALTHOFF et al., DESY 83-089; G. HERTEN, Brighton Conference 1983; E. LOHRMANN, DESY 83-102; A. BÖHM, DESY 83-103; B. NAROSKA, DESY 83-111; E. FERNANDEZ et al., Phys. Rev. Lett. **50** (1983) 1238; SLAC-PUB-3133 (1983); H. V. MARTYN, Vanderbilt Conference 1984, DESY 84-48; I. P. DUERDOTH, HEP '85 Conference, Bari 1985.
- [5] Proceedings of the LEP Summer Study, CERN 79-01 (1979); Proceedings of the SLC Workshop, SLAC-Report-247 (1982).
- [6] G. 'T HOOFT, Nucl. Phys. **B 33** (1971) 173, Nucl. Phys. **B 35** (1971) 167.
- [7] Proceedings of the Topical Conference on Radiative Corrections in $SU(2)_L \times U(1)$, Miramare-Trieste, 6–8 June 1983, ed. B. W. Lynn and J. Wheeler, Singapore 1984.
- [8] D. YU. BARDIN, P. CH. CHRISTOVA, O. M. FEDERENKO, Nucl. Phys. **B 175** (1980) 435; **B 197** (1982) 1.
- [9] G. PASSARINO, M. VELTMAN, Nucl. Phys. **B 160** (1979) 151; M. CONSOLI, Nucl. Phys. **B 160** (1979) 208.
- [10] A. SIRLIN, Phys. Rev. **D 22** (1980) 971; W. J. MARCIANO, A. SIRLIN, Phys. Rev. **D 22** (1980) 2695; A. SIRLIN, W. J. MARCIANO, Nucl. Phys. **B 189** (1981) 442.
- [11] J. FLEISCHER, F. JEGERLEHNER, Phys. Rev. **D 23** (1981) 2001.
- [12] D. A. ROSS, J. C. TAYLOR, Nucl. Phys. **B 51** (1973) 25; S. SAKAKIBARA, Phys. Rev. **D 24** (1981) 1149; E. A. PASCHOS, M. WIRBEL, Nucl. Phys. **B 194** (1982) 189; M. WIRBEL, Z. Phys. **C 14** (1982) 293; I. LIEDE, E. A. PASCHOS, M. ROOS, S. SAKAKIBARA, Preprint HU-TFT-83-45/DO-TH-83-21 (1983).
- [13] F. ANTONELLI, G. CORBO, M. CONSOLI, O. PELLEGRINO, Nucl. Phys. **B 183** (1981) 475; M. CONSOLI, S. LO PRESTI, L. MAIANI, Nucl. Phys. **B 223** (1983) 474.
- [14] C. H. LLEWELLYN SMITH, J. F. WHEATER, Phys. Lett. **105 B** (1981) 486; J. F. WHEATER, C. H. LLEWELLYN SMITH, Nucl. Phys. **B 208** (1982) 27.
- [15] K. I. AOKI, Z. HIOKI, R. KAWABE, M. KONUMA, T. MUTA, Progr. Theor. Phys. **64** (1980) 707; **65** (1981) 1001; Suppl. Progr. Theor. Phys. **73** (1982) 1.
- [16] W. WETZEL, Nucl. Phys. **B 227** (1983) 1; R. W. BROWN, R. DECKER, E. A. PASCHOS, Phys. Rev. Lett. **52** (1984) 1192.
- [17] J. COLE, in [7], and Nucl. Phys. **B** (to be published).
- [18] M. GRECO, G. PANCHERI-SRIVASTAVA, Y. SRIVASTAVA, Nucl. Phys. **B 171** (1980) 118; F. A. BERENDS, R. KLEISS, S. JADACH, Nucl. Phys. **B 202** (1982) 63; M. BÖHM, W. HOLLIK, Nucl. Phys. **B 204** (1982) 45.
- [19] M. BÖHM, W. HOLLIK, Z. Phys. **C 23** (1984) 31.
- [20] M. BÖHM, W. HOLLIK, Phys. Lett. **139 B** (1984) 213.
- [21] L. D. FADDEEV, V. N. POPOV, Phys. Lett. **25 B** (1967) 29.
- [22] C. BECCHI, A. ROUET, R. STORA, Phys. Lett. **52 B** (1974) 344; Comm. Math. Phys. **42** (1975) 127.
- [23] A. A. SLAVNOV, Theor. Math. Phys. **10** (1972) 99; J. C. TAYLOR, Nucl. Phys. **B 33** (1971) 436.
- [24] J. C. WARD, Phys. Rev. **78** (1950) 1824.
- [25] G. 'T HOOFT, M. VELTMAN, Nucl. Phys. **B 44** (1972) 189.
- [26] Particle Data Group, Phys. Lett. **111 B** (1982).
- [27] J. GASSER, H. LEUTWYLER, Ann. Phys. (N.Y.) **136** (1981) 62; Phys. Rep. **87 C** (1982) 77.
- [28] F. A. BERENDS, G. J. KOMEN, Phys. Lett. **63 B** (1976) 432. F. YNDURAIN, Nucl. Phys. **B 136**, (1978) 533.
- [29] M. BÖHM, W. HOLLIK, H. SPIESBERGER, Z. Phys. **C 27** (1985) 523.
- [30] CHARM Collaboration, F. BERGSMAN et al. Contributed paper, Neutrino 84, Nordkirchen near Dortmund (1984); M. Murtagh, this conference. Paper submitted to the HEP '85 Conference, Bari 1985.

$$\begin{aligned} \overline{\text{ghost}}^a \text{ghost}^a &= i \left[k^2 \left(\delta \bar{Z}^a - \frac{1}{2} \delta \xi_1^a \right) - M_a^2 \left(\delta \bar{Z}^a + \frac{\delta M_a^2}{M_a^2} + \frac{1}{2} \delta \xi_2^a \right) \right]; \\ a &= \pm, Z, \gamma, \end{aligned}$$

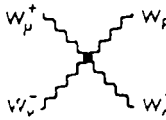
$$\overline{\text{ghost}}^Y \text{ghost}^Z = -i \left[k^2 \left(\delta \bar{Z}^{\gamma Z} - \frac{1}{2} \delta \xi_1^{\gamma Z} \right) + M_Z^2 \left(\delta Z_1^{\gamma Z} - \frac{3}{2} \delta Z_2^{\gamma Z} + \delta \bar{Z}^{\gamma Z} \right) \right],$$

$$\overline{\text{ghost}}^Z \text{ghost}^Y = -i \left[k^2 \left(\delta \bar{Z}^{\gamma Z} - \frac{1}{2} \delta \xi_1^{\gamma Z} \right) + M_Z^2 \left(\delta Z_1^{\gamma Z} - \frac{3}{2} \delta Z_2^{\gamma Z} + \frac{1}{2} \delta \xi_2^{\gamma Z} \right) \right],$$

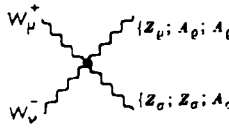
$$\begin{aligned} i\sigma \text{---} x \text{---} i\sigma &= i \left[k \left(\delta Z_L^i \frac{1 - \gamma_5}{2} + \delta Z_R^{i\sigma} \frac{1 + \gamma_5}{2} \right) \right. \\ &\quad \left. - m_{i\sigma} \left(\frac{1}{2} \delta Z_L^i + \frac{1}{2} \delta Z_R^{i\sigma} \right) - \delta m_{i\sigma} \right], \end{aligned}$$



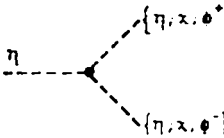
$$\begin{aligned} \text{Diagram} &= -ie \left\{ -\frac{c}{s}; 1 \right\} [g_{\mu\nu}(k^+ - k^0)_\nu + g_{\nu e}(k^- - k^+)_\mu \\ &\quad + g_{e\mu}(k^0 - k^-)_\nu] (1 + \delta Z_1^W), \end{aligned}$$



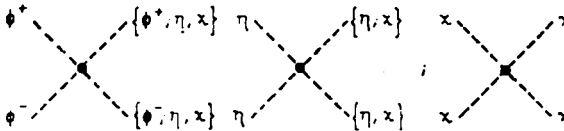
$$= ie^2 \frac{1}{s^2} [2g_{\mu\sigma}g_{\nu e} - g_{\mu\nu}g_{e\sigma} - g_{\mu e}g_{\nu\sigma}] \cdot (1 + 2\delta Z_1^W - \delta Z_2^W),$$



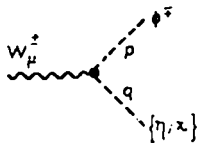
$$\begin{aligned} &= -ie^2 \left\{ \frac{c^2}{s^2}; -\frac{c}{s}; 1 \right\} [2g_{\mu\nu}g_{e\sigma} - g_{\mu e}g_{\nu\sigma} - g_{\mu\sigma}g_{\nu e}] \\ &\quad \times (1 + 2\delta Z_1^W - \delta Z_2^W), \end{aligned}$$



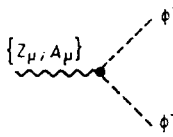
$$= -i \frac{e}{2s} \frac{M_H^2}{M_W} \{3; 1; 1\} \left(1 - \frac{\delta v}{v} + \delta Z^I \right),$$



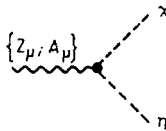
$$= -i \frac{e^2}{4s^2} \frac{M_H^2}{M_W^2} \{2; 1; 1; 3; 1; 3\} \times (1 + \delta Z^I),$$



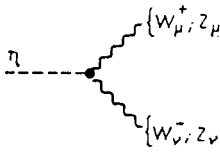
$$= \frac{e}{2s} (p - q)_\mu \{ \mp i; 1 \} (1 + \delta Z^{\nu} + \delta Z_1^W - \delta Z_2^W),$$



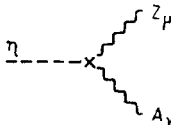
$$= -ie(p - q)_\mu \left\{ \frac{s^2 - c^2}{2cs}; 1 \right\} \left(1 + \delta Z^\varphi + \left\{ \delta Z_1^Z - \delta Z_2^Z + \frac{2cs}{c^2 - s^2} (\delta Z_1^{\gamma Z} - \delta Z_2^{\gamma Z}); \delta Z_1^\gamma - \delta Z_2^\gamma + \frac{c^2 - s^2}{2cs} (\delta Z_1^{\gamma Z} - \delta Z_2^{\gamma Z}) \right\} \right),$$



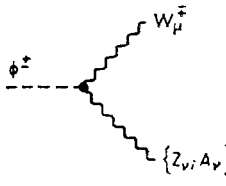
$$= \frac{e}{2cs} (p - q)_\mu \{ 1 + \delta Z^\varphi + \delta Z_1^Z - \delta Z_2^Z; \delta Z_2^{\gamma Z} - \delta Z_1^{\gamma Z} \},$$



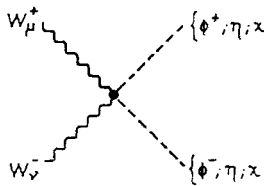
$$= i \frac{e}{s} M_W g_{\mu\nu} \left\{ 1; \frac{1}{c^2} \right\} \left(1 + \frac{1}{2} \delta Z^\varphi + \frac{\delta M_{W;Z}}{M_{W;Z}} + \delta Z_1^{W;Z} - \frac{1}{2} \delta Z_2^{W;Z} \right),$$



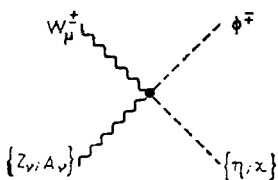
$$= -i \frac{e}{c^2 s} M_W g_{\mu\nu} (\delta Z_1^{\gamma Z} - \delta Z_2^{\gamma Z}),$$



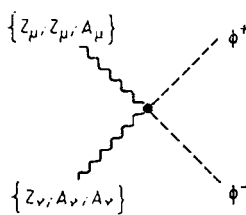
$$= -ie M_W g_{\mu\nu} \left\{ \frac{s}{c}; 1 \right\} \left(1 - \frac{1}{2} \delta Z^\varphi + \frac{\delta M_W}{M_W} + \frac{1}{2} \delta Z_2^W + \delta Z_1^B - \delta Z_2^B \right),$$



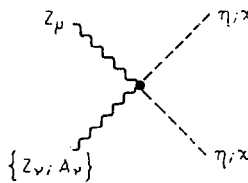
$$= i \frac{e^2}{2s^2} g_{\mu\nu} (1 + \delta Z^\varphi + 2\delta Z_1^W - 2\delta Z_2^W),$$



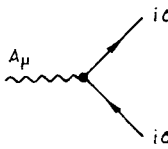
$$= -i \frac{e^2}{2} g_{\mu\nu} \left\{ \frac{1}{c}; \frac{1}{s} \right\} \{ 1; \pm i \} (1 + \delta Z^\varphi + \delta Z_1^W - \delta Z_2^W + \delta Z_1^B - \delta Z_2^B),$$



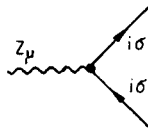
$$= ie^2 g_{\mu\nu} \left\{ \begin{aligned} & \frac{(c^2 - s^2)^2}{2c^2 s^2} \left(1 + \delta Z^\varphi + 2\delta Z_1^Z - 2\delta Z_2^Z \right. \\ & \quad \left. - \frac{4cs}{c^2 - s^2} (\delta Z_1^{\gamma Z} - \delta Z_2^{\gamma Z}) \right), \\ & \frac{s^2 - c^2}{cs} \left(1 + \delta Z^\varphi + \delta Z_1^\gamma - \delta Z_2^\gamma + \delta Z_1^Z - \delta Z_2^Z \right. \\ & \quad \left. + \frac{1}{2cs(c^2 - s^2)} (\delta Z_1^{\gamma Z} - \delta Z_2^{\gamma Z}) \right) \\ & 2 \left(1 + \delta Z^\varphi + 2\delta Z_1^\gamma - 2\delta Z_2^\gamma \right. \\ & \quad \left. + \frac{c^2 - s^2}{cs} (\delta Z_1^{\gamma Z} - \delta Z_2^{\gamma Z}) \right), \end{aligned} \right.$$



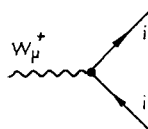
$$= i \frac{e^2}{2c^2 s^2} g_{\mu\nu} \{ 1 + 2\delta Z_1^Z - 2\delta Z_2^Z + \delta Z^\varphi; \delta Z_2^{\gamma Z} - \delta Z_1^{\gamma Z} \},$$



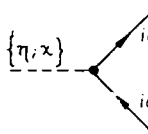
$$= -ieQ^{i\sigma} \gamma_\mu \left(1 + \delta Z_1^\gamma - \delta Z_2^\gamma + \delta Z_L^i \frac{1 - \gamma_5}{2} + \delta Z_R^{i\sigma} \frac{1 + \gamma_5}{2} \right) - ie\gamma_\mu (v_{i\sigma} - \gamma_5 a_{i\sigma}) (\delta Z_1^{\gamma Z} - \delta Z_2^{\gamma Z}),$$



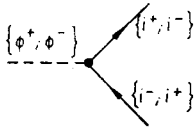
$$= ie\gamma_\mu (v_{i\sigma} - \gamma_5 a_{i\sigma}) (1 + \delta Z_1^Z - \delta Z_2^Z) + i \frac{e}{cs} \gamma_\mu \left[(I_3^\sigma - s^2 Q^{i\sigma}) \frac{1 - \gamma_5}{2} \delta Z_L^i - s^2 Q^{i\sigma} \frac{1 + \gamma_5}{2} \delta Z_R^{i\sigma} + cs Q^{i\sigma} (\delta Z_1^{\gamma Z} - \delta Z_2^{\gamma Z}) \right],$$



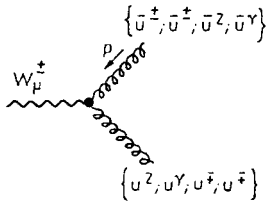
$$= i \frac{e}{\sqrt{2}s} \gamma_\mu \frac{1 - \gamma_5}{2} (1 + \delta Z_1^W - \delta Z_2^W + \delta Z_L^i),$$



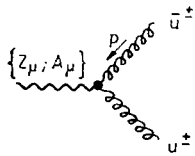
$$= -\frac{e}{2s} \frac{m_{i\sigma}}{M_W} \{ i; 2I_3^\sigma \gamma_5 \} \left(1 + \frac{\delta m_{i\sigma}}{m_{i\sigma}} + \frac{\delta v}{v} + \frac{1}{2} \delta Z_L^i + \frac{1}{2} \delta Z_R^{i\sigma} \right),$$



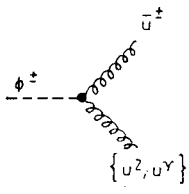
$$\begin{aligned}
 &= i \frac{e}{\sqrt{2} s} \frac{1}{M_W} \left(\frac{1 \mp \gamma_5}{2} m_{i\pm} \left(1 + \frac{\delta m_{i\pm}}{m_{i\pm}} + \frac{\delta v}{v} \right. \right. \\
 &\quad \left. \left. + \frac{1}{2} \delta Z_R^{i\pm} + \frac{1}{2} \delta Z_L^i \right) - \frac{1 \pm \gamma_5}{2} m_{i-} \right. \\
 &\quad \left. \times \left(1 + \frac{\delta m_{i-}}{m_{i-}} + \frac{\delta v}{v} + \frac{1}{2} \delta Z_R^{i-} + \frac{1}{2} \delta Z_L^i \right) \right),
 \end{aligned}$$



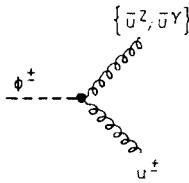
$$\begin{aligned}
 &= \pm i e p_\mu \left\{ \frac{c}{s}; -1; -\frac{c}{s}; 1 \right\} \left(1 + \delta \tilde{Z}^W + \delta Z_1^W - \delta Z_2^W \right. \\
 &\quad \left. - \frac{1}{2} \{ \delta \xi_1^W; \delta \xi_1^W; \delta \xi_1^3; \delta \xi_1^3 \} \right),
 \end{aligned}$$



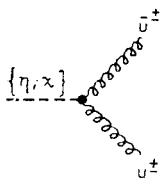
$$= \mp i e p_\mu \left\{ \frac{c}{s}; -1 \right\} \left(1 + \delta \tilde{Z}^W - \frac{1}{2} \delta \xi_1^W + \delta Z_1^W - \delta Z_2^W \right),$$



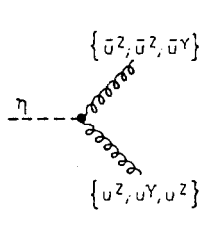
$$\begin{aligned}
 &= i e M_W \left\{ \frac{s^2 - c^2}{2cs}; 1 \right\} \left(1 - \frac{\delta v}{v} + \delta Z^\varphi + \delta Z_1^W - \frac{3}{2} \delta Z_2^W \right. \\
 &\quad \left. + \left\{ \frac{c^2}{c^2 - s^2}; \frac{1}{2} \right\} \left(\delta Z_1^W - \frac{3}{2} \delta Z_2^W + \delta \tilde{Z}^W + \delta \xi_2^W \right) \right. \\
 &\quad \left. + \left\{ \frac{-s^2}{c^2 - s^2}; \frac{1}{2} \right\} \left(\delta Z_1^B - \frac{3}{2} \delta Z_2^B + \delta \tilde{Z}^B + \delta \xi_2^W \right) \right),
 \end{aligned}$$



$$\begin{aligned}
 &= i \frac{e}{2cs} M_W \left\{ 1 - \frac{\delta v}{v} + \delta Z^\varphi + \delta Z_1^Z - \frac{3}{2} \delta Z_2^Z + \delta Z_1^W \right. \\
 &\quad \left. - \frac{3}{2} \delta Z_2^W + \delta \tilde{Z}^W + \frac{1}{2} \delta \xi_2^Z; -\delta Z_1^{\gamma Z} + \frac{3}{2} \delta Z_2^{\gamma Z} - \frac{1}{2} \delta \xi_2^{\gamma Z} \right\},
 \end{aligned}$$



$$\begin{aligned}
 &= -i \frac{e}{2s} M_W \{ 1; \pm i \} \left(1 - \frac{\delta v}{v} + \delta Z^\varphi + 2\delta Z_1^W - 3\delta Z_2^W + \delta \tilde{Z}^W \right. \\
 &\quad \left. + \frac{1}{2} \delta \xi_2^Z \right),
 \end{aligned}$$



$$= -i \frac{e}{2c^2 s} M_W \cdot \begin{cases} \left(1 - \frac{\delta v}{v} + \delta Z^v + 2\delta Z_1^z - 3\delta Z_2^z + \delta \tilde{Z}^z + \frac{1}{2} \delta \xi_2^z \right), \\ \left(-\delta Z_1^{\gamma z} + \frac{3}{2} \delta Z_2^{\gamma z} - \delta \tilde{Z}^{\gamma z} \right), \\ \left(-\delta Z_1^{\gamma z} + \frac{3}{2} \delta Z_2^{\gamma z} - \frac{1}{2} \delta \xi_2^{\gamma z} \right). \end{cases}$$

Appendix B:

1. The finite part of the scalar self energy $F(k^2; M_1, M_2)$:

$$F(k^2; M_1, M_2) = 1 + \left(\frac{M_1^2 - M_2^2}{k^2} - \frac{M_1^2 + M_2^2}{M_1^2 - M_2^2} \right) \ln \frac{M_2}{M_1}$$

$$+ \begin{cases} \frac{1}{k^2} [((M_1 + M_2)^2 - k^2)((M_1 - M_2)^2 - k^2)]^{1/2} \\ \times \ln \frac{\sqrt{(M_1 + M_2)^2 - k^2} + \sqrt{(M_1 - M_2)^2 - k^2}}{\sqrt{(M_1 + M_2)^2 - k^2} - \sqrt{(M_1 - M_2)^2 - k^2}}, \\ k^2 < (M_1 - M_2)^2 \\ - \frac{2}{k^2} [(M_1 + M_2)^2 - k^2]^{1/2} [k^2 - (M_1 - M_2)^2]^{1/2} \\ \times \arctan \frac{\sqrt{k^2 - (M_1 - M_2)^2}}{\sqrt{(M_1 + M_2)^2 - k^2}}, \\ (M_1 - M_2)^2 < k^2 < (M_1 + M_2)^2 \\ - \frac{1}{k^2} [k^2 - (M_1 + M_2)^2]^{1/2} [k^2 - (M_1 - M_2)^2]^{1/2} \\ \times \left\{ \ln \frac{\sqrt{k^2 - (M_1 + M_2)^2} + \sqrt{k^2 - (M_1 - M_2)^2}}{\sqrt{k^2 - (M_1 - M_2)^2} - \sqrt{k^2 - (M_1 + M_2)^2}} - i\pi \right\}, \\ k^2 > (M_1 + M_2)^2. \end{cases} \tag{B.1}$$

2. The function $B_1(k^2; M_1, M_2)$ is defined by:

$$\frac{i}{16\pi^2} k_\mu B_1(k^2; M_1, M_2) = \mu^{4-D} \int \frac{d^D q}{(2\pi)^D} \frac{q_\mu}{(q^2 - M_1^2 + i\varepsilon)((q + k)^2 - M_2^2 + i\varepsilon)}$$

and related to B_0 :

$$2k^2 B_1(k^2; M_1, M_2) = A(M_2) - A(M_1) + (M_2^2 - M_1^2 - k^2) B_0(k^2; M_1, M_2). \tag{B.2}$$

This gives for equal masses:

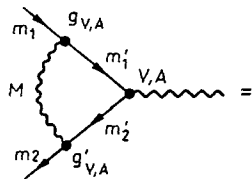
$$B_1(k^2; M, M) = -\frac{1}{2} B_0(k^2, M, M). \tag{B.2'}$$

3. The vertex functions $A_{1,\dots,4}$:

The contributions of the photonic diagrams of fig. 7a to the vertex function Γ_μ (of sect. 5.2f) for $|k^2| \gg m^2$, $\not{p} = \not{q} = m$ have already been calculated [18, 19]. After splitting off the UV divergent parts and the coupling constants remains the function $A_1(k^2, m)$:

$$\begin{aligned}
 A_1(0, m) &= 0, \\
 A_1(k^2, m) &= -2 \ln \frac{|k^2|}{\lambda^2} \left(\ln \frac{|k^2|}{m^2} - 1 \right) + \ln \frac{|k^2|}{m^2} + \ln^2 \frac{|k^2|}{m^2} \\
 &\quad + \begin{cases} 4 \left(\frac{\pi^2}{3} - 1 \right) + 2\pi i \left(\ln \frac{k^2}{\lambda^2} - \frac{3}{2} \right) & \text{for } k^2 \gg m^2, \\ 4 \left(\frac{\pi^2}{12} - 1 \right) & \text{for } -k^2 \gg m^2. \end{cases}
 \end{aligned} \tag{B.3}$$

The diagrams of fig. 7b describing the exchange of the heavy bosons Z and W lead to the following integral:



$$\begin{aligned}
 &= \mu^{4-D} \int \frac{d^D l}{(2\pi)^D} \frac{\gamma_\nu (g_V \gamma_{V'} - g_A \gamma_{A'}) (-\not{q} - \not{l} + m_2') \gamma_\mu (V - A \gamma_5) (\not{p} - \not{l} + m_1') \gamma^\nu (g_V - g_A \gamma_5)}{(l^2 - M^2) ((p-l)^2 + m_1'^2) ((q+l)^2 - m_2'^2)} \\
 &= \frac{i}{16\pi^2} \gamma_\mu (\lambda_V - \lambda_A \gamma_5) \cdot \begin{cases} \left[\Delta_M - \frac{1}{2} \right] & \text{for } k^2 = 0, \\ \left[\Delta_M - \frac{1}{2} + \Delta_2(k^2, M) \right] & \text{for } k^2 \gg m_{1,2}^2, m_{1,2}'^2 \end{cases}
 \end{aligned}$$

with

$$\lambda_V = V(g_V g_{V'} + g_A g_{A'}) + A(g_V g_{A'} + g_{V'} g_A),$$

$$\lambda_A = A(g_V g_{V'} + g_A g_{A'}) + V(g_V g_{A'} + g_{V'} g_A),$$

and

$$\Delta_2(k^2, M) = -\frac{5}{2} + \ln w + 2(1+w)^2 \frac{d}{dw} \left(\frac{J(w)}{1+w} \right), \quad w = \frac{M^2}{k^2}.$$

The parameter integral

$$J(w) = \int_0^1 dx \int_0^1 dy y \ln [w(1-y) - y^2 x(1-x) - i\epsilon]$$

can be evaluated with help of the dilogarithm

$$\text{Sp}(z) = - \int_0^1 dt \frac{\ln(1-zt)}{t}$$

and yields for A_2 the expression:

$$A_2(k^2, M) = -\frac{7}{2} - 2w - (2w + 3) \ln(-w) + 2(1 + w)^2 \left[\text{Sp} \left(1 + \frac{1}{w} \right) - \frac{\pi^2}{6} \right]$$

for $k^2 < 0$,

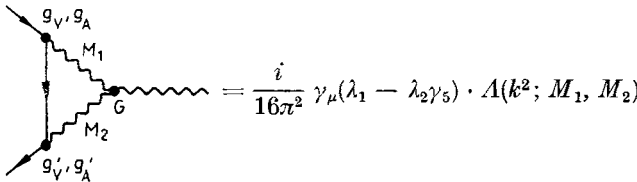
(B.4)

$$A_2(k^2, M) = -\frac{7}{2} - 2w - (2w + 3) \ln(w) + 2(1 + w)^2 \left[\ln(w) \ln \left(\frac{w + 1}{w} \right) - \text{Sp} \left(-\frac{1}{w} \right) \right] - i\pi \left[3 + 2w - 2(1 + w)^2 \ln \left(\frac{1 + w}{w} \right) \right]$$

for $k^2 > 0$.

In fig. 22 we show $A_2(k^2, M_Z)$, $A_2(k^2, M_W)$, $A_3(k^2, M_W)$, and $A_4(k^2; M_Z, M_W)$.

In a similar way we have obtained the invariant functions belonging to the diagram 7c containing the triple boson vertex:



with

$$\lambda_1 = (g_V g_{V'} + g_A g_{A'}) G, \quad \lambda_2 = (g_V g_{A'} + g_A g_{V'}) G$$

and

$$A(k^2; M_1, M_2) = \begin{cases} 3 \left[\Delta_M - \frac{1}{6} + A_3(k^2, M) \right] & \text{for } M_1 = M_2 = M, \\ 3 \left[\frac{\Delta_{M_1} + \Delta_{M_2}}{2} + \frac{5}{6} - \frac{M_1^2 + M_2^2}{M_1^2 - M_2^2} \ln \frac{M_1}{M_2} + A_4(k^2; M_1, M_2) \right] & \text{for } M_1 \neq M_2. \end{cases}$$

(B.5)

The remaining functions have the properties

$$A_3(0, M) = A_4(0, M_1, M_2) = 0,$$

$$A_4(k^2, M_1, M_2) = A_4(k^2, M_2, M_1).$$

They read for $|k^2| \gg m_f^2$ ($w = M^2/k^2$):

$$A_3(k^2, M) = \frac{5}{6} - \frac{2w}{3} + \frac{2w + 1}{3} \sqrt{1 - 4w} \ln \frac{\sqrt{1 - 4w} + 1}{\sqrt{1 - 4w} - 1} + \frac{2}{3} w(w + 2) \left(\ln \frac{\sqrt{1 - 4w} + 1}{\sqrt{1 - 4w} - 1} \right)^2 \quad \text{for } k^2 < 0,$$

$$\begin{aligned}
 A_3(k^2, M) &= \frac{5}{6} - \frac{2w}{3} + \frac{2}{3} (2w + 1) \sqrt{4w - 1} \arctan \frac{1}{\sqrt{4w - 1}} \\
 &\quad - \frac{8}{3} w(w + 2) \left(\arctan \frac{1}{\sqrt{4w - 1}} \right)^2 \quad \text{for } 0 < k^2 < 4M^2,
 \end{aligned}
 \tag{B.6}$$

$$\begin{aligned}
 A_3(k^2, M) &= \frac{5}{6} - \frac{2w}{3} + \frac{2w + 1}{3} \sqrt{1 - 4w} \ln \frac{1 + \sqrt{1 - 4w}}{1 - \sqrt{1 - 4w}} \\
 &\quad + \frac{2}{3} w(w + 2) \left[\ln^2 \left(\frac{1 + \sqrt{1 - 4w}}{1 - \sqrt{1 - 4w}} - \pi^2 \right) \right] \\
 &\quad - i\pi \left[\frac{2w + 1}{3} \sqrt{1 - 4w} + \frac{2}{3} w(w + 2) \ln \frac{1 + \sqrt{1 - 4w}}{1 - \sqrt{1 - 4w}} \right] \\
 &\hspace{15em} \text{for } k^2 > 4M^2
 \end{aligned}$$

and with $w_1 = M_1^2/k^2, w_2 = M_2^2/k^2$:

$$\begin{aligned}
 &A_4(k^2; M_1, M_2) \\
 &= \frac{1}{6} + \frac{w_1 + w_2}{w_1 - w_2} \ln \frac{M_1}{M_2} - \frac{w_1 - w_2}{3} \ln \frac{M_1}{M_2} + \frac{w_1 + w_2 + 1}{3} \left(\ln \frac{M_1}{M_2} - 1 \right) \\
 &\quad + \frac{w_1 + w_2 + 1}{3} \left[x_1 \ln \frac{x_1}{x_1 - 1} + x_2 \ln \frac{-x_2}{1 - x_2} \right] \\
 &\quad - \frac{2}{3} (w_1 + w_2 + w_1 w_2) \ln \frac{x_1}{x_1 - 1} \ln \frac{-x_2}{1 - x_2},
 \end{aligned}
 \tag{B.7}$$

$$x_{1,2} = \begin{cases} \frac{1 - w_1 + w_2}{2} \pm \frac{1}{2} \sqrt{(1 - w_1 + w_2)^2 - 4w_2} \\ \text{for } k^2 < (M_1 - M_2)^2 \text{ and } k^2 > (M_1 + M_2)^2, \\ \frac{1 - w_1 + w_2}{2} \pm \frac{i}{2} \sqrt{4w_2 - (1 - w_1 + w_2)^2} \\ \text{for } (M_1 - M_2)^2 < k^2 < (M_1 + M_2)^2. \end{cases}$$

The imaginary part of A_4 is obtained from (B.7).

$$\begin{aligned}
 \text{Im } A_4(k^2; M_1, M_2) &= -\pi \cdot \theta(k^2 - (M_1 + M_2)^2) \\
 &\quad \times \left\{ \frac{w_1 + w_2 + 1}{3} \sqrt{(1 - w_1 + w_2)^2 - 4w_2} \right. \\
 &\quad \left. + \frac{2}{3} (w_1 + w_2 + w_1 w_2) \left(\ln \frac{x_1}{1 - x_1} + \ln \frac{x_2}{1 - x_2} \right) \right\}.
 \end{aligned}
 \tag{B.8}$$

In the case $M_2 = 0$, i.e. if one of the bosons is a photon, the mass m of the fermion coupled to the photon has to be respected. In that special case we have to use the following

expression, valid for $|k^2| \gg m^2$ (with $w = M^2/k^2$):

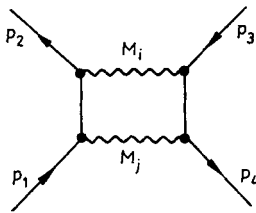
$$A_4^m(k^2; M, 0) = \frac{1}{2} - \frac{w}{3} + \frac{1-w^2}{3} \ln \frac{w-1}{w} + \frac{2}{3} \ln \frac{M^2}{m^2} + \frac{w}{3} \left[\ln^2 \left(\frac{M^2-k^2}{m^2} \right) - \left(\ln \frac{M^2}{m^2} \right)^2 + 2 \operatorname{Sp} \left(\frac{1}{1-w} \right) \right]. \quad (\text{B.9})$$

For $k^2 \cong M^2$ replace $M^2 \rightarrow M^2 - iM\Gamma$.

Fig. 23 shows $A_4^m(k^2; M, 0)$ for $m = m_e, M = M_W$.

4. The box diagrams:

We write down the explicit expressions for the s -channel box diagrams. The matrix element can be written as:



$$= \frac{\alpha}{2\pi} \frac{1}{s} \{ \bar{v}(p_2) \gamma_\mu (\lambda_1^V - \lambda_1^A \gamma_5) u(p_1) \cdot \bar{u}(p_4) \gamma^\mu (\lambda_2^V - \lambda_2^A \gamma_5) v(p_3) \cdot I^{ij}(s, t) + \bar{v}(p_2) \gamma_\mu \gamma_5 (\lambda_1^V - \lambda_1^A \gamma_5) u(p_1) \cdot \bar{u}(p_4) \gamma^\mu \gamma_5 (\lambda_2^V - \lambda_2^A \gamma_5) v(p_3) \cdot I_5^{ij}(s, t) \} \quad (\text{B.10})$$

with

$$\lambda_1^V = v_1 v_2 + a_1 a_2, \quad \lambda_1^A = v_1 a_2 + v_2 a_1, \\ \lambda_2^V = v_3 v_4 + a_3 a_4, \quad \lambda_2^A = v_3 a_4 + v_4 a_3,$$

where the v_i, a_i are the vector and axial vector couplings of the i 'th fermion to the internal boson according to the labelling of fermion momenta in the above diagram.

$$s = (p_1 + p_2)^2, \quad t = (p_2 - p_3)^2, \quad u = (p_1 - p_3)^2$$

are the usual Mandelstam variables.

In order to obtain the expression for the crossed box one should substitute $t \leftrightarrow u$ and reverse the sign of I^{ij} :

$$I^{ij}(s, t) \rightarrow -I^{ij}(s, u) \quad \text{and} \quad I_5^{ij}(s, t) \rightarrow I_5^{ij}(s, u). \quad (\text{B.11})$$

The following results [33], given in a form which is convenient for numerical evaluation, are valid for $s, |t|, |u| \gg m_f^2$. Because of (B.11) we give for the neutral-current boxes only that part of I , which is antisymmetric under $t \leftrightarrow u$:

$$I_5^{\gamma\gamma}(s, t) = \frac{\alpha}{2\pi} \left\{ \frac{s}{2(s+t)} \ln \frac{t}{s+i\epsilon} - \frac{s(s+2t)}{4(s+t)^2} \left[\ln^2 \left(\frac{t}{s+i\epsilon} \right) + \pi^2 \right] \right\} \quad (\text{B.12}) \\ I^{\gamma\gamma}(s, t) - I^{\gamma\gamma}(s, u) = \frac{\alpha}{2\pi} \left\{ -2 \ln \frac{t+i\epsilon}{-s} \ln \left(\frac{-s}{\lambda^2} - i\epsilon \right) \right\} + I_5^{\gamma\gamma}(s, t) - I_5^{\gamma\gamma}(s, u);$$

$$I_5^{\gamma Z}(s, t) = \frac{\alpha}{2\pi} \frac{s - M_Z^2}{2(s + t)} \left\{ \ln \frac{t}{s - M_Z^2} - \frac{M_Z^2}{s} \ln \frac{M_Z^2}{M_Z^2 - s} + \frac{s + 2t + M_Z^2}{s + t} \right. \\ \left. \times \left[\text{Sp} \frac{s}{M_Z^2} - \text{Sp} \frac{-t}{M_Z^2} + \ln \frac{-t}{M_Z^2} \cdot \ln \frac{M_Z^2 - s}{M_Z^2 + t} \right] \right\}, \tag{B.13}$$

$$I^{\gamma Z}(s, t) - I^{\gamma Z}(s, u) = I_5^{\gamma Z}(s, t) - I_5^{\gamma Z}(s, u) + \frac{\alpha}{2\pi} \left(\text{Sp} \frac{M_Z^2 + t}{t} \right. \\ \left. + \frac{1}{2} \ln \frac{t^2}{s^2} \ln \frac{M_Z^2}{M_Z^2 - s} - \ln \left(\frac{-t}{s} + i\epsilon \right) \ln \frac{M_Z^2}{\lambda^2} \right).$$

$$I_5^{ZZ}(s, t) = \frac{\alpha}{2\pi} \frac{s}{s + t} \left\{ \frac{2t + s + 2M_Z^2}{2(s + t)} \left[\text{Sp} \left(1 + \frac{t}{M_Z^2} \right) - \frac{\pi^2}{6} - \left(\ln \frac{-y_1}{y_2} \right)^2 \right] \right. \\ \left. + \frac{1}{2} \ln \frac{-t}{M_Z^2} + \frac{y_2 - y_1}{2} \ln \frac{-y_1}{y_2} \right. \\ \left. + \frac{s + 2t - 4tM_Z^2/s + 2M_Z^4/t - 2M_Z^4/s}{2(s + t)(x_2 + x_1)} \right. \\ \left. \times \left[\text{Sp} \frac{x_1}{x_1 - y_1} + \text{Sp} \frac{x_1}{x_1 - y_2} - \text{Sp} \frac{x_2}{x_2 - y_2} - \text{Sp} \frac{x_2}{x_2 - y_1} \right] \right\}, \tag{B.14}$$

$$I^{ZZ}(s, t) = I_5^{ZZ}(s, t) + \frac{\alpha}{2\pi} \left\{ 2 \left(\ln \frac{-y_1}{y_2} \right)^2 + \frac{2}{x_1 - x_2} \right. \\ \left. \times \left[\text{Sp} \frac{x_1}{x_1 - y_1} + \text{Sp} \frac{x_1}{x_1 - y_2} - \text{Sp} \frac{x_2}{x_2 - y_2} - \text{Sp} \frac{x_2}{x_2 - y_1} \right] \right\}$$

with

$$x_{1/2} = \frac{1}{2} \left(1 \pm \sqrt{1 - 4M_Z^2/s(1 + M_Z^2/t)} \right) \\ y_{1/2} = \frac{1}{2} \left(1 \pm \sqrt{1 - 4M_Z^2/s} \right). \tag{B.15}$$

The expressions for the form factors I^{ZZ} , I_5^{ZZ} are valid for $s \leq 2 \text{ Re } M^2$; those for the WW -box are obtained from (B.14, 15) by the substitution $M_Z^2 \rightarrow M_W^2$ (the gauge boson masses include as imaginary part $-iM\Gamma$).

As an illustration we present for $\sqrt{s} = 93 \text{ GeV}$ the functions I and I_5 for the ZZ and WW boxes in Figs. 24a, b. Only the t -channel expressions have an imaginary part comparable to the real part. In the other cases $\text{Im } I$ is of the order of magnitude $\alpha/2\pi \cdot 10^{-2}$ or even smaller.